“Combined optical and wireless/wireline access based on existing requirements”

D5.3

‘Accordance_D5.3_WP5_2011_30September_UH_v1.0.docx’

Version: 1.0

Last Update: 30/9/2011 22:09:00 119/P9

Distribution Level: PU

- ***Distribution level***
  PU = Public,
  RE = Restricted to a group of the specified Consortium,
  PP = Restricted to other program participants (including Commission Services),
  CO= Confidential, only for members of the ACCORDANCE Consortium (including the Commission Services)

The ACCORDANCE Project Consortium groups the following organizations:

Partner Name	Short name	Country
JCP-Consult	JCP	FR
Research and Education Laboratory in Information Technologies	AIT	GR
Alcatel-Lucent Deutschland	ALUD	DE
Deutsche Telekom AG	DTAG	DE
Intracom Telecom	ICOM	GR
Telefónica Investigación y Desarrollo	TID	ES
University of Hertfordshire	UH	UK
Karlsruhe Institute of Technology	KIT	DE
Universitat Politècnica de Catalunya	UPC	ES
Euprocom	EPC	EE

Abstract:
This document provides a detailed analysis with reference to the technological concepts identified at the workpackage 5 of the ACCORDANCE project with respect to optical/wireless and wireline integration. To that effect the network architectures and their requirements, identified in preceding deliverables (mainly D5.1 and D5.2), have been examined, to provide detail description of the wireless interfacing options with PON followed with the performance evaluations of the digital and analog variants and deployment scenarios for the optical/wireless and wireline segments of the ACCORDANCE network. An executive summary outlining the key contributes of the undertaken work is included at the opening section of this deliverable.

"The research leading to these results has received funding from the European Community's Seventh Framework Programme (FP7/2007-2013) under grant agreement n° 248654"

Document Identity

Title:	Combined optical and wireless/wireline access based on existing requirements
Subject:	Performance evaluation studies for optical/wireless and wireline segments
File name:	Accordance_D5.3_WP5_2011_30September_UH_v1.0.docx
Last Update:	Friday, September 30, 2011

Revision History

No.	Version	Edition	Author(s)	Date
1	0	1	Milos Milosavljevic	04/07/11
	Comments:	Initial Release of ToC		
2	0	2	Frank Schaich	11/08/11
	Comments:	first input		
3	0	3	Milos Milosavljevic	06/09/11
	Comments:	ToC reorganisation. Abstract, partial ex. summary and introduction added		
4	0	4	Milos Milosavljevic	16/09/11
	Comments:	UH input and review ready version		
5	0	5	Milos Milosavljevic	25/09/11
	Comments:	Address first reviewer comments		
6	0	6	Milos Milosavljevic	30/09/11
	Comments:	Formatting and minor modifications to some parts of the contents		
7	0	7	Milos Milosavljevic	30/09/11
	Comments:	Final version		
8	1	0	Roman Kaurson	30/09/11
	Comments:	Released version		
9				
	Comments:			
10				
	Comments:			
11				
	Comments:			
12				
	Comments:			
13				
	Comments:			
14				
	Comments:			
15				
	Comments:			

Table of Contents

Executive Summary

A detailed analysis of the ACCORDANCE optical/wireless and wireline network architectures and elements, including its extended features and technological challenges are provided in D5.1 and D5.2 with the latter focusing primarily on the requirements aspects. Taking into consideration the scope of D5.3, being to evaluate the combined optical and wireless/wireline access solutions for ACCORDANCE based on the outcomes of D5.1 and D5.2, an assessment of the wireless/wireline convergence and interfacing requirements for different backhauling and fronthauling options, (i.e. IP backhauling, split eNB (evolved NodeB), CPRI (Common Public Radio Interface) and RoF (Radio-over-Fibre)) are included at this deliverable's opening sections.

To that extent, Section 2 gives some insight with respect to the achievable and especially rational degree of wireless/wireline convergence. Depending on the network scenario (rural and urban) the degree of convergence has to be balanced accordingly.

Section 3 provides an exclusive summary of the foreseen interfacing challenges with respect to the different LTE Layer-1 terminations. The signal generation and detection principles at the MCO (Main Central Office) and the site were described for each option where IP backhauling variant performs complete baseband and MAC (Medium Access Control) processing at the site compared to CPRI and RoF fronthauling where full centralisation could be achieved at the MCO. A trade-off in terms of complexity, bandwidth requirements and degree of centralisation could be considered with split eNB scenarios.

Section 4 of the deliverable presents the bandwidth requirements for each of the optional interfacing points. For digital fronthauling these rates range from several hundreds of Mbit/s (soft-bit fronthauling) up to several Gbit/s (CPRI fronthauling) for the given scenario (10 MHz, 4 Rx antennas). The analog (RoF) requires minimum bandwidth (around 300 MHz per site) but it is more susceptible to errors.

In section 5 performance evaluation of digital and analog fronthauling is described. For the digital fronthauling BER (Bit Error Rate) of various options (soft-bit, burst and frame fronthauling) and modulation formats (QPSK and QAM) were considered where PON is modelled solely to introduce bit errors into the system. In terms of RoF, wireless signal performance is experimentally demonstrated over various fibre distances. The effect of limited power budget and optical modulation index was clearly visible. In addition, due to these limitations the subcarrier insertion in the optical OFDM spectrum is not feasible.

Section 6 covers aspects regarding inter-cell communication. This is followed with the comparison evaluation of all optical/wireless options, in Section 7, clearly demonstrating that no obvious solution for the back- or fronhauling is available.

Furthermore, Section 8 is focusing on xDSL transmission evaluation over the integrated architectural platform as well as its deployment scenarios.

Finally, Section 9 provides some concluding remarks.

References

[1] *ACCORDANCE: Deliverable 2.4 (D2.4)* [Online]. Available: http://ict-accordance.eu

[2] "ACCORDANCE: Deliverable 5.2 (D5.2)," *http://ict-accordance.eu)*.

[3] S. Sesia, I. Toufik, and M. Baker, *LTE The UMTS long term evolution*: John Wiley & Sons Ltd., 2009.

[4] H. Ekstrom, "QoS control in the 3GPP evolved packet system," *IEEE Communications Magazine*, vol. 47, pp. 76-83, (2009).

[5] *ACCORDANCE: Deliverable 5.1 (D5.1)* [Online]. Available: http://ict-accordance.eu

[6] *Common Public Radio Interface (CPRI); Specificaiton v4.1*, http://www.cpri.info, 2009

[7] "IEEE Standard for Local and metropolitan area networks Part 16: Air Interface for Fixed and Mobile Broadband Wireless Access Systems Amendment 2: Physical and Medium Access Control Layers for Combined Fixed and Mobile Operation in Licensed Bands and Corrigendum 1," *IEEE Std 802.16e-2005 and IEEE Std 802.16-2004/Cor 1-2005 (Amendment and Corrigendum to IEEE Std 802.16-2004)*, pp. 0_1-822, (2006).

[8] W. Hofmann, E. Wong, G. Bohm, M. Ortsiefer, N. H. Zhu, and M. C. Amann, "1.55-um VCSEL Arrays for High-Bandwidth WDM-PONs," *Photon. Technol. Lett.*, vol. 20, pp. 291-293, (2008).

[9] Anritsu. (2011, July 10), *Mobile WiMAX Base Station Troubleshooting Guide* [Online]. Available: http://www.anritsu.com

[10] *Real Decreto 401/2003 de 4 de abril de 2003 por el que se aprueba el Reglamento Regulador de las Infraestructuras Comunes de Telecomunicación* [Online]. Available: http://www.coit.es/pub/ficheros/rd4012003_62428266.pdf

[11] *ACCORDANCE: Deliverable 2.1 (D2.1)* [Online]. Available: http://ict-accordance.eu

1. Introduction

With developments in broadband wireless networks, driven primarily by long term evolution (LTE), data rates in the range of hundreds of Mbps are expected to be supported over next generation radio cells. This will unavoidably lead to a higher density of base station deployment and a requirement for increased spectral efficiency. High bandwidth, cost-effective feeder links will be required as a result to connect each of these base stations to a common main central office (MCO). In addition, efficient data transport on the feeder is required without degrading the wireless performance across a cell. Since the application of current solutions, such as SDH and IP is anticipated to be expensive to both deploy and operate, lower-cost optical infrastructures, such as ACCORDANCE, have been suggested, required also to allow sharing of network resources among different sites and/or different operators.

To that extent, the aim of this deliverable is to provide solutions to the aforementioned problems. The parameters and scenarios used in these investigations are based on the findings in D5.1 and D5.2 that were dealing with definitions of the optical/wireless architectural options and corresponding requirements respectively.

The optical-wireless interfacing and bandwidth requirements for each option were analysed followed with the evaluation measure in order to provide an optimum PHY structure for the ACCORDANCE scenario. As it will be described, there was no obvious solution since each option has its own benefits and the choice will primarily depend on deployment scenarios.

2. Wireless/wireline convergence

To start with the convergence aspects, looking at one of the original architecture sketches developed in ACCORDANCE, we can identify the two different degrees: infrastructural and convergence based on transport mechanism.

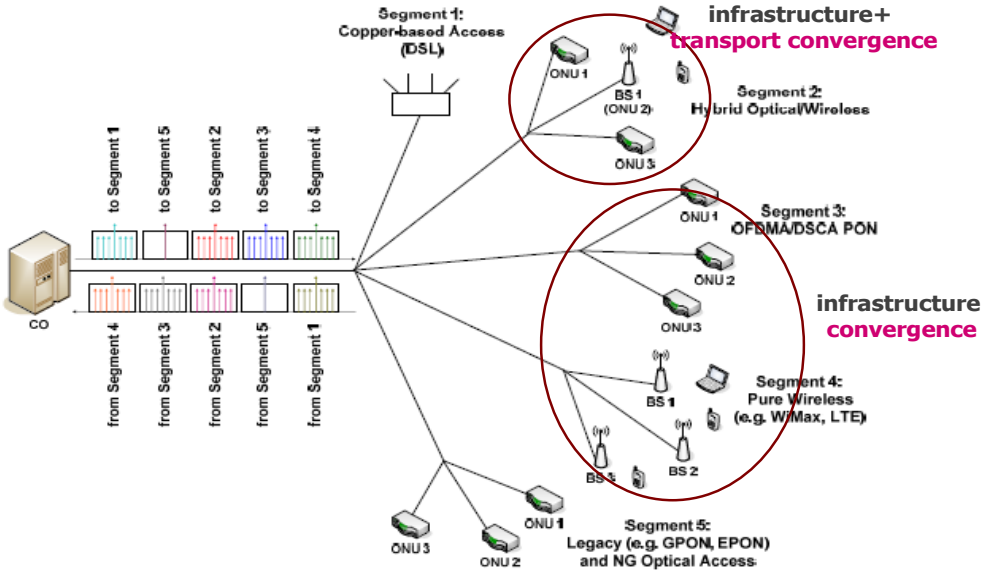

Figure 1: ACCORDANCE architecture – grades of wireless/wireline convergence

As displayed in figure above, Segment 2 is fed via a single wavelength and contains both fibre-to-the-home (FTTH) and mobile back/fronthauling links. Consequently, we have both convergence with respect to the infrastructure and with respect to the transport mechanism (i.e. both services are multiplexed into the same OFDM subsystem). Segment 3 and segment 4 on the other side deliver purely FTTH and wireless services, respectively. In this case convergence is limited to sharing the infrastructure.

Depending on the wireless network scenario and connected to this the optimal wireless back/fronthauling option different approaches are to be favored:

- If the wireless subsystem is fully decentralised (e.g. rural scenario), i.e. the equipment at the sites are equipped with fully functional eNBs, the ACCORDANCE network has to transport IP packets to the various wireless nodes. In this case the wireless medium access control (MAC) processing is performed at the sites and the stringent latency requirements described in former deliverables are not present. The required rates on the PON per eNB are in the same range as the rates transported via the air and varying in time. Subsequently, sharing the transport mechanism between FTTH and wireless backhauling is an option and may produce statistical multiplexing gains. In this case the ACCORDANCE network tunnels the IP packets between the serving gateway and the eNBs.
- On the other side, if the MAC and parts of the baseband processing are centralized (e.g. urban scenario), things are different. Now, the HARQ (Hybrid Automatic Repeat reQuest) anchor point is at the respective main central office and the harsh latency requirements are to be met. In addition, depending on the degree of baseband centralisation (from soft-bit fronthauling up to CPRI fronthauling) the required rates on the PON to feed a single eNB are rising tremendously. The more the baseband gets

centralized the less time varying the required PON rates (up to constant bit rates for frame and CPRI backhauling) are and the less favorable the convergence of the transport mechanism gets.

In D2.4 [1] a more detailed analysis with respect to wireless/wireline convergence will be presented.

2.1. WIRELESS NETWORK SCENARIOS

This section provides an outline of the possible network scenarios for urban and rural settings.

Urban setting:
In urban regions the demand for capacity is rather high and heterogeneously dispersed. So, the distribution of wireless network nodes should follow this, leading to a heterogeneous network topology:

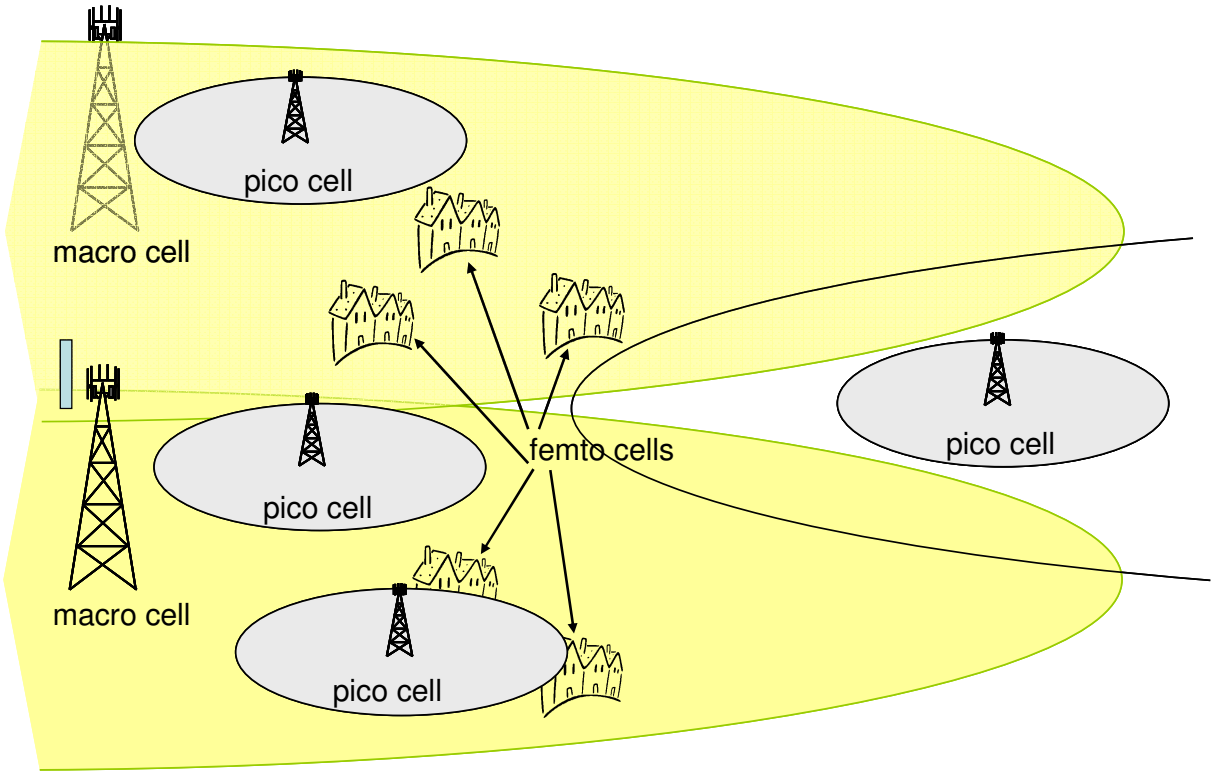

Figure 2: Wireless networking scenario in urban regions.

Full coverage is reached through macro cells. More or less regularly towers are placed feeding their surroundings. To achieve a given capacity per region inter-site-distance is in the range of [0.2…0.5] km. To meet local capacity peeks, pico cells are placed in regions with high user densities. Naturally their locations are within macro cells. Both macro and pico cells feed wireless services to open subscriber groups. Macro cells are always on, pico cells are active on demand. Finally, femto cells deliver WLAN-like services to closed subscriber groups. They are mostly indoor and active on demand.

In urban settings we have many cell borders in locations with high user density (both between macro cells, and between macro and pico cells). So, the use of collaborative schemes is a must and has the potential to provide high gains. Therefore, a centralized approach (both for the

macro and pico cells) is favorable. As femto cells are mostly located indoor and to prohibit the need of fat back-/fronthauling pipes, IP backhauling is to be favored for femtos.

D2.4 [1] will treat this in more detail.

Rural setting:
In rural settings the user density is by far lower. Macro cells still provide full coverage, but with much higher inter-site-distances up to 5 km. The need for pico-cells is less crucial. Femtos are still present for the provision of indoor services. So the overall site density is much lower and the distances for back/fronthauling are much higher in average. Cell borders are most likely located in regions with low user density. All these arguments make the need and gain of centralised processing less relevant. So, in rural settings a decentralised approach (eNB@site) with IP backhauling is favourable.

3. Interfacing and wireless system consolidation

This chapter provides an overview about the available options for the integration of the wireless subsystem into the converged network.

We have two kinds of wireless system consolidation:

- MAC centralisation
- Baseband (PHY) centralisation

The main functionalities handled by the MAC layer are multi user scheduling, HARQ processing and user ranging [2, 3]. For the MAC layer we have two options: complete centralisation and strict decentralised MACs. In the following, we assume the MAC functionalities to be handled by the central entity in any case beside with option (a), i.e. IP backhauling.

The PHY layers duty is to synthesize/analyse the baseband signal and to provide measurements to the higher layers. Here, we have more degrees of freedom as we can vary the grade of centralisation by choosing the appropriate interfacing point. For the sake of simple referencing in later sections we once more present the baseband processing chains for uplink and downlink of wireless communication systems relying on OFDM and the available points of interfacing:

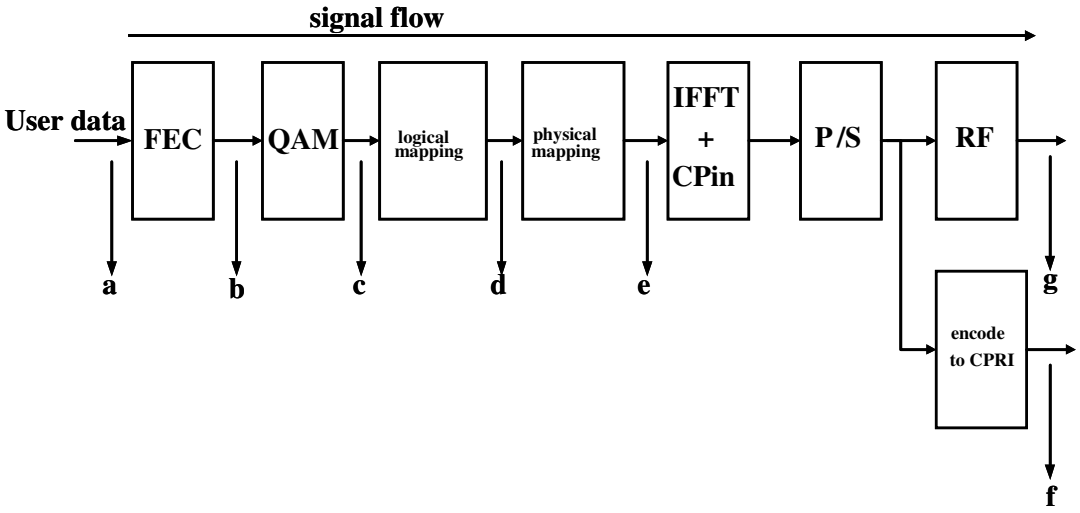

Figure 3: Baseband processing chain – downlink.

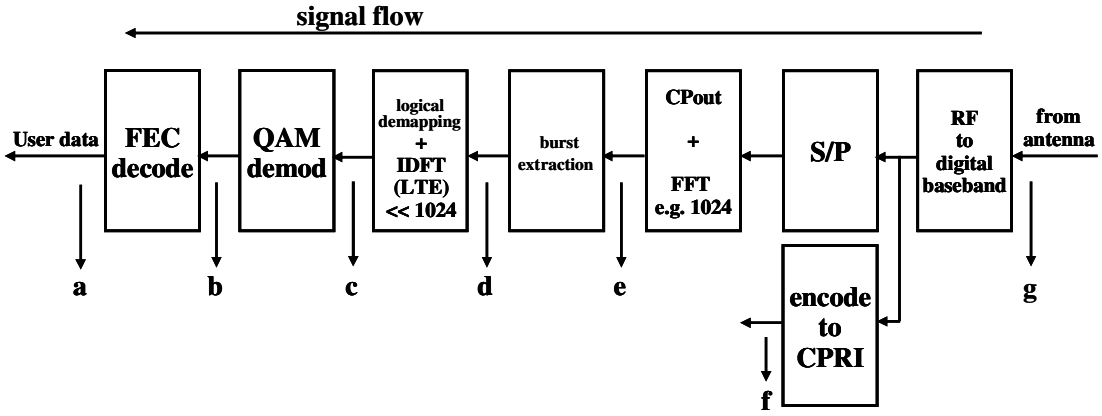

Figure 4: Baseband processing chain – uplink.

Each interfacing point has various implications to the operation of the system and the architectures both within the CO and at the sites as described in the following sections.

3.1. IP BACKHAULING (A)

With IP backhauling signal generation/detection is performed completely at the sites therefore the bandwidth pipes needed on the PON are rather small. The MAC centralization would still be possible, but would generate severe signaling needs as the measurements are taken by the PHY layer located at the site and used by the MAC layer at the central office. Consequently, although baseband processing is performed near the user, the target of low latency and slim eNB is not reached anymore.

In order to enable appropriate operation however, the IP backhauling requires an effective quality of service (QoS) mapping mechanism between PON priority queues and LTE QoS class identifier (QCI) IP flows. In particular, the mapping has to identify which LTE IP flow should be stored in which PON priority queue for equivalent QoS. For LTE the QoS model is based on the concept of bearers [4] where each bearer has assigned QCI (as it was described in D5.1 [5]) and is composed of a radio bearer and mobility tunnel.

The Figure 3 below describes a converged architecture and the requirements for the optical/wireless QoS mapping mechanism. Only PHY and MAC layers functionalities are presented for optical and LTE nodes.

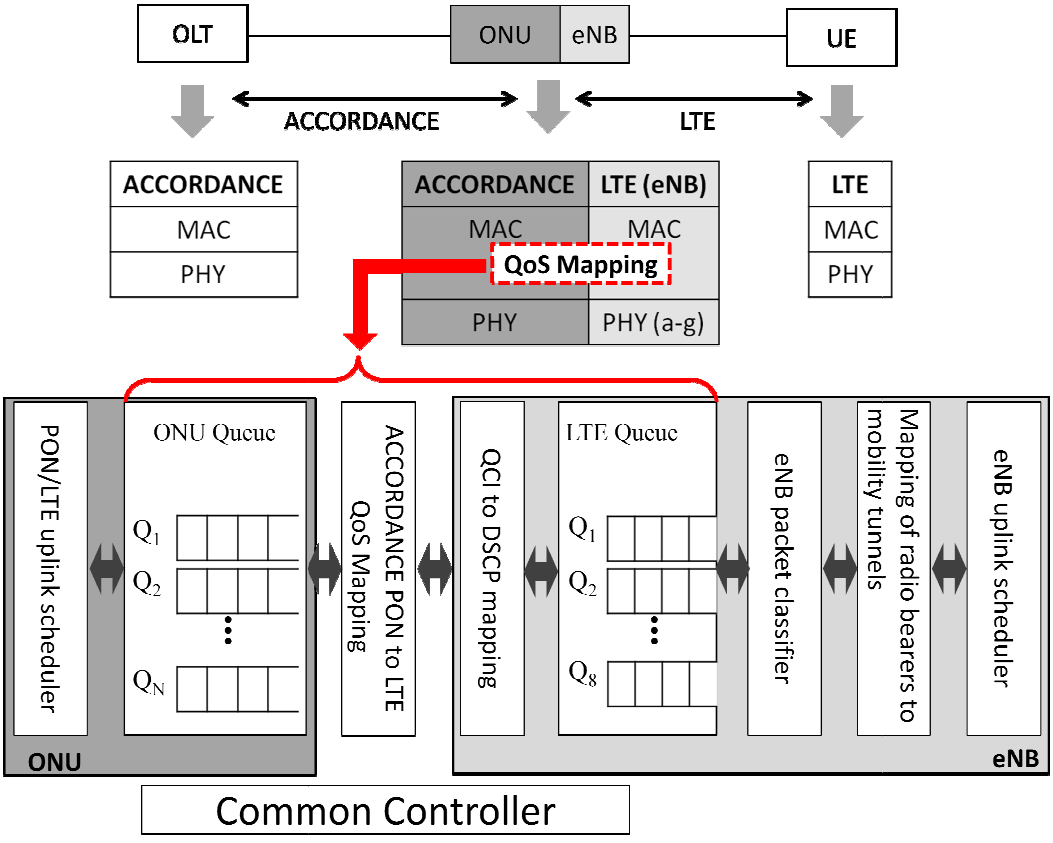

Figure 5: QoS mapping requirements between ACCORDANCE PON and LTE.

As it can be seen from the figure once the radio bearers are received at the eNB they are directly mapped to mobility tunnels based on their bearer ID [4]. This is followed with the packet classification and queue mapping. The queue mapping is essential process in providing class of service separation and is indentified by its corresponding IP packet. LTE defines eight

standardized QCIs that classify data traffic into eight different classes of service, ranging from real-time gaming to the lowest priority best-effort data.

To allow for traffic separation in the transport network, each QCI is mapped onto a corresponding diffserv code point (DSCP) in order to translate a bearer-based QoS (QCI) to transport-based QoS (DSCP), as shown in Figure 3. Using this mapping function, packets on a bearer associated with a specific QCI are marked with a specific DSCP for forwarding in the transport network [4]. The QCI to DSCP mapping is performed based on operator policies, which are configured into the network nodes. The central office performs the mapping for downlink packets while eNB performs it for uplink packets.

This is then forwarded to the packet classifier (i.e. QoS mapping mechanism between ACCORDANCE PON and LTE) which needs to be carefully designed in order to enable satisfactory QoS performance for wireless users.

To that extent, the typical PON's dynamic bandwidth allocation (DBA) and QoS support must be modified at both the ONUs and OLTs. For instance, the most common centralized PON architectures support differentiated upstream QoS via two independent scheduling mechanisms namely scheduling at the OLT and scheduling at the ONU. However, none of these scheduling mechanisms can guarantee bandwidth for real-time IP flows. Thus, each ONU is required to reserve bandwidth for its real-time IP flows for the whole duration of the flow.

Also, since the bearers are not visible to the ONUs/OLTs, each and every ONU/OLT must be directly configured with all eight LTE's standardized QCIs (QoS characteristics) or more precisely with the corresponding ACCORDANCE priority queues as mentioned before. With this approach the common scheduler manages the QoS mapping between ONU's queues and eNB's queues.

Since this deliverable is providing solutions mainly at Layer-1, the detail mapping mechanisms and QoS performance, aspects of Layer-2, are out of the scope and will be investigated and presented in D5.4 ('Mapping of radio signals to optical resources and distribution of mapping within the network') instead.

Finally, the IP backhauling requires the following physical interfaces:

- a single connection for user's IP packets stream at the central office and the site
- communication interface between the wireless and optical MAC unit within the site for effective QoS mapping

3.2. PARTIAL BASEBAND CENTRALISATION: SPLIT ENB (B-E)

Figure 6, Figure 8, Figure 10 and Figure 12 depict the CO architectures for soft-bit fronthauling (b), soft-symbol fronthauling (c), burst fronthauling (d) and frame fronthauling (e) (once parts of the baseband processing is done at the central office we no more talk about backhauling, but instead we say fronthauling). The left blocks include the wireless processing units (upper half UL Rx, lower half DL Tx) the right ones the units in charge of the optical transport. Radio Link Control (RLC) and MAC are centralized and site comprehensive.

Figure 7, Figure 9, Figure 11 and Figure 13 depict the respective counterparts, i.e. the architectures of the site equipment. Here, the left blocks include the processing units dealing with the optical transport the right ones are handling the signals being transported via the air.

3.2.1. Soft-bit fronthauling (b)

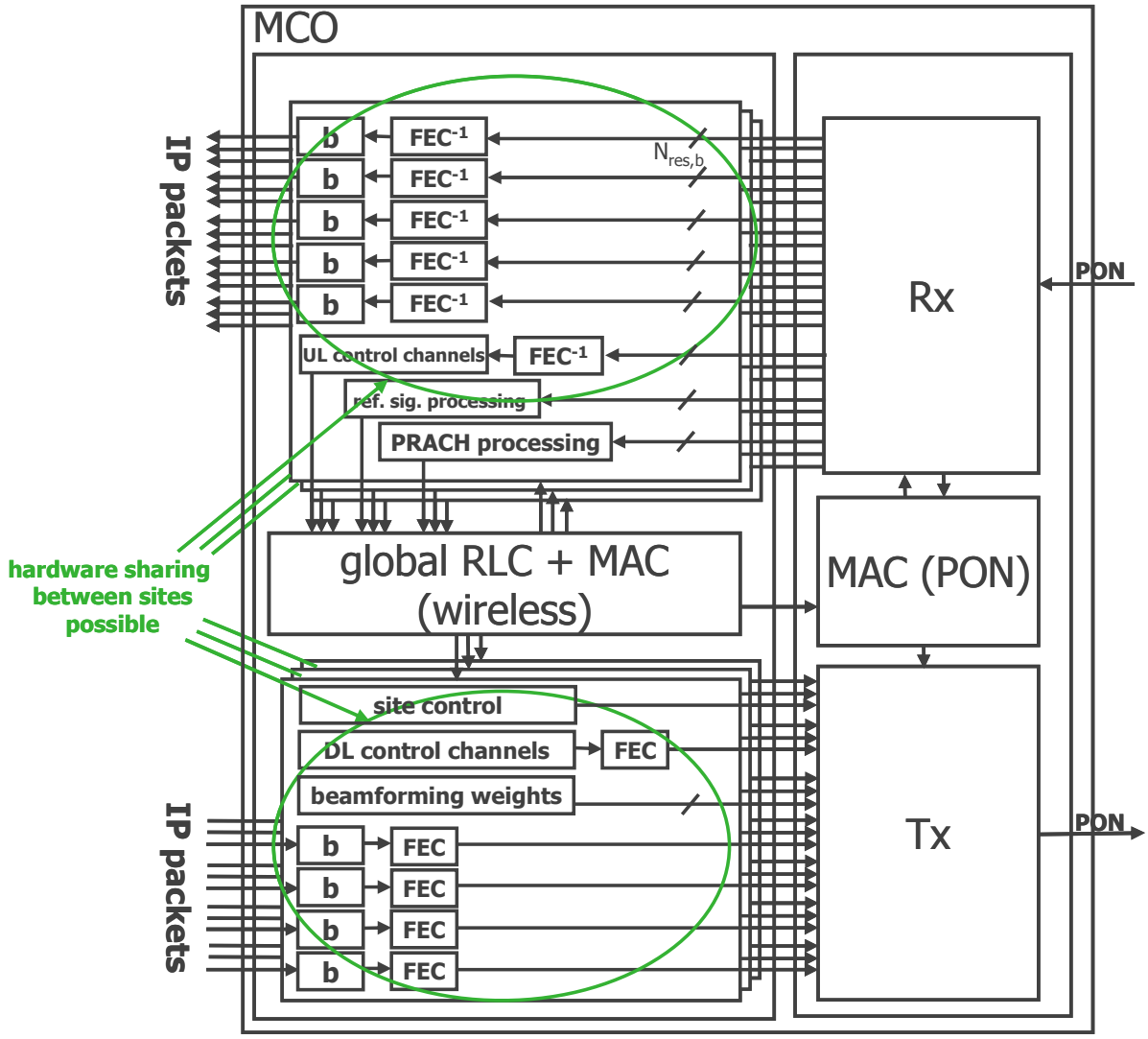

Figure 6: MCO architecture for soft-bit fronthauling (b).

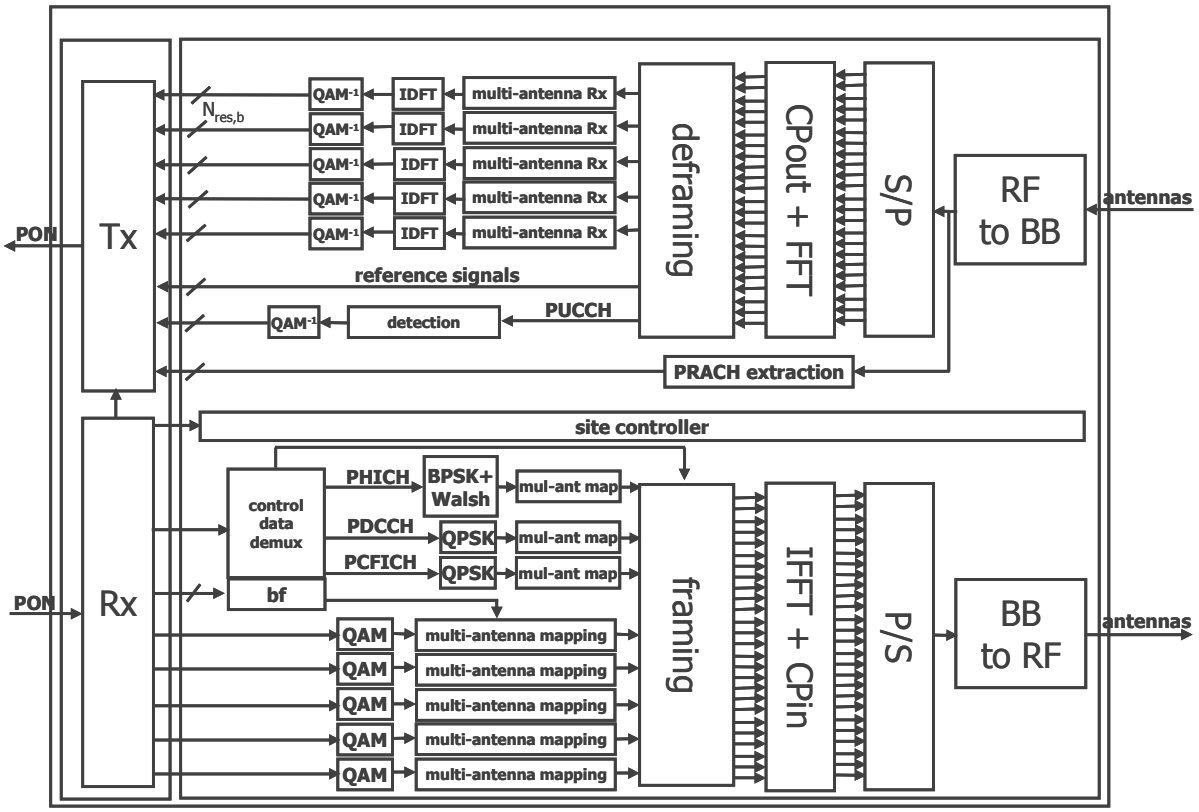

Figure 7: Site architecture for soft-bit fronthauling (b) (not drawn: control inputs to baseband processing elements).

DL (MCO → site):

Incoming IP packets (from the Super Metro Central Office, SMCO) are buffered and FEC (Forward Error Correction) processed (segmentation, encoding, rate matching). DL control includes all standard specific control messages (for LTE: PHICH, PDCCH and PCFICH), site control covers all non-standard specific control messages with which the equipment at the site can be controlled (e.g. SON commands, Self-Organized Networks) and messages needed for signal generation which are not part of the control channels (e.g. beamforming vectors).

The outputs of the FEC blocks and of the site control block are hard bits. So, they directly can be fed into the transmitter (thus, the naming soft-bit backhauling is somewhat out-of-place for the fronthauling of the downlink signals, however, we still stick to this name, as in uplink we still have to transport soft-bits). Obviously the data to be transmitted via the PON is still per user and thus has to be clearly identifiable by the site equipment either implicitly or explicitly via appropriate MAC headers. The MAC controlling the transport via the PON has to take this into account (both for the user data and the control messages). Therefore the wireless MAC/RLC entity has to be able to communicate with the optical MAC. The data fed into the transmitter at a given time instant (e.g. once per Transmission Time Interval (1 ms), TTI) are sharing the LTE sub-frame and thus have to be transmitted conjointly and virtually instantly.

The receiver at the site extracts the bits out of the optical signal and feeds the respective subsequent processing units. The site control commands are fed into the site controller. The DL control channel commands are demultiplexed and the DL control channels (PHICH, PDCCH, PCFICH) are synthesized according to the standard. The user data is QAM modulated and mapped according to respective multi-antenna mode. To do so these elements must have access to the respective burst profiles (part of the PDCCH). These connections are

not drawn within the figure for clarity reasons. As the receiver has to extract relevant information out of the LTE control channels latency is somewhat increased. Then the actual sub-frame is generated (again according to the commands within the control channels), i.e. the bursts and control channels are placed and the reference signals included. Then the OFDM symbol is transformed into time domain. After the insertion of the cyclic prefix and parallel-to-serial conversion the baseband processing is completed and the signal is ready for RF processing.

So, the necessary interfaces between the respective wireless and optical processing units are:

- a connection per user stream with a width of one bit (both within the metro-central office (MCO) and at the site)
- a connection for the DL control commands with a width of one bit (both within the MCO and at the site)
- a connection for the site control messages with a width of one bit (both within the MCO and at the site)
- communication interface between the wireless RLC/MAC unit and the optical MAC (within the MCO)

UL (site → MCO):
First the received wireless signal is converted to baseband. The characteristics of the PRACH significantly diverts from the characteristics of the other uplink channels (much smaller subcarrier spacing and thus much longer symbol length). So, the PRACH symbols have to be extracted and transmitted separately via the PON. The processing regarding the remaining channels (both carrying data and control information) is straightforward: After serial-to-parallel conversion the cyclic prefix is removed. Then the multi-carrier symbol is converted into frequency domain and the user bursts, the reference signals and the PUCCH are extracted out of the sub-frame (to do so these processing elements need access to the control commands within the control channels, these connections are again not drawn due to clarity reasons). The uplink control channel is analyzed and the control commands are extracted (up to the soft-demapping). The same holds for the user bursts. For proper FEC decoding the soft-bits are weighted according to the signal to noise ratio (SNR) the originating subcarrier had been confronted with (i.e. the subcarrier which hat carried the QAM symbol containing the respective bit).

The receiver at the MCO extracts the relevant data and feeds the corresponding processing chains. The outcomes of PRACH processing and channel sounding (with the help of the sounding reference signals) are fed into the MAC for later use (network entry, ranging, multi-user scheduling). Both the control channels and the user streams are decoded and processed. The former are fed into the RLC/MAC unit, the latter are buffered. Once an IP packet is fully received it is forwarded to the SCO.

So, the needed interfaces between the respective blocks are:

- a connection per user stream with a width of $N_{res,b}$ bits (both within the MCO and at the site)
- a connection for the reference signals with a width of $N_{res,b}$ bits (both within the MCO and at the site)
- a connection for the PRACH symbols with a width of $N_{res,b}$ bits (both within the MCO and at the site)
- a connection for the UL control commands with a width of $N_{res,b}$ bits (both within the MCO and at the site)

As highlighted within Figure 6 for some of the processing steps (e.g. FEC encoding) hardware sharing can be applied within the MCO. This is one of the benefits of baseband centralization.

3.2.2. Soft-symbol fronthauling (c)

Soft-symbol fronthauling goes one step further with respect to baseband centralization. Compared to soft-bit fronthauling QAM processing (modulation and demodulation) is done within the main central office in addition.

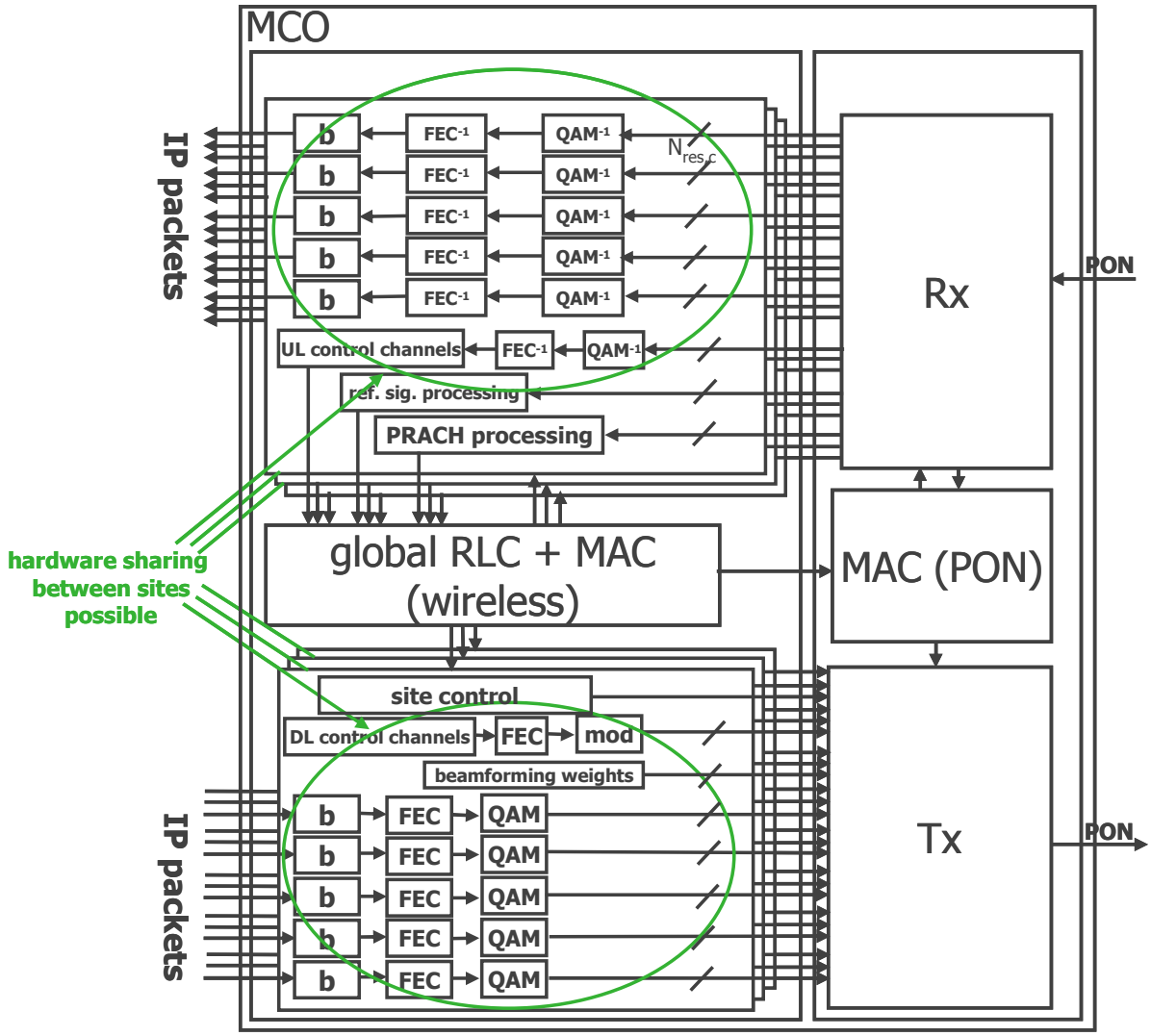

Figure 8: MCO architecture for soft-symbol fronthauling (c).

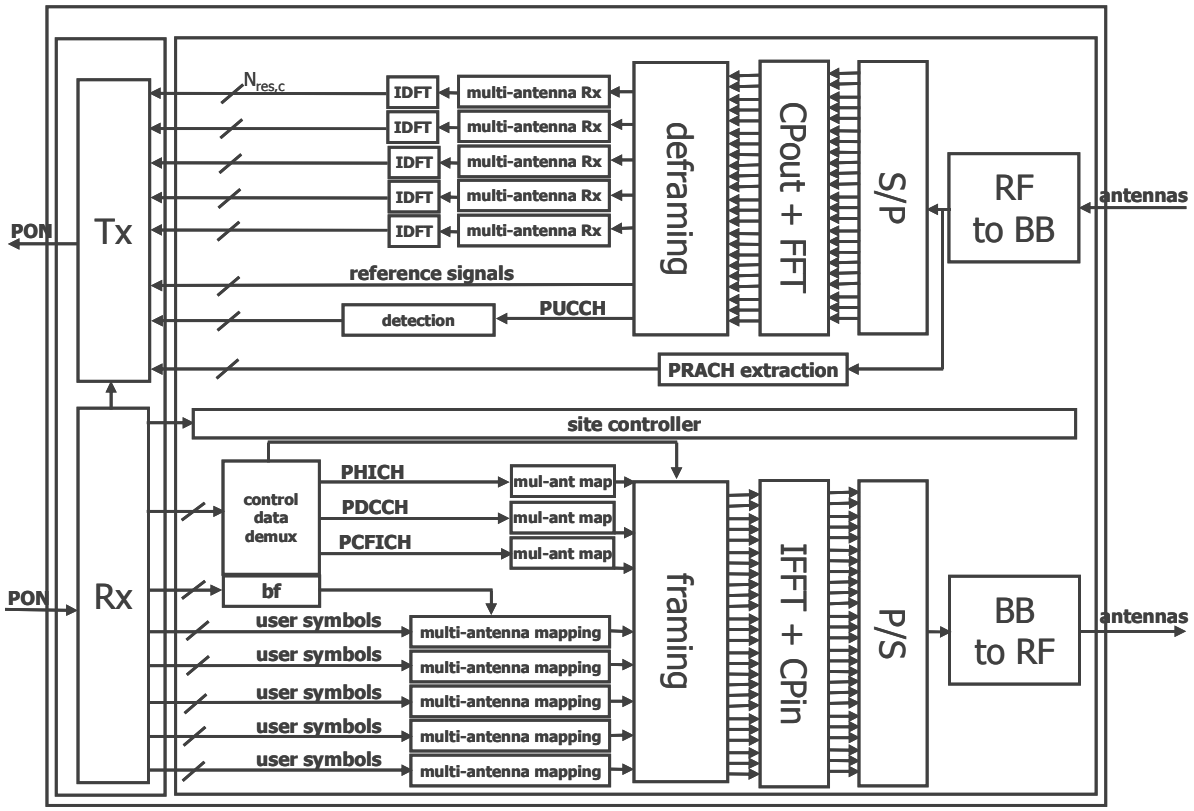

Figure 9: Site architecture for soft-symbol fronthauling (c) (not drawn: control inputs to baseband processing elements).

Processing is similar as it has been described in the former section covering soft-bit fronthauling. Now, beside FEC encoding/decoding QAM modulation/demodulation (according to their burst profiles) is shifted away from the site and into the main central office in addition. Thus, QAM symbols are fed into the optical Tx block in downlink, in uplink binary representations (of the I/Q components of the QAM symbols) are to be transmitted via the PON, as FEC decoding relies on soft inputs (this holds both for the user bursts and the control channels). This variant is not to be favored compared to the others, as no additional binary processing steps (such as FEC for the optical transport) can be applied in downlink and the modulation grade cannot be adapted to the quality of the optical channel. So, in the following we abandon this option. All statements posted within the former section (streams are per user, this has to be taken into account by the optical MAC and the need for instantaneous and conjoint transport, increased latency as the receiver at the site has to extract the relevant control data) are holding here, either. The treatment of the reference signals and PRACH symbols has not changed.

Interface between the wireless baseband units and the optical modem:

- a connection per user stream (DL: QAM symbols, UL: binary representations of noisy and unequalized symbols with a width of $N_{res,c}$ bits)
- a connection for the DL control commands
- a connection for the site control messages with a width of one bit (both within the MCO and at the site)
- communication interface between the wireless RLC/MAC unit and the optical MAC (within the MCO)

- a connection for the reference signals with a width of $N_{res,c}$ bits (both within the MCO and at the site)
- a connection for the PRACH symbols with a width of $N_{res,c}$ bits (both within the MCO and at the site)
- a connection for the UL control commands with a width of $N_{res,c}$ bits (both within the MCO and at the site)

Again hardware sharing can be applied within the MCO.

3.2.3. Burst fronthauling (d)

Burst fronthauling again goes one step further with respect to baseband centralization. Now multi antenna mapping (e.g. beamforming) and multi-antenna reception (e.g. maximum ratio combining) is performed at the main central office.

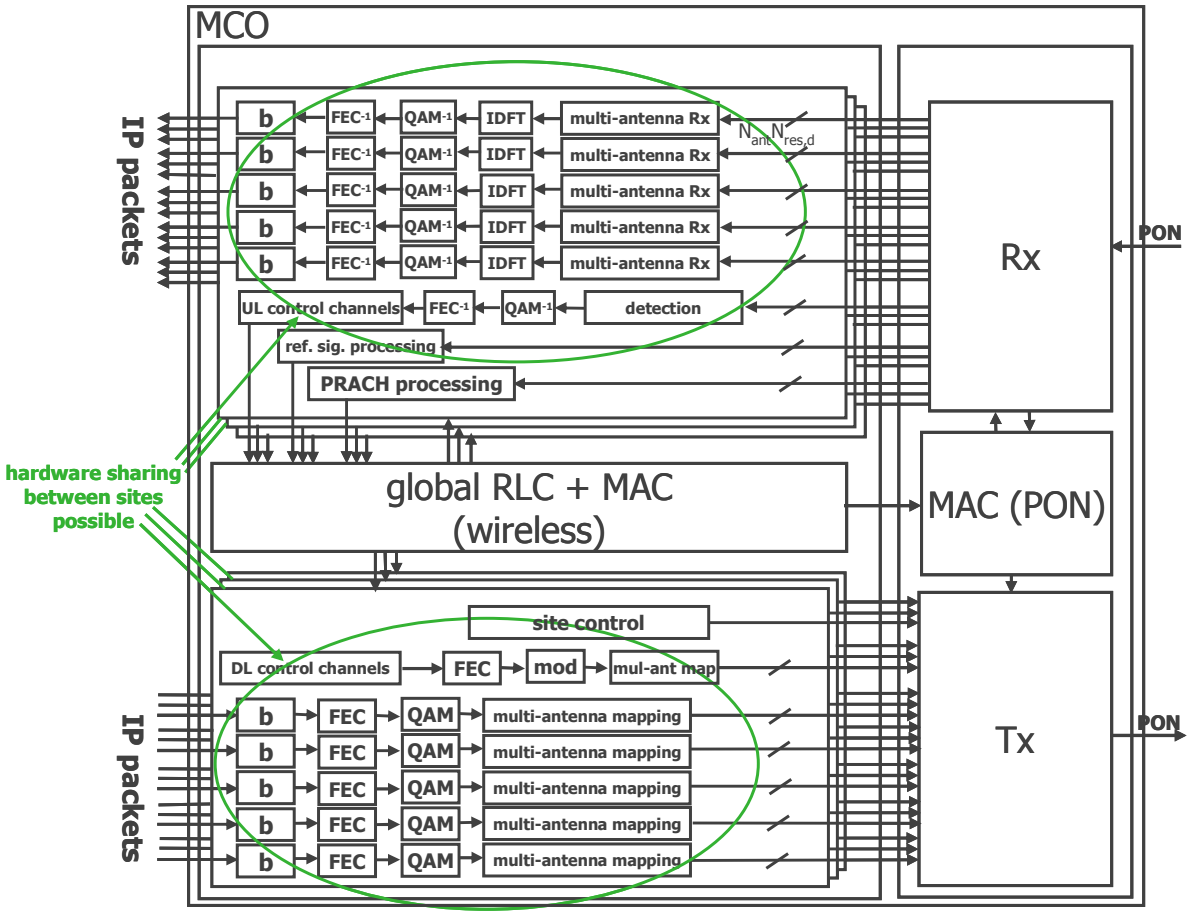

Figure 10: MCO architecture for burst fronthauling (d).

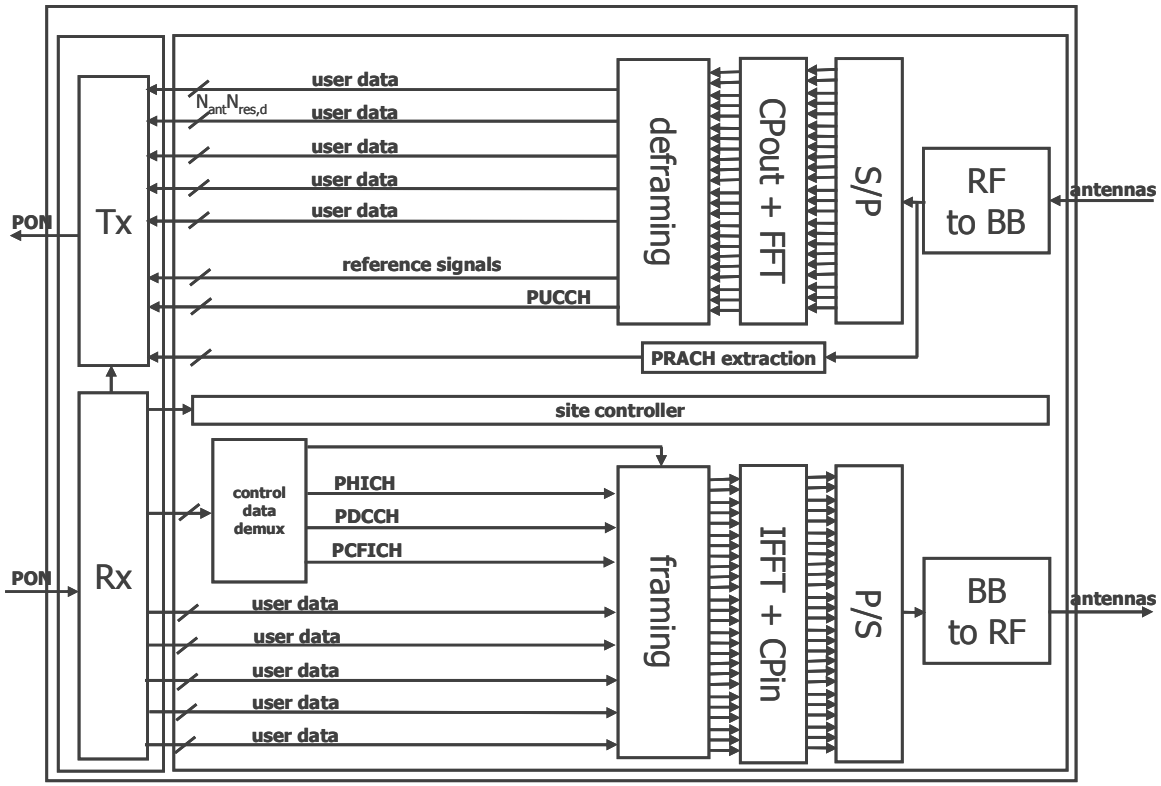

Figure 11: Site architecture for burst fronthauling (d) (not drawn: control inputs to baseband processing elements).

With burst fronthauling – as the name indicates – fully processed user bursts and control channels (i.e. up to multi-antenna mapping), ready for being placed into the sub-frame, are to be transmitted via the PON. Input to the optical Tx blocks are binary representations of the complex symbols to be transmitted via the air (DL) and been transmitted via the air (UL), respectively. Again, all statements posted within the former sections (streams are per user, this has to be taken into account by the optical MAC and the need for instantaneous and conjoint transport, increased latency as the receiver at the site has to extract the control data) are holding here, either, and the treatment of the reference signals and PRACH symbols has not changed.

Interface between the wireless baseband units and the optical modem:

- a connection per user stream with a width of $N_{res,d}$ bits per antenna stream (binary representations of possibly (if beamforming is applied) complex weighted (DL) symbols and noisy/unequalized (UL) symbols, respectively)
- a connection for the DL control commands with a width of $N_{res,d}$ bits
- a connection for the site control messages with a width of one bit (both within the MCO and at the site)
- communication interface between the wireless RLC/MAC unit and the optical MAC (within the MCO)
- a connection for the reference signals with a width of N_{res} bits per antenna stream (both within the MCO and at the site)
- a connection for the PRACH symbols with a width of N_{res} bits per antenna stream (both within the MCO and at the site)
- a connection for the UL control commands with a width of N_{res} bits per antenna stream (both within the MCO and at the site)

Hardware sharing can be applied within the MCO in this case even to a higher extend.

For downlink we abandon this version, as it does not make sense to do multi-antenna mapping (e.g. beamforming) followed by A/D-conversion. It is much more efficient to transport the bits to be transported via the air together with the respective commands (burst profiles and beamforming vector) as it is done with soft-bit fronthauling.

3.2.4. Frame fronthauling (e)

Finally frame fronthauling is the last option we have with distributed baseband processing at the main central office and at the site. Here, multiplexing/demultiplexing of user bursts and control channels is performed at the central office.

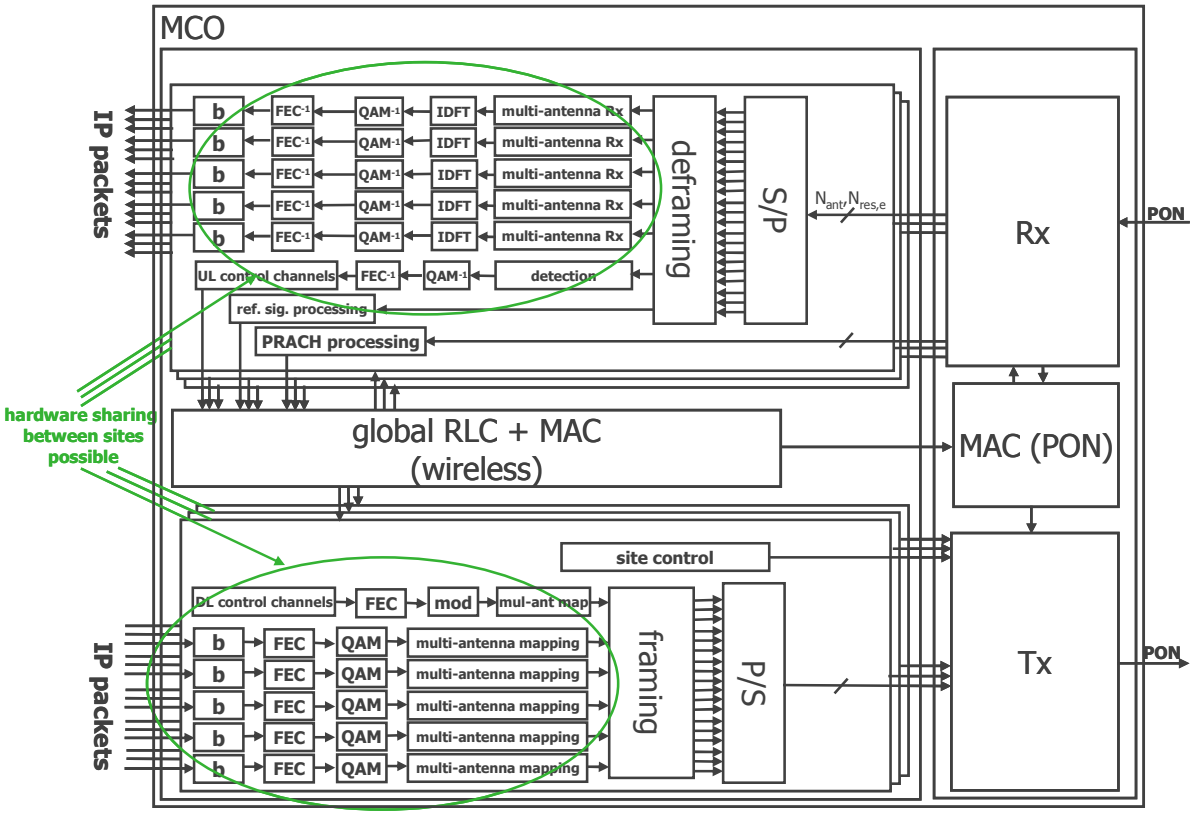

Figure 12: MCO architecture for frame fronthauling (e).

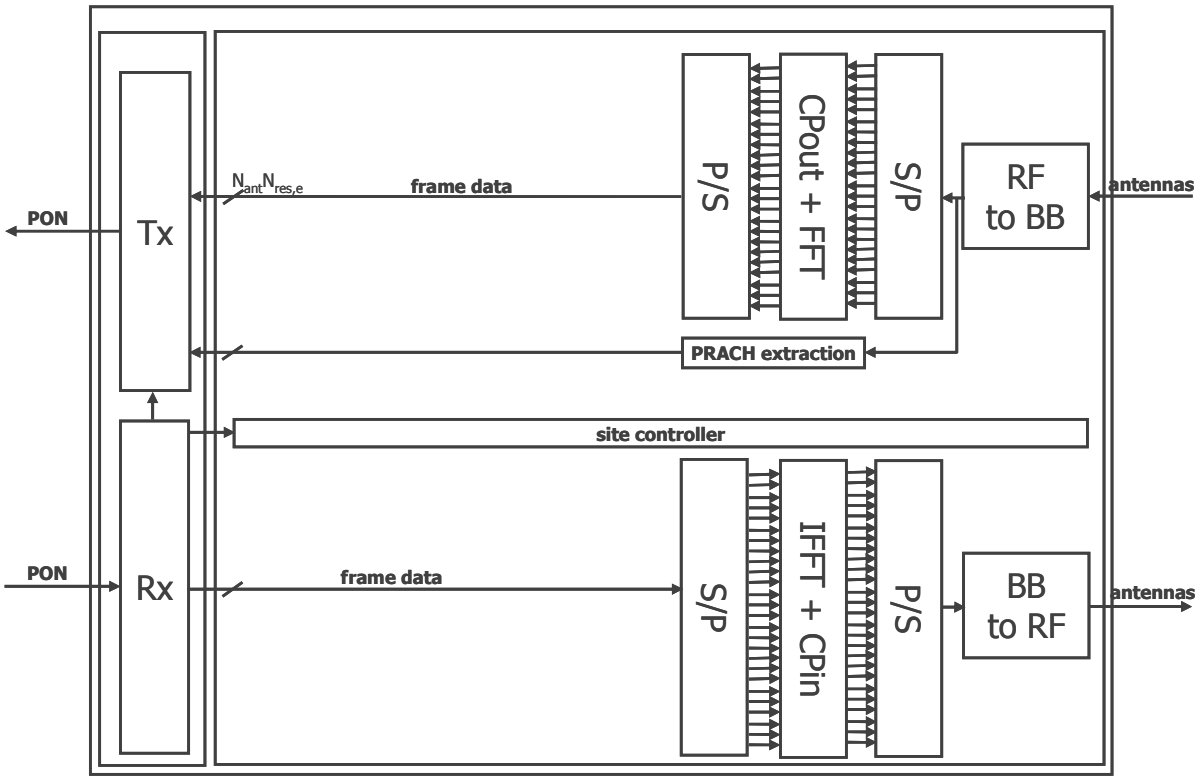

Figure 13: Site architecture for frame fronthauling (e).

With frame fronthauling completely assembled sub-frames (including user bursts, control channels, reference signals) are to be transmitted via the PON. Input to the optical Tx blocks are binary representations of the symbols carried by the sub-carriers to be transmitted via the air (DL) and been transmitted via the air (UL), respectively. Now the optical transport no more has to handle a stream per wireless user. Again, once a sub-frame is assembled/received and fed into the optical transport units, it has to be transmitted via the PON instantly. PRACH handling is the same as presented in the former descriptions.

- a single connection for the frame data (both user data and control data) with a width of $N_{res,e}$ bits per antenna stream (binary representations of possibly (if beamforming is applied) complex weighted symbols (DL) and noisy/unequalized (UL) symbols, respectively)
- a connection for the site control messages with a width of one bit (both within the MCO and at the site)
- communication interface between the wireless RLC/MAC unit and the optical MAC (within the MCO)
- a connection for the PRACH symbols with a width of $N_{res,e}$ bits per antenna stream (both within the MCO and at the site)

PRACH processing:
With respect to PRACH processing (network entry, ranging) we have three options:

- PRACH extraction at the site and transport to the central office, PRACH processing (e.g. offset measurements) at the central office, generation of the random access response message within the central office (the figures in the preceding sections display this option)

- PRACH extraction and processing at the site, transport of measurement results to the central office, generation of the random access message within the central office
- PRACH extraction and processing at the site, generation of the random access response message at the site (not applicable with frame fronthauling)

The first option requires the most transport resources on the PON and the least processing power at the site. The second option requires more processing power at the site (to perform the measurements) and some resources on the PON (to transport the measurements, e.g. timing and frequency offsets). The last option requires no resources on the PON (as the MCO is bypassed) but the most processing power at the site (to perform the measurements and generate the random access response message). With respect to latency the last option outclasses the former two, as the delay due to the transport via the PON is omitted (in [2] we have introduced the timings connected to network entry). The disadvantage of the third option is the loss of the global view with respect to users entering the network. Additionally, the third option contradicts to the centralization of the MAC and is to be abandoned.

The tasks connected to PRACH processing are beyond the scope of this deliverable. The interested reader is referred to [3].

3.3. CPRI FRONTHAULING (F)

In contrast to the above approaches the CPRI fronthauling provides for complete MAC and baseband centralization. Figure 14 and Figure 15 demonstrate the MCO and site configuration respectively.

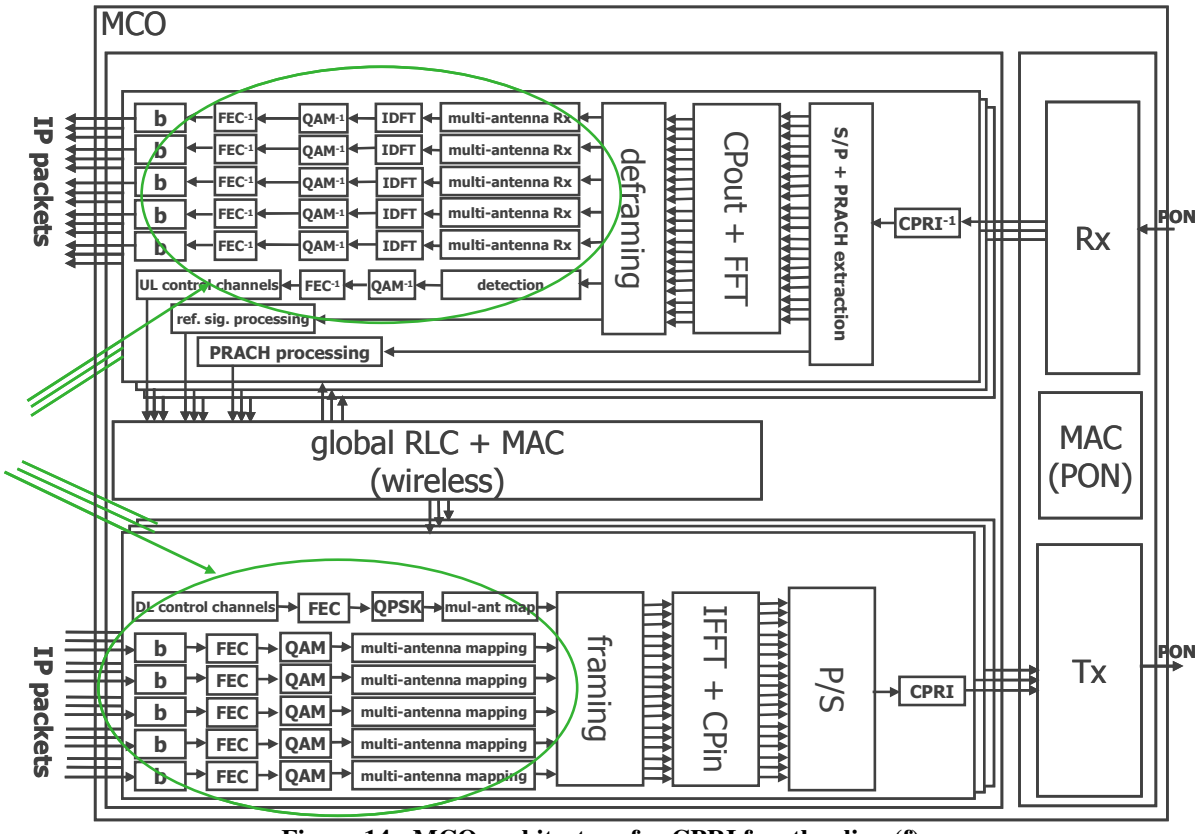

Figure 14: MCO architecture for CPRI fronthauling (f).

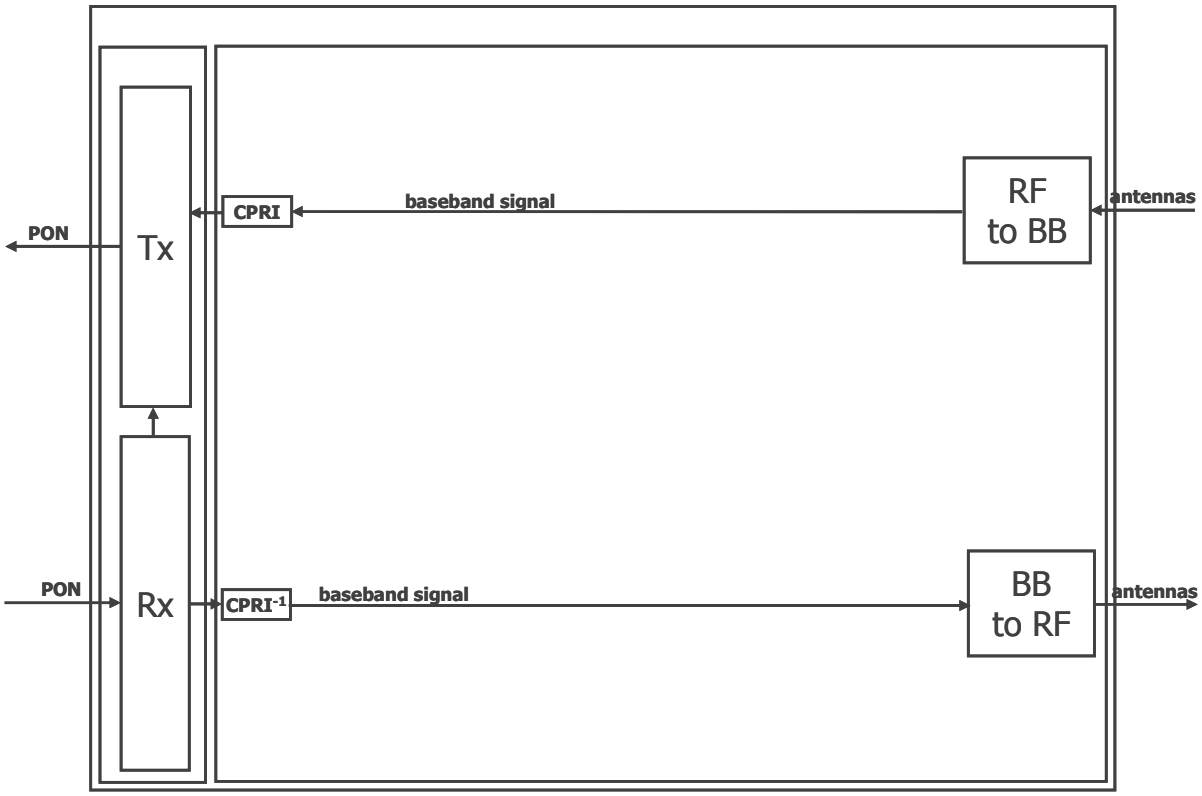

Figure 15: Site architecture for CPRI fronthauling (f).

At the MCO, after baseband processing the signal is CPRI encoded prior to transmission over the PON downstream (via WDM). The CPRI encoding and operation principles as well as latency requirements are described in D5.1 [5] and D5.2 [2]. No dedicated site control messages can be transmitted separately as with the former options. At the site the baseband signal gets retrieved out of the CPRI stream and processed for transmission via the air.

In upstream, as shown in Figure 15, the received signal (at the site) gets converted to baseband, CPRI encoded and transmitted via the PON (via WDM). The MCO retrieves the baseband signal out of the CPRI stream and performs the respective wireless baseband processing steps.

Significantly, the data fed into the transmitter at the MCO and at the site at a given time instant have to be transmitted instantaneously on the PON in order to meet latency requirements. Therefore, no buffering is allowed.

In addition, similar as before, the hardware sharing is still possible at the MCO.

Finally, interface requirement between the wireless baseband and PON is given below:

- a single connection for the CPRI signal at the MCO and the site (both for UL and DL)

3.4. RoF (G)

Similarly to CPRI, the analog radio over fibre (RoF) schemes offer a solution for the complete centralisation of wireless equipment enabling link transparency and lower transmission bandwidth per base station compared to digital-over-fibre approaches (as described later in

the deliverable). Following the same trend as before, the MCO and site configurations are shown in Figure 16 and Figure 17 respectively.

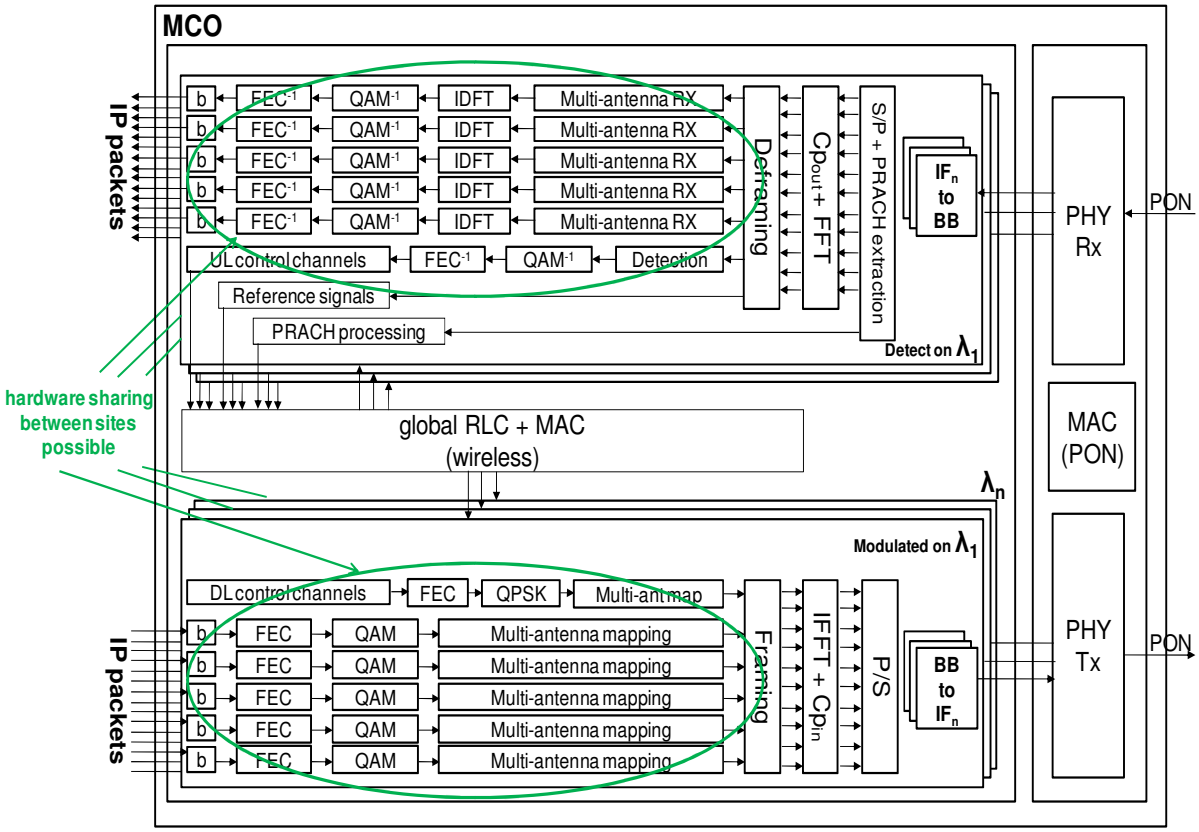

Figure 16: MCO architecture for RoF fronthauling (g).

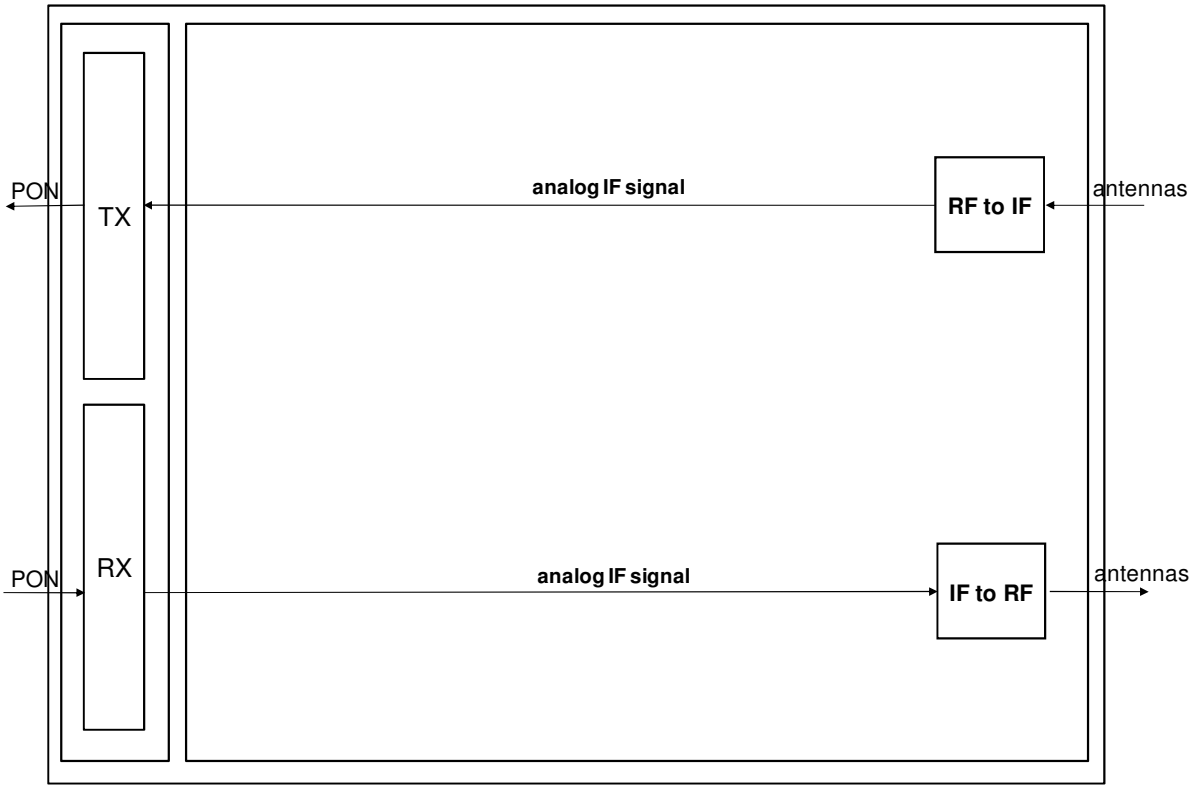

Figure 17: Site architecture for RoF fronthauling (g).

In downstream, at the MCO, after baseband processing the resulting signals are upconverted to an analog intermediate frequency (IF) prior to transmission over the PON (via wavelength division multiplexing (WDM)). Due to analog nature of the link the frequency division multiplexing (FDM) of IF frequencies and multi-wavelength (i.e. WDM/FDM approach) are used in order to address individual antenna ports and sites respectively. The IF is selected due to ease of implementation and low distortion on the PON. At the site the received FDM window is processed (i.e. IF to RF conversion) for transmission via the air channel.

For upstream, the received signal at the site gets frequency shifted to an IF frequency and transmitted via the PON using WDM. The MCO retrieves the baseband signal by downshifting and performs the respective wireless baseband processing steps. Similarly to downstream, mainly due to frequency reuse of 1, the FDM window is transmitted in upstream as well.

Significantly, it is important to mention that WDM/FDM is also utilised since it reduces the effect of sharing the power budget between different sites as it is extensively described in Sections 4 and 5.

In addition, as with CPRI, the analog signal fed into the transmitter at the MCO and at the site at a given time instant has to be transmitted instantaneously on the PON in order to meet the latency requirements.

Finally, a single analog interface between wireless and PON is required at both MCO and site for DL and UL.

4. Bandwidth requirements on the PON

As already pointed out in D2.2 [2] the required rate on the PON per eNB depends on the chosen interfacing point. In the following we will follow up on this and provide quantitative measures.

4.1. DIGITAL FRONTHAULING

The least amount of PON resources is needed in the case of IP backhauling (option (a)):

$$R_a = R_{IP} \tag{1}$$

The needed rate on the PON simply equals the amount of granted IP rates to the mobile users by the wireless base station. This measure is highly varying in time as the mix of users and accessed services varies. Statistical multiplexing gains can be achieved by exploiting the point to multi-point nature of the PON.

IP packets vary in size and are typically not matching the amount of resources granted to a single user within the respective wireless frame. So the first baseband processing step in downlink is packet concatenation/segmentation. These packets are arranged to so-called FEC blocks and turbo encoded. The amount of overhead depends on the chosen modulation and coding scheme of user i (decided by the scheduling algorithm based on the channel quality the respective user has to deal with). So compared to option (a) the amount of resources needed on the PON is increased due to the FEC overhead ($R_{FEC,i}$), if I user are scheduled into the sub-frame:

$$R_b = \sum_{i=1}^{I} N_{res,i,b} \frac{R_{0,i}}{R_{FEC,i}} \tag{2}$$

$R_{0,i}$ is the instantaneous raw bit rate of user i being transmitted via the air including the HARQ overhead and spatial multiplexing gains, but excluding the FEC overhead (here we slightly differ from the approach used in D2.2 [2]). In downlink the outputs of the FEC encoder are to be transmitted via the PON. Naturally those are hard-bits and can thus be directly fed into the optical transmitter ($N_{res,i,b} = 1$). In uplink this is different. Here, soft-bits are to be transmitted via the PON, as the FEC decoder relies on statistical properties. So, to reliably transport the soft-bits via the PON they have to be represented by $N_{res,i,b}$ Bits. This rate naturally varies in time as the user mix allocated to the actual wireless resources is different from one TTI to the next (upper bounded due to the amount of subcarrier resources).

In the case of burst fronthauling the required rate on the PON can be calculated as follows:

$$R_d = \sum_{i=1}^{I} 2N_{ant,i,d} N_{res,i,d} \frac{R_{0,i}}{R_{FEC,i} N_{q,i}} \tag{3}$$

Now, multi-antenna mapping is performed within the central office. If for the transport of the data of user i beamforming or transmit diversity is applied, the required rate on the PON is

increased according to the number of used antennas ($N_{ant,i}$). This does not hold if spatial multiplexing is used. In that case a higher $R_{0,i}$ is achieved. $N_{res,i,d}$ again accounts for the A/D conversion of the symbols to be transmitted. Now, in downlink the symbols to be transported via the PON may be weighted with a complex factor (e.g. beamforming coefficients). So, directly modulating those symbols onto the optical subcarriers is not practical anymore. Instead we have to represent them by $N_{res,i,d}$ Bits both in uplink and in downlink.

With frame fronthauling the user multiplexing is performed within the central office. This, the streams to be transported via the PON are no more per user (visible through the absence of the index i):

$$R_e = 2N_{ant,e}N_{res,e}\frac{N_{scrr}N_{symb}}{T_{subframe}} \quad (4)$$

$N_{ant,e}$ reflects the number of antenna streams generated for the given sub-frame, $N_{res,e}$ the applied resolution. N_{scrr} (= 600 for 10 MHz bandwidth) is the number of modulated subcarriers (both data and control signals and reference symbols) per multi-carrier symbol, N_{symb} (= 14 in 1 ms) the number of multi-carrier symbols within the considered time span $T_{subframe}$ (LTE: 1 ms).

Finally with CPRI fronthauling we have:

$$R_f = 2N_{ant,f}N_sN_{res,f}N_{ovhd}N_{8B10B} \quad (5)$$

Again, $N_{ant,f}$ reflects the number of antenna streams, $N_{res,f}$ the applied resolution. N_s (LTE: 15.36 MHz for a channel width of 10 MHz) is the sampling rate, N_{ovhd} (= 16/15) the CPRI control overhead and N_{8B10B} (= 10/8) the overhead due to the 8B/10B coding.

Having measures for all variants of digital fronthauling, we need to assess the parameters, which we not yet have given quantities for, to be able to evaluate them. Therefore, link-level and system-level simulations have been performed presented within the following chapters.

4.2. ASSESSMENT OF THE PARAMETERS

System-level simulations cover multi-user/multi-cell aspects. The average signal to interference and noise ratio (SINR) a user observes at a given position within the cell is their output, typically. Using these measurements $R_{0,i}$ R_{FEC} and N_q can be calculated.
System-level simulations are rather abstract with respect to baseband processing not to have overflowing simulation run times. So, the impact of quantization (N_{res}) cannot be assessed via system-level simulations. Instead link-level simulations covering all baseband processing steps in detail but neglecting multi-user aspects have been used, here.

Before heading to the actual assessment of the parameters the simulation frameworks are covered in the following.

Figure 18 depicts the cell-deployment simulated by the system-level simulator. The dark blue dots are the locations of the sites covering 3 cells each. Interfering cells are light blue, the cell under investigation is depicted in orange.

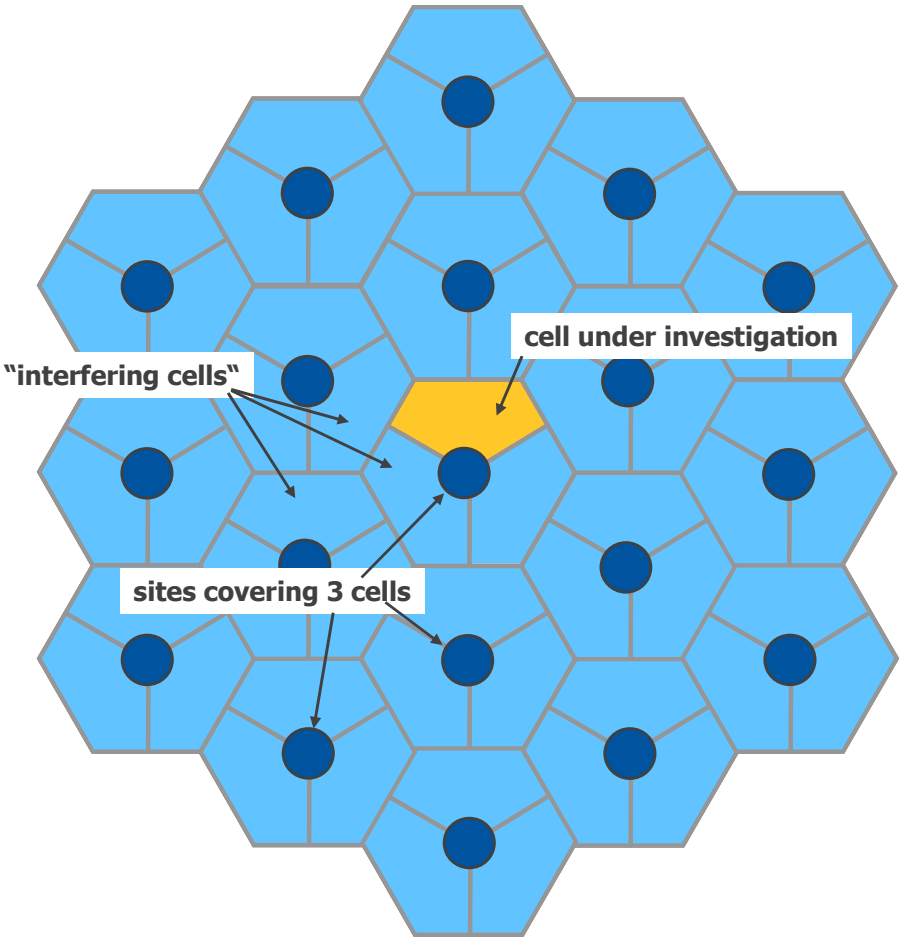

Figure 18: Cell deployment used within the system-level simulations.

At the beginning of each drop the user equipments (UEs) are randomly placed into each interfering cell and the available transmission resources are evenly distributed. We apply frequency re-use 1, thus, each cell is served via the same carrier frequency. Once the placement is ready, the actual signal transmissions are carried out. Then, the SINR at each point of a predefined grid within the cell under investigation is calculated. At the end the outcomes of all drops are averaged. Table 1 summarizes the simulation framework.

Table 1: Parameters of the system-level simulations:

Bandwidth	10 MHz @ 2 GHz
# of modulated subcarriers per multi-carrier symbol	600, 15 kHz spacing (LTE)
# of simulated sites	19
# of cells per site	3
site distance	500 m
channel model	SCME, urban macro angular spread: 15°
path-loss model	Cost-Hata
height site antenna	32 m
height UE antenna	1.5 m
# of UEs per cell	10
indoor/outdoor ratio	1/2
wall penetration loss	20 dB

For downlink we have investigated both a scenario without (scenario I) and a scenario with beamforming (scenario II) [1]. No dedicated beam-coordination has been applied.

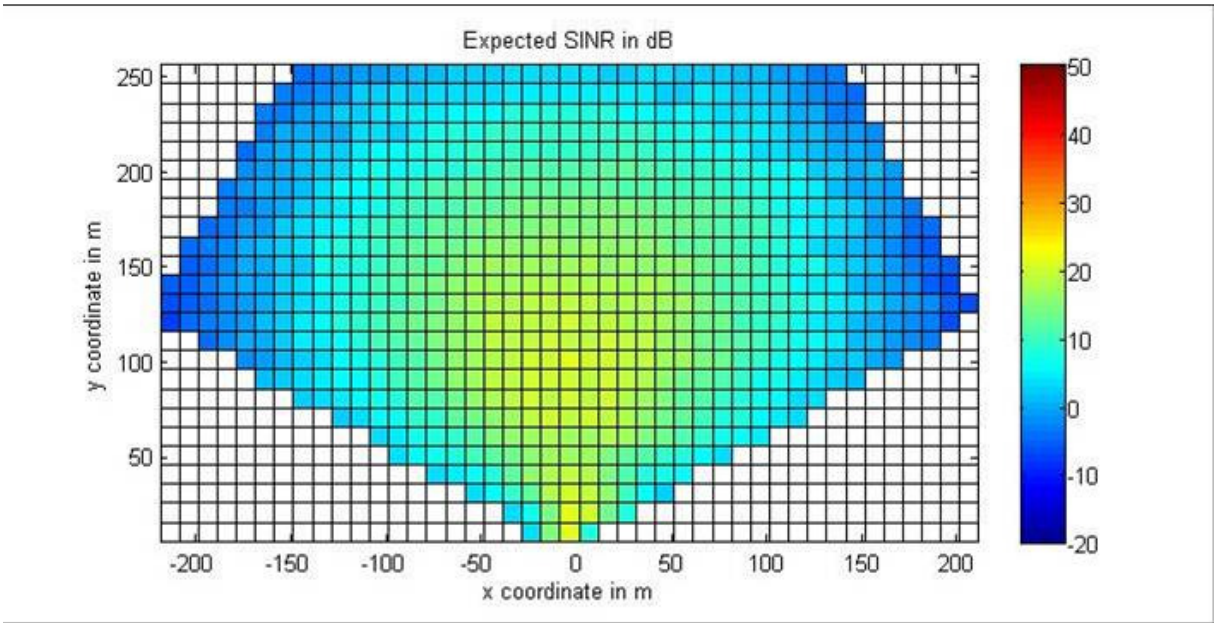

Figure 19: SINR users are experiencing with scenario I.

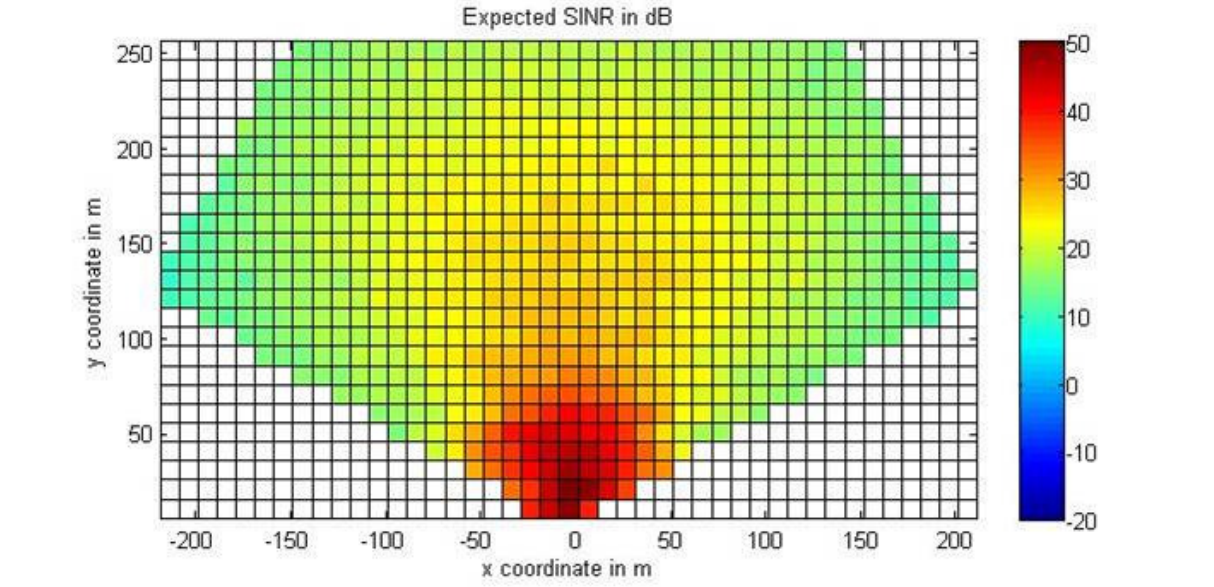

Figure 20: SINR users are experiencing with scenario II.

The overall capacity gain and the quality improvement at the cell edge due to the use of beamforming is apparent. With the help of the SINR grids we can calculate the probabilities for all available modulation and coding schemes (MCS) to be chosen. To do so we have to decide for a block error rate (BLER) we want to achieve at least. Then, for each grid point we determine the MCS with the highest capacity that still performs better than the chosen BLER. Once all grid points are evaluated we can calculate the probability of occurrence of each MCS for the given scenario. Table 1 summarizes the outcomes. The third column includes the SINR ranges for which the respective MCS is picked (we have used a BLER of 10 %, this is a typical choice, if the system applies HARQ). The fourth and the fifth columns contain the probabilities of occurrence for the two scenarios.

Table 2: Probability of occurrence for the available MCS (DL):

index	MCS (R=code rate)	SINR range [dB]	P[MCS], (I)	P[MCS], (II)
1	QPSK, R=1/9	x<-7	0.1867	0.0161
2	QPSK, R=1/6	-7<x<-3	0.0251	0.0036
3	QPSK, R=0.21	-3<x<-2.2	0.0267	0.0043
4	QPSK, R=1/4	-2.2<x<-1.4	0.036	0.0066
5	QPSK, R=1/3	-1.4<x<-0.4	0.0384	0.0081
6	QPSK, R=0.42	-0.4<x<0.8	0.0397	0.0098
7	QPSK, R=1/2	0.8<x<1.8	0.0402	0.0116
8	QPSK, R=0.58	1.8<x<2.8	0.0419	0.0139
9	QPSK, R=2/3	2.8<x<3.8	0.0414	0.0161
10	QPSK, R=0.73	3.8<x<4.8	0.0415	0.0186
11	16 QAM, R=0.43	4.8<x<5.8	0.0177	0.0083
12	16 QAM, R=0.46	5.8<x<6.2	0.0243	0.0139
13	16 QAM, R=1/2	6.2<x<6.8	0.033	0.0197
14	16 QAM, R=0.54	7.6<x<8.2	0.0244	0.0153
15	16 QAM, R=0.58	8.2<x<8.6	0.0161	0.0112
16	16 QAM, R=0.61	8.6<x<9.4	0.0313	0.0233
17	16 QAM, R=2/3	9.4<x<10.6	0.0453	0.0399
18	16 QAM, R=0.73	10.6<x<11.6	0.0366	0.0359
19	16 QAM, R=4/5	11.6<x<12.8	0.0419	0.0459
20	64 QAM, R=0.58	12.8<x<13.6	0.0267	0.0323
21	64 QAM, R=0.62	13.6<x<14.4	0.0245	0.0337
22	64 QAM, R=2/3	14.4<x<15	0.0177	0.0264
23	64 QAM, R=0.70	15<x<15.8	0.0227	0.0362
24	64 QAM, R=0.74	15.8<x<16.8	0.025	0.0449
25	64 QAM, R=4/5	16.8<x<17.8	0.0225	0.0457
26	64 QAM, R=0.85	17.8<x<19	0.0224	0.0544
27	64 QAM, R=0.90	19<x	0.0502	0.4043

Figure 21 depicts the results graphically. Again the gain through the use of beamforming, even if not in a coordinated manner, is apparent. Without beamforming almost 20 % (the ones located at the cell edges) of the users are stuck with the MCS delivering the lowest rate (QPSK, 1/9). With beamforming on the other side more than 40 % of the users can apply the MCS delivering the highest rate (64 QAM, 9/10).

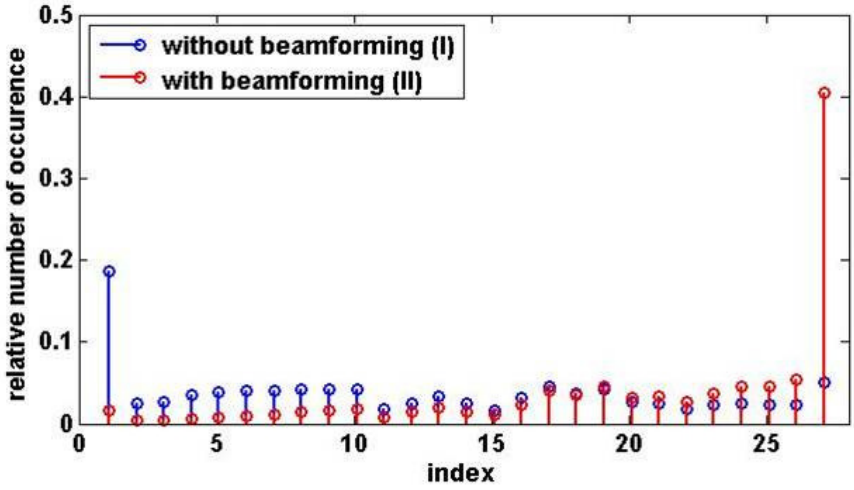

Figure 21: Relative number of occurrence for the available MCS (DL).

For uplink we have equipped the basestations with two (scenario I) and four (scenario II) receiving antennas. The received replicas are combined following the maximum ratio principle. Again, we use a target BLER of 10%. The results for the uplink scenarios can be found in Table 3:

Table 3: Probability of occurrence for the available MCS (UL):

index	MCS (R=code rate)	SINR range [dB]	P[MCS], (I)	P[MCS], (II)
1	QPSK, R=1/9	x<-7	0.0081	0.0022
2	QPSK, R=1/6	-7<x<-3	0.01	0.0034
3	QPSK, R=0.21	-3<x<-2.2	0.0045	0.002
4	QPSK, R=1/4	-2.2<x<-1.4	0.0106	0.0036
5	QPSK, R=1/3	-1.4<x<-0.4	0.0186	0.0068
6	QPSK, R=0.42	-0.4<x<0.8	0.025	0.0101
7	QPSK, R=1/2	0.8<x<1.8	0.0311	0.0132
8	QPSK, R=0.58	1.8<x<2.8	0.0398	0.0185
9	QPSK, R=2/3	2.8<x<3.8	0.048	0.0246
10	QPSK, R=0.73	3.8<x<4.8	0.0509	0.0301
11	16 QAM, R=0.43	4.8<x<5.8	0.0276	0.0163
12	16 QAM, R=0.46	5.8<x<6.2	0.0321	0.0198
13	16 QAM, R=1/2	6.2<x<6.8	0.0459	0.0304
14	16 QAM, R=0.54	7.6<x<8.2	0.0482	0.0335
15	16 QAM, R=0.58	8.2<x<8.6	0.0442	0.0329
16	16 QAM, R=0.61	8.6<x<9.4	0.0608	0.0483
17	16 QAM, R=2/3	9.4<x<10.6	0.0904	0.0802
18	16 QAM, R=0.73	10.6<x<11.6	0.0901	0.0907
19	16 QAM, R=4/5	11.6<x<12.8	0.077	0.0885
20	64 QAM, R=0.58	12.8<x<13.6	0.0406	0.0519
21	64 QAM, R=0.62	13.6<x<14.4	0.0401	0.0565
22	64 QAM, R=2/3	14.4<x<15	0.0355	0.0554
23	64 QAM, R=0.70	15<x<15.8	0.0332	0.0576
24	64 QAM, R=0.74	15.8<x<16.8	0.0318	0.062
25	64 QAM, R=4/5	16.8<x<17.8	0.0235	0.053
26	64 QAM, R=0.85	17.8<x<19	0.0165	0.0442
27	64 QAM, R=0.90	19<x	0.0159	0.0642

The gain through the use of four antennas instead of two is visible through the shift to higher MCS:

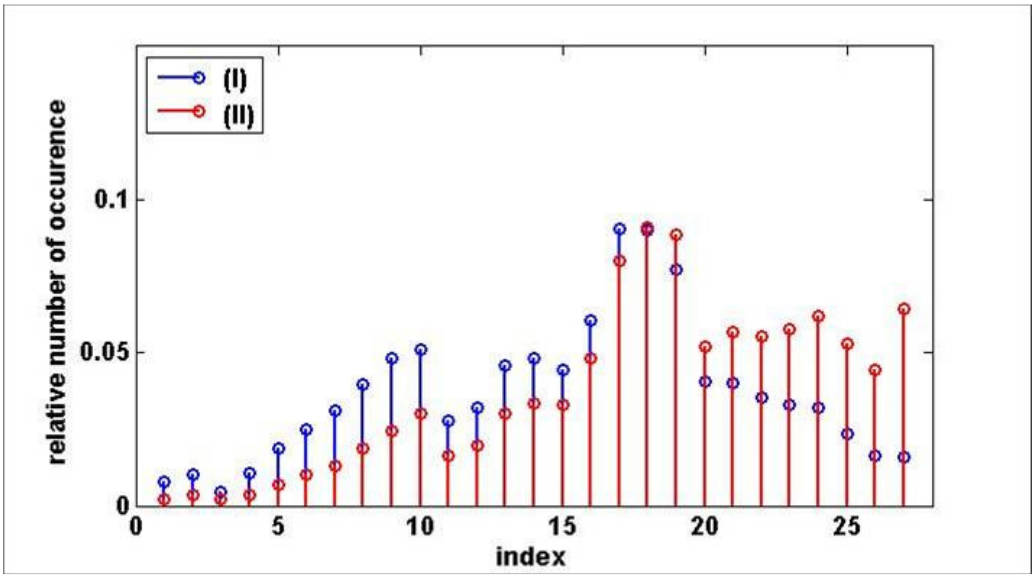

Figure 22: Relative number of occurrence for the available MCS (UL).

With the help of these results $R_{0,i}$, R_{FEC} and N_q can be calculated.

4.2.1. Representative user rates ($R_{0,i}$), code rates ($R_{FEC,i}$) and modulation orders ($N_{q,i}$)

Now that we have the probabilities for the available MCS to be chosen, we have the tools to generate the expectation values $E[R_{FEC,i}]$ and $E[N_{q,i}]$. The average raw bit-rate $E[R_{0,i}]$ naturally depends on the load factor of the cell in addition (i.e. the fraction of resources used for transmission):

Table 4: expectation values (raw bit-rate, FEC overhead, number of bits per QAM symbol)

	$E[R_{0,i}]$, full load	$E[R_{FEC,i}]$	$E[N_{q,i}]$
scenario (II), DL	25.3 Mbit/s	0.75	5.14
scenario (II), UL	17.9 Mbits/s	0.68	4.66

However, we are not only interested in the expectation values, but in addition we want to get aware of the statistical characteristics of the occurring rates (R_b, R_c and R_d), e.g. to be able to assess the gains through statistical multiplexing (covered in a later deliverable). Therefore we drop x users into the cell at random positions. With the help of the grid of SINRs we have gained through the system-level simulations, we can determine the MCS these users are able to use during this drop. To assess the rates per user and the overall rates for the given sub-frame, we have to decide for the amount of resources each user gets. Therefore, we have divided the available resources into y equal shares and allocated each of the x users one share. This way we can evaluate cases with full load (y=x) and cases where the cell is in not in full-buffer mode (x<y). The load factor is defined as follows:

$$L = \frac{x}{y} 100 \quad [\%] \tag{6}$$

The actual results are gathered in a later section.

4.2.2. N_{ant}

Both in downlink (for beamforming) and in uplink (for receive diversity: maximum ration combining, MRC) we equip the basestations with 4 antennas. Thus we have $N_{ant} = 4$ in any case.

4.2.3. N_{res}

The resolution we apply for the binary representation of the bits/symbols highly affects the bandwidth needs on the PON. Thus, we have to assess the lowest resolution we can apply without having performance losses (i.e. the required average SNR to achieve a BER of 1% does not increase). To do so we have performed link-level simulations. The relevant parameters of the simulation framework are as follows:

Table 5: simulation framework

subcarrier modulation	QPSK, 64 QAM
coding scheme	CTC, coderate 1/2, 4 iterations
channel model	Ped B, 3 km/h

To be independent on pilot placements and estimation schemes we have assumed perfect synchronization and ideal channel knowledge. Transmitter and receiver (regarding the feeder link) are placed back2back, thus, no bit errors are introduced by the PON (the impact of bit errors occurring on the PON will be covered later in this deliverable). The wireless channel is modelled according to the ITU channel model PedB with a UE speed of 3 km/h. The following figure depicts the fading behaviour of the absolute value of the subcarrier channel gain normalized to its average (following a Rayleigh distribution):

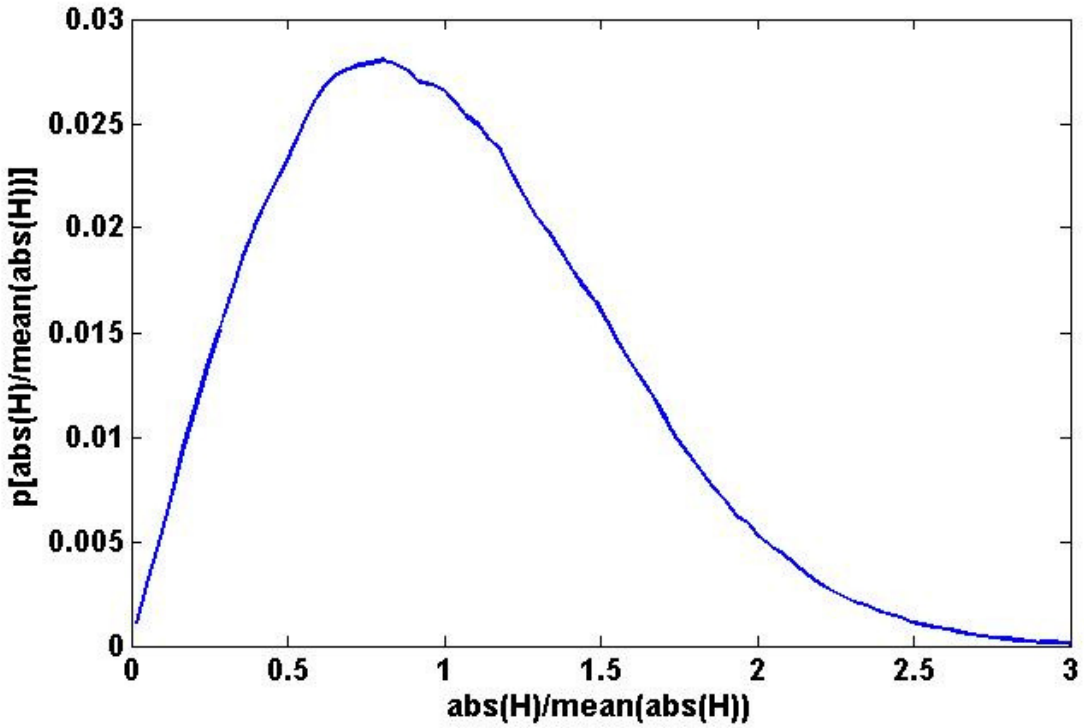

Figure 23: Probability density function of the absolute value of the channel gain H.

No dedicated power control and no frequency selective scheduling is applied. So, the range of channel qualities the user symbols is confronted with is somewhat wider than with power control and/or frequency selective scheduling.
Outcome of the simulations are BER curves depending on the SNR for various clipping values (following the principle set and keep). The clipping value is set in that way that a given relative number of samples monitored over a long period (this design parameter is called sample coverage ratio in the following) is below the threshold (as described in D5.1 [5]). With the help of the BER curves the required SNR to achieve a given error ratio (1%) can be assessed. This way the sensibility to variations of the clipping and the least possible resolution can be determined. We can expect two effects:

- with increasing dynamic range quantisation noise increases, increasing the required average SNR
- once the resolution is high enough soft-value clipping will occur (degrading the error correction capabilities of the decoder) with too small dynamic ranges

We start with option (b), i.e. soft-bit fronthauling:

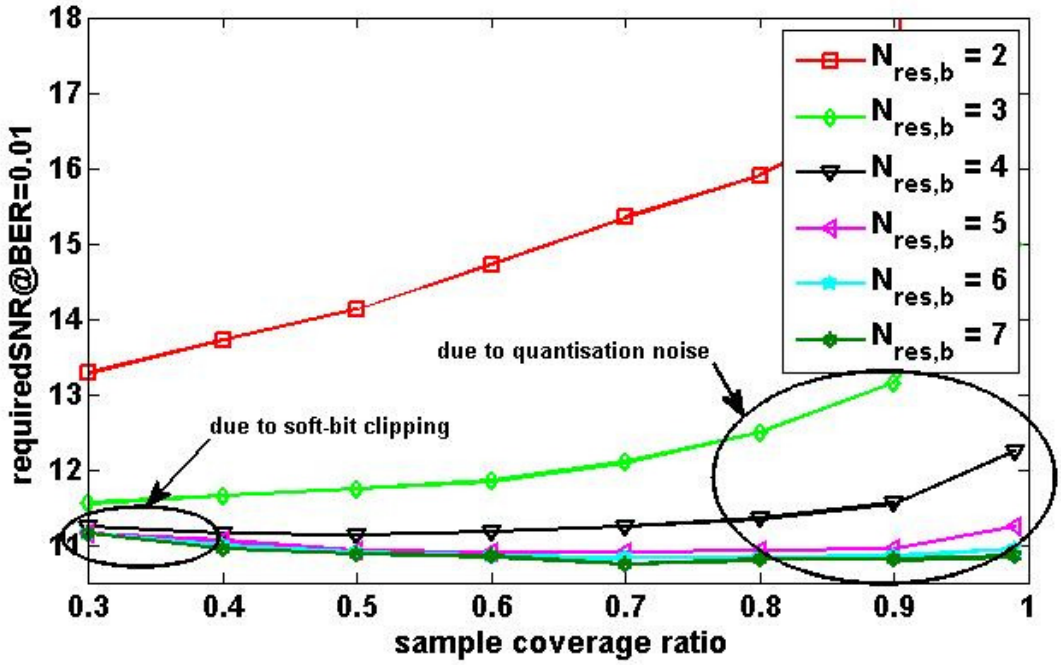

Figure 24: required SNR to stay below 1% error rate (soft-bit fronthauling, QPSK)

With $N_{res,b} = 5$ we practically have no losses due to the quantisation (required SNR = 11 dB). If a slightly higher required SNR (1/2 dB) can be tolerated we even can reduce the resolution to $N_{res,b} = 4$. Obviously, the adjustment of the dynamic range is rather tolerant. With $D < 0.4$ soft-bit clipping starts to have an impact. Quantisation noise is negligible up to $D = 0.9$. In between we have almost no impact at all.

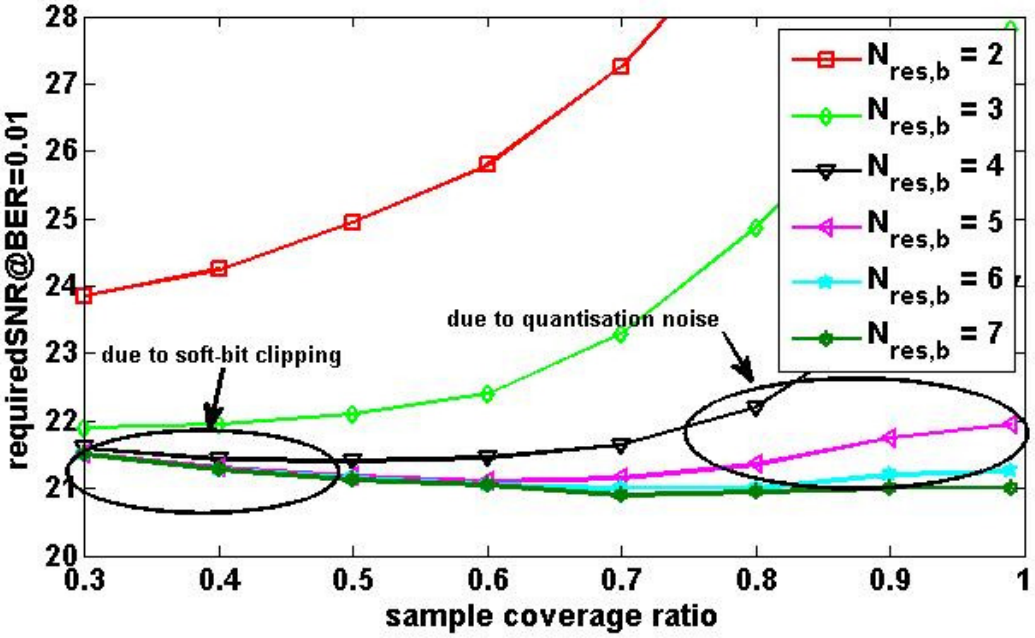

Figure 25: required SNR to stay below 1% error rate (soft-bit fronthauling, 64QAM)

When soft-bits originating from 64 QAM constellations are to be quantized we have to apply a higher resolution as quantisation noise has a higher impact. With $N_{res,b}$ = 6 performance is near to optimum (required SNR = 21 dB), if small losses (~ 1/2 dB) can be tolerated $N_{res,b}$ = 5 is enough. Again dependency on the dynamic range D is small with high enough resolution.

Now we head to burst fronthauling (d):

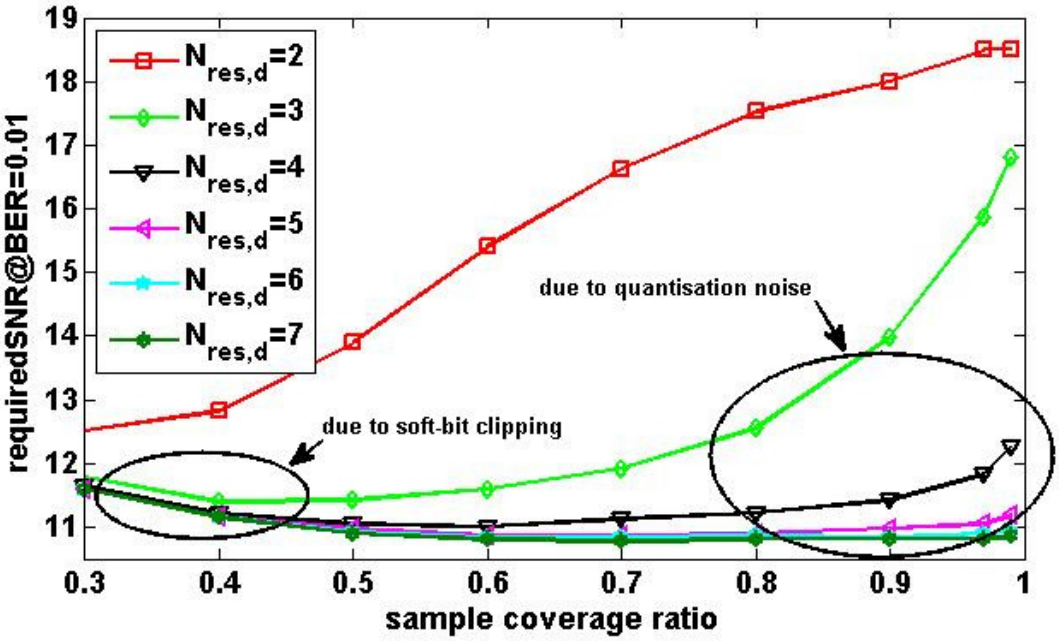

Figure 26: required SNR to stay below 1% error rate (burst fronthauling, QPSK)

Here, $N_{res,d}$ = 5 are sufficient, if small losses may be acceptable $N_{res,d}$ = 4 are possible, either. Again dependency on the dynamic range ratio is rather small, once the resolution is high enough.

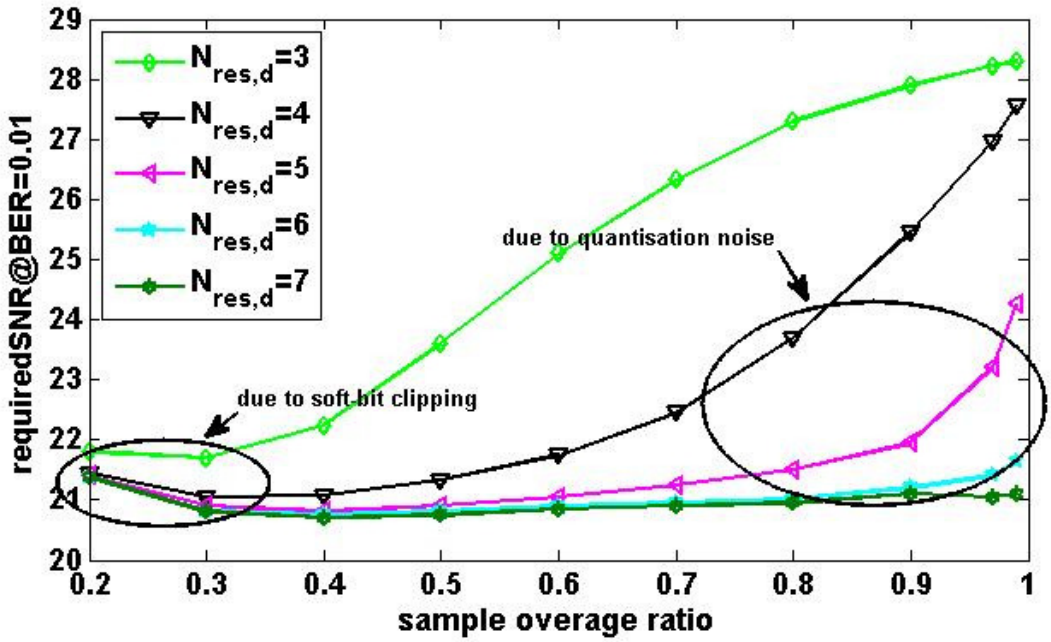

Figure 27: required SNR to stay below 1% error rate (burst fronthauling, 64 QAM)

Fronthauling bursts carrying 64 QAM symbols requires optimally $N_{res,d}$ = 6. With a decreased independency of the dynamic range $N_{res,d}$ = 5 still delivers acceptable performance.

The advantage of burst backhauling is the fact, that the dynamic range and the resolution can be applied per user. This is different with frame backhauling. Here, no user demultiplexing is performed at the site. Thus, the resolution and the dynamic range have to be set in a way avoiding losses for all possible modulation orders and code rates.

The lower bound for the dynamic range is strictly set by the bursts carrying 64 QAM data. If the applied dynamic range would be lower, soft-bit clipping would occur degrading the error correction capability of the FEC decoder. The following figure depicts the histograms of the realpart of the received QAM symbols for QPSK (blue) and 64 QAM (black) at different SNRs (we assume the noise power to be fixed):

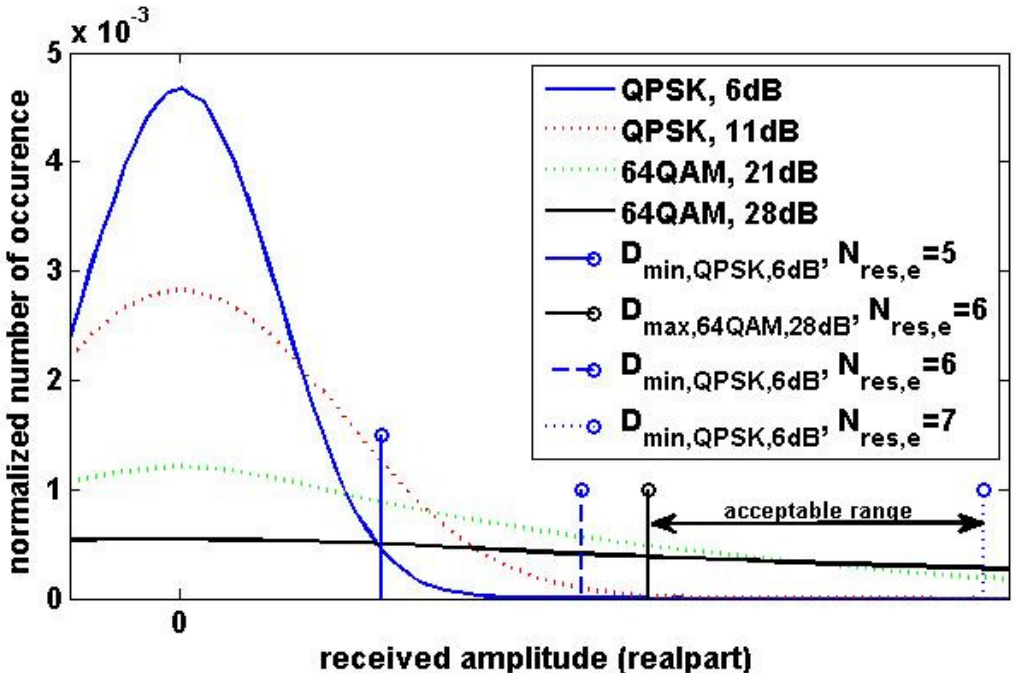

Figure 28: Determination of the minimal resolution for frame fronthauling.

The black vertical line depicts the lowest value for the dynamic range delivering lossless performance for 64 QAM@28 dB. The blue vertical lines are the upper bounds for the dynamic range leading to lossless performance in case of 5, 6 and 7 bits per sample for QPSK@6 dB. Naturally the acceptable width of dynamic ranges lies above the lower bound (the black one) and below the upper bound (the blue ones). Luckily the upper bounds can be shifted to higher values by increasing the resolution (a single bit doubles the bound). So looking at Figure 28 with a resolution of 7 bits we start having values for the dynamic range delivering lossless conversion (lossless with respect to the error rate, naturally not with respect to the error vector magnitude) both for QPSK and 64QAM. If even higher receive powers are present even higher resolutions might be necessary (as in this case, the black bound even gets higher). A smart approach would be not to schedule both extreme cases (UEs with the highest signal quality and UEs with the lowest signal quality) within a single sub-frame. Then, if per the parameters (clipping value and resolution) are set per sub-frame sensitivity is lower.

The following table summarizes the results, i.e. the resolutions (representing the the lower borders) we have applied for the calculation of the bandwidths needs (later in this deliverable):

Table 6: Resolutions (i.e. number of bits) applied for the fronthauling options:

	QPSK	16 QAM	64 QAM
soft-bit fronthauling	5	5	5
burst fronthauling	5	6	6
frame fronthauling	7	7	7
CPRI fronthauling	15	15	15

4.3. ANALOG FRONTHAULING (ROF)

With RoF the analog RF/IF signal is generated at the CO and transmitted to remote radio heads. In upstream the received signal at the eNBs from mobile users is transmitted directly over the PON without any processing as described in Section 3. Therefore, due to analog nature of the signal transmitted over the optical network the bandwidth for the analog fronthauling is measured in units of Hz instead of bits/s.

Compared to digital options with analog the bandwidth estimation is simpler. Due to the effects analog signal experience over the fibre, as detailed in D5.2 [2], available power budget on the PON is the limiting factor. Therefore, with FDM approach, due to the shared budget with different eNBs the maximum number of subcarriers and consequently the base stations is significantly limited. To avoid this issue WDM of the FDM analog signals would be beneficial.

To that extent, Figure 29 illustrates the possible analog wireless overlay over ACCORDANCE based on WDM/FDM technique. The total bandwidth requirement per single wavelength (e.g. λ3) will then depend on the subcarrier spacing. The results in Section 4.2 confirm that spacing around 40 MHz (assuming 10 MHz of wireless bandwidth) could be sufficient for satisfactory performance. Therefore, assuming 2x2 transmit and receive antennas at the eNB, 3 sectors and guard band this would lead to the bandwidth requirements in the range of 300 MHz (6 subcarriers) per wavelength per base station.

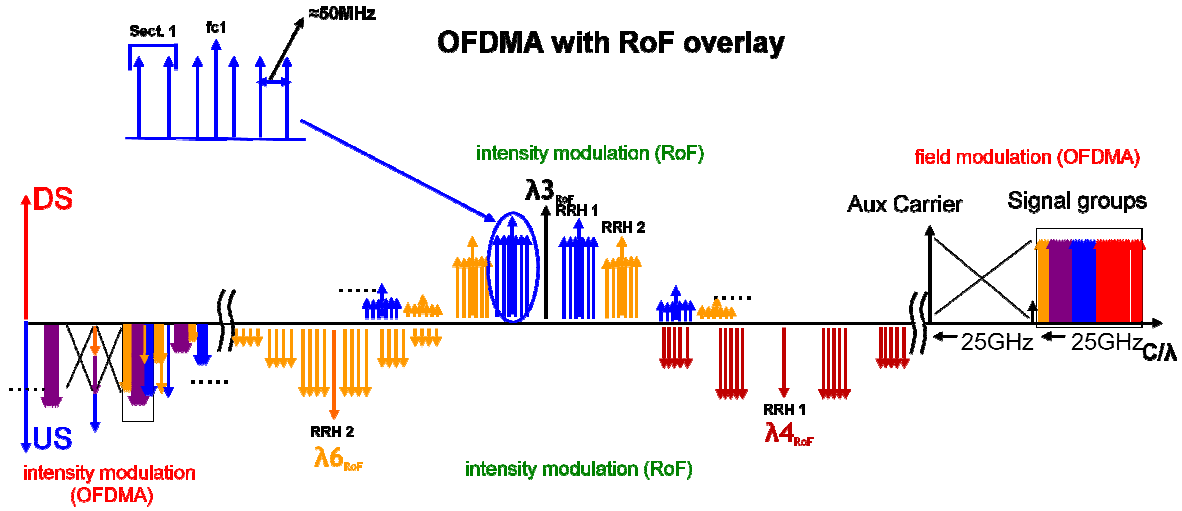

Figure 29: Multi-wavelength overlay over ACCORDANCE PON with RoF FDM.

The total number of wavelengths available, leading to the total number of supported base stations, will be determined by the wavelength plan as it will be further elaborated in D2.4 ('Migration and convergence scenarios') [1].

4.4. RESULTS

A key differentiation characteristic between the fronthauling options we have proposed is their bandwidth need on the PON. The lower this value the more sites can be consolidated. Before heading to the actual numbers we need to quantify the relative amount of overhead LTE requires (reference signals, control channels). The fronthauling options which are per user (b-d) need to transport those overheads separately. The others (e-f) do not, as these are already multiplexed into the frame.

DL:
In downlink we have the pilots, the reference symbols and the control channels.

Depending on the number of spatial multiplexing streams (1, 2, 4) pilot overhead is varying (5%, 11%, 24%). In downlink always all pilots are radiated. There is no need to transport the pilots via the PON as they simply can be placed by the site equipment according to the burst profiles communicated via the control channel.

LTE applies two downlink synchronization signals (the primary synchronization signal and the secondary synchronization signal) with which the UE can synchronise itself with respect to timing and frequency and can assess critical system information (such as physical layer ID of the cell). The amount of resources needed for the transmission of the synchronization signals is negligible. Both kinds are transmitted twice per radio frame consuming 72 subcarriers within a single multi-carrier symbol (so, per radio frame we have 4 * 72 = 288 subcarriers being occupied by the synchronization signals). This number is rather low compared to the number of available resources (< 1%) and thus can be neglected here. Again this must not be transmitted via the PON and can be placed by the site equipment autonomously.

Finally the control channel consumes resources either. It is to be transmitted once per sub-frame and placed at the beginning. Depending on the amount of control information to be transmitted one, two or three multi-carrier symbols can be dedicated to this matter. So, the overhead due to the control channel is depending on the load of the cell. If the load is low only few control messages are to be communicated and a single multi-carrier symbol may be sufficient (~ 7% overhead), if the load is high up to three multi-carrier signals might be needed (~ 21% overhead).

UL:
In uplink resources have to be spent for the reference signals, the control channel and the PRACH transmissions.

We have two kinds of reference signals, the demodulation reference signal and the sounding reference signal. The former is placed within the user allocations and can be used by the basestation for estimating the channel for proper signal reception (~ 14% overhead). The latter are occasionally to be transmitted by each UE within the sounding region. With their help the basestation is able to get a view on the channel characteristics the UEs are confronted with (~ 7% overhead). This information is used by the frequency selective scheduler. The demodulation reference signal is depending on the load factor of the cell as only resource blocks carrying user data are containing demodulation reference signals. The overhead due to the sounding reference signal is independent from the load.

The uplink control channel covers up to 16% of the available resources. However, if not necessary this fraction may be decreased. Thus, the actual overhead due to the control channel is depending on the load of the cell.

Various PRACH formats are available (for various cell sizes). For cell sizes up to 14 km the duration of a single PRACH slot is a single TTI (i.e. the length of a sub-frame, 1ms). In frequency direction the PRACH slot covers the range of 72 data subcarriers. So, if we assume

a periodicity of 10ms (i.e. one PRACH slot per frame) and 10 MHz bandwidth, we have an overhead of around 1.2%.

The following tables include the resulting required fronthauling rates for uplink (only user data, the overhead due to the control signals will be covered in the next deliverable) with scenario II (i.e. 4-antenna MRC):

Table 7: Peak fronthauling rates (UL, only user data, scenario II) [Mbps]

	10% load	30% load	50% load	100% load
R_b	19.6	54.7	91.2	165.9
R_d	31.1	87.6	146.0	265.4
R_e	470.4			
R_f	2457.6			

Table 8: Average fronthauling rates (UL, only user data, scenario II) [Mbps]

	10% load	30% load	50% load	100% load
R_b	15.2	42.5	70.9	128.9
R_d	30.7	85.9	143.2	260.4
R_e	470.4			
R_f	2457.6			

In Table 7 the peak values, in Table 8 average numbers are shown. As reminder:

- R_b → transport of soft-bits (DL) and hard-bits (UL) plus control info
- R_d → transport of bursts (i.e. frequency domain I/Q samples + control info)
- R_e → transport of frames (again frequency domain I/Q samples)
- R_f → CPRI fronthauling (i.e. time domain I/Q samples)

Figure 30 depicts the required peak fronthauling rates (scenario II, UL) in case of various cell loads. The tremendous decrease by shifting parts of the baseband processing to the site is apparent.

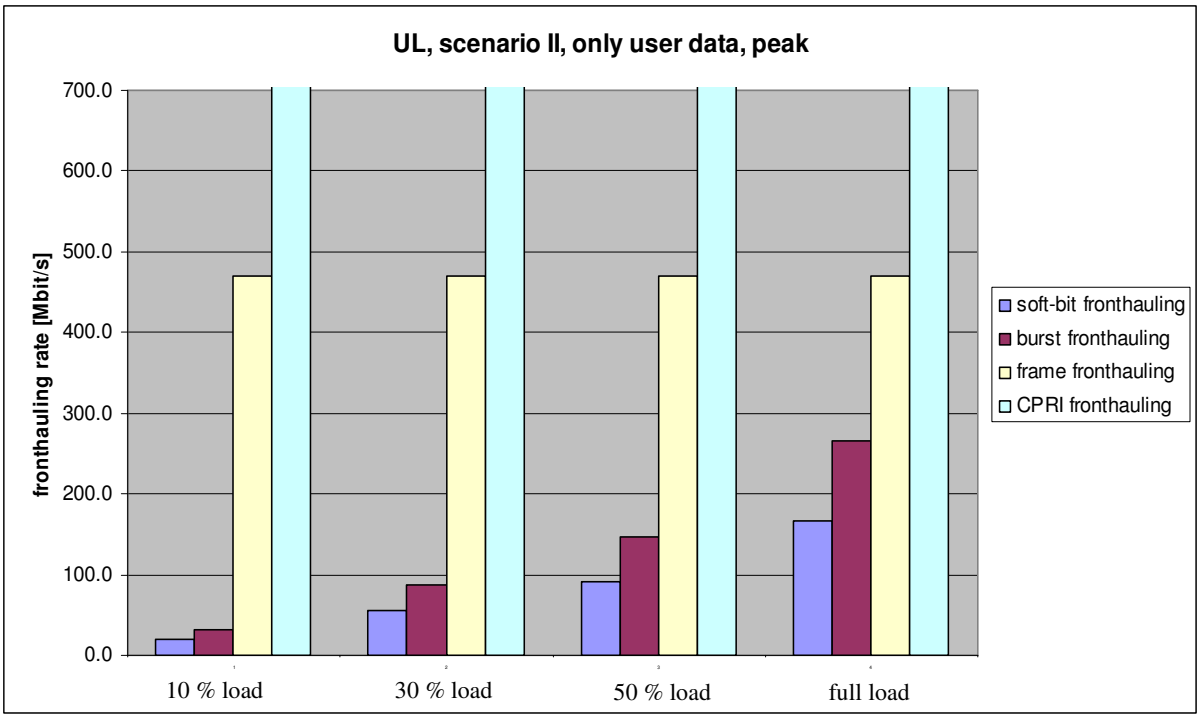

Figure 30: Required peak fronthauling rates (UL).

Obviously, by shifting parts of the baseband processing chain to the PON leaves (i.e. into the site equipment) the amount of fronthauling resources decreases significantly. As soft-bit and burst fronthauling are on a per user basis, the required rates are load dependent. Comparing the two tables soft-bit fronthauling is user mix dependant in addition (the difference between the average rates and the peak rates makes this apparent). If a lot of cell-center UEs are scheduled (high fraction of 64QAM within the sub-frame) the amount of soft-bits to be transported via the PON is much higher than if a lot of cell-edge UEs (high fraction of QPSK within the sub-frame) are scheduled. With burst backhauling this is different, as the number of QAM symbols to be fronthauled is independent from the user-mix. With frame backhauling and CPRI backhauling the rates are fixed in any case.

To visualize the dependency of the fronthauling rates on the user mix and on the load factor Figure 31 depicts the average fronthauling rates normalized to the respective peak rates in full load:

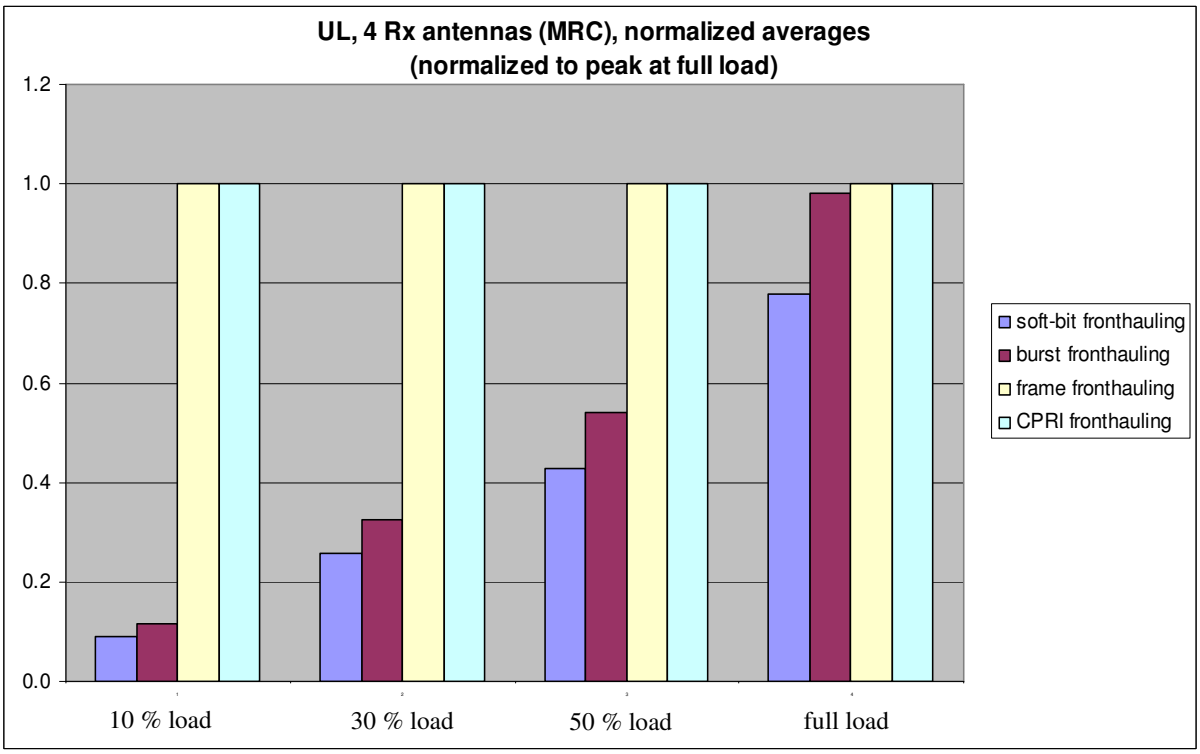

Figure 31: Average fronthauling rates normalized to the respective peak rates in full load (UL).

The normalized averages are defined as follows:

$$r_* = \frac{R_*(\text{average}, x\%\,\text{load})}{R_*(\text{peak}, \text{full load})} \qquad (7)$$

The normalized averages for r_e and r_f equal one in any case. This is due to the fact, that these rates are independent both from the user mix and the load factor. r_d (burst backhauling) is near one in case of full load, thus r_d is slightly user dependent (due to the fact, that 64 QAM symbols need a higher resolution the QPSK symbols and thus the overall rate depends on the ratio of 64 QAM symbols and QPSK symbols within the subframe). With 50% load r_d is far away from one, this is due the load dependency. r_b obviously depends both on the user mix (normalized average in case full load is smaller than one) and on the load level (normalized average in case of 50% load is even smaller then the normalized average in case of full load).

In downlink we get:

Table 9: Peak fronthauling rates (DL, scenario II) [Mbps]

	10% load	30% load	50% load	100% load
R_b	4.5	12.3	20.6	37.7
R_e	470.4			
R_f	2457.6			

Table 10: Average fronthauling rates (DL, scenario II) [Mbps]

	10% load	30% load	50% load	100% load
R_b	3.8	10.6	17.6	32.3
R_e	470.4			
R_f	2457.6			

R_b is tremendously lower than in uplink. This is due to the fact that in downlink we do not need a high resolution for transporting the data as we actually have to transport hard-bits (naturally, as the data not yet has passed the wireless channel at this stage).

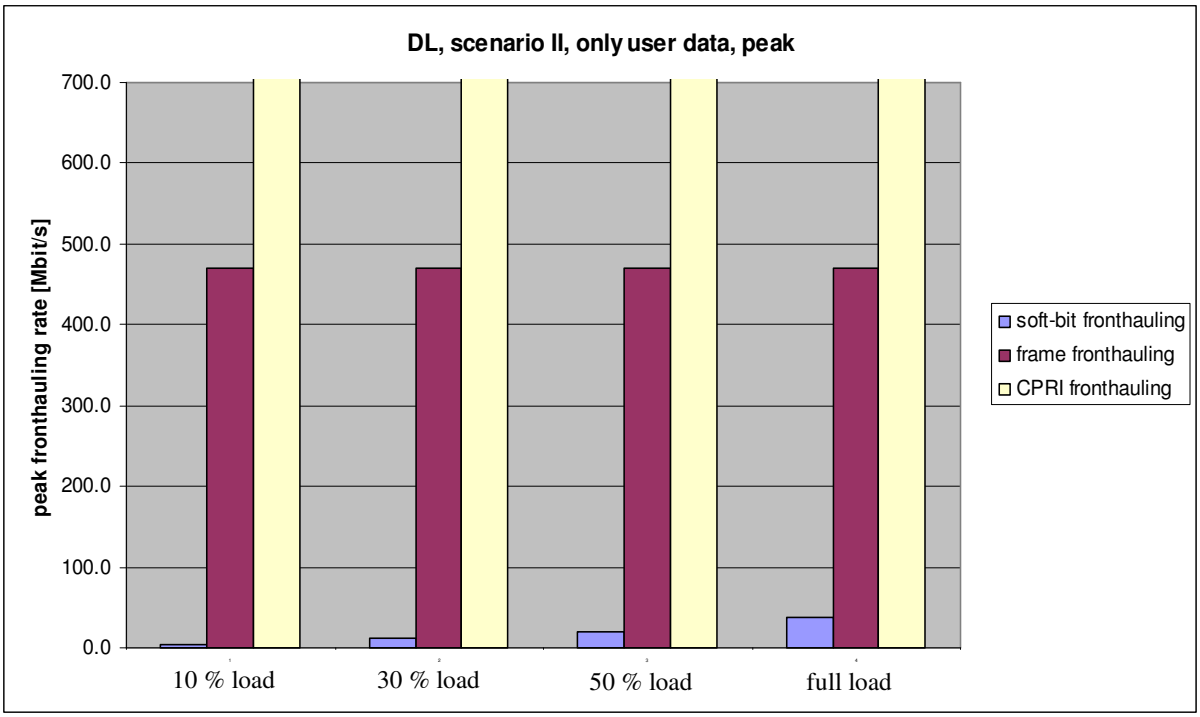

Figure 32: Required peak fronthauling rates (DL).

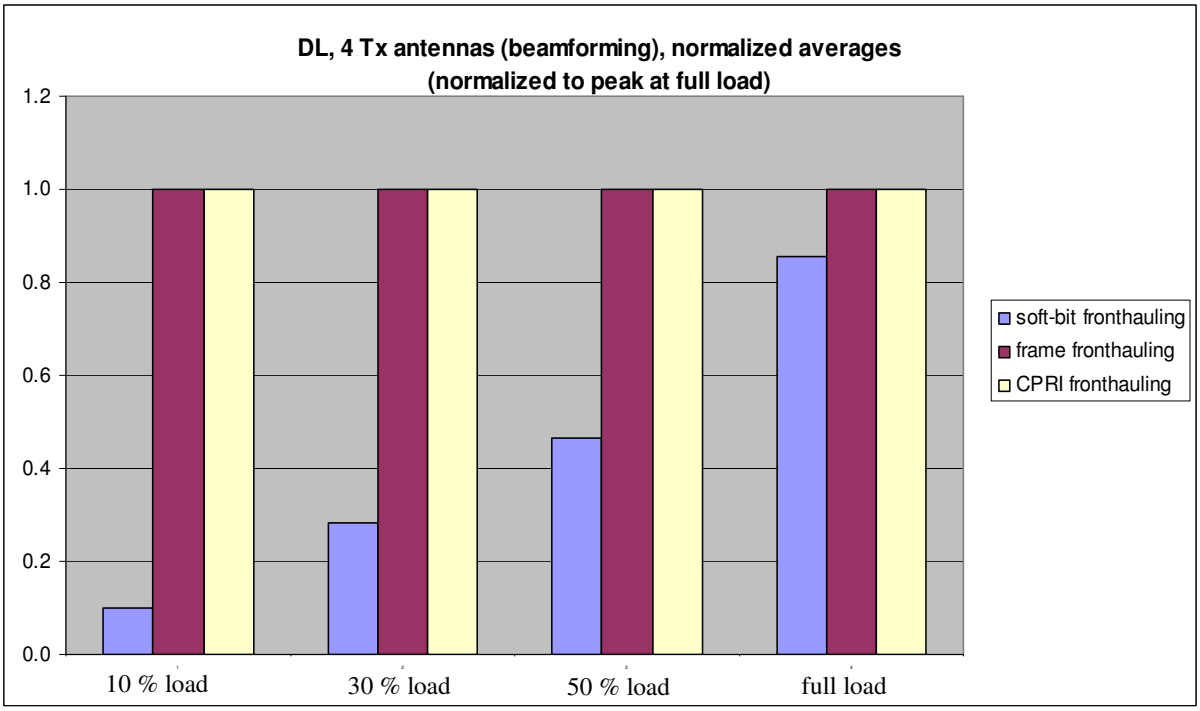

Figure 33: Average fronthauling rates (50% and full load) normalized to the respective peak rates in full load (DL).

Similar conclusions can be drawn as with uplink.

5. Performance requirements for the optical transport

5.1. DIGITAL FRONTHAULING

As stated on D5.2 [2] if we apply digital fronthauling we can model the fibre transmission in the following way:

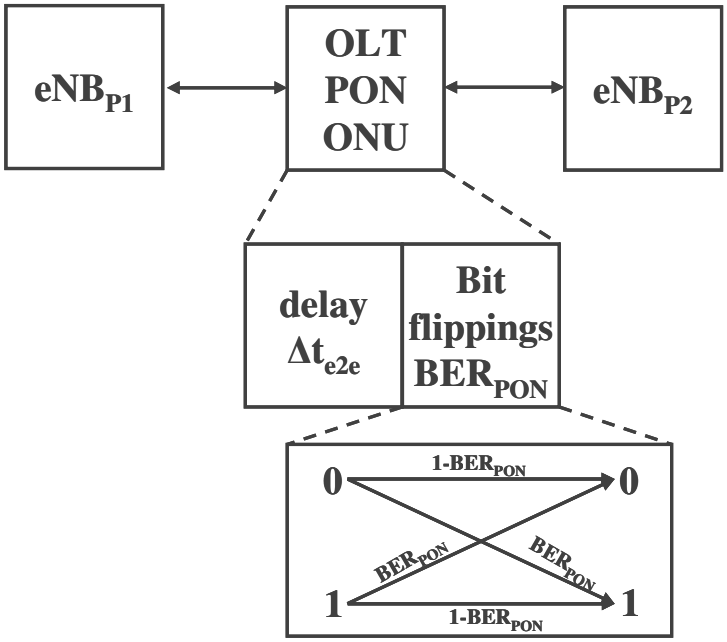

Figure 34: OLT-PON-ONU link in the view of the wireless subsystem (for digital fronthauling). eNB$_{P1}$ is the part of the wireless baseband processing performed centrally, eNB$_{P2}$ includes the parts performed at the site.

So, delay is introduced (covered in a later chapter) and bit errors occur. Here, we will discuss the impact bit errors, occurring on the fronthauling link, have to the wireless transport of data. In the following, we omit the index in $N_{res,x}$ (x=[b, d, e]) identifying the respective interfacing point, as it is obvious through the naming of the sections.

Soft-bit fronthauling:

In downlink encoded bits are to be transported via the PON. So, the fibre link and the wireless link share the budget of acceptable bit errors. So, the overall bit error rate we achieve end-to-end (i.e. from the central office to the UE) is as follows:

$$\begin{aligned} BER_{e2e} &= P[\text{bit error on the fibre link}] \cdot P[\text{no bit error on the air link}] \\ &\quad + P[\text{no bit error on the fibre link}] \cdot P[\text{bit error on the air link}] \\ &= BER_{fibre} \cdot (1 - BER_{air}) + (1 - BER_{fibre}) \cdot BER_{air} \\ &= BER_{fibre} + BER_{air} - 2(BER_{fibre} \cdot BER_{air}) \end{aligned} \quad (8)$$

Solving this equation for BER_{fibre} we get:

$$BER_{fibre} = \frac{BER_{e2d} - BER_{air}}{1 - 2BER_{air}} \tag{9}$$

So, now we have an equation for the error rate the fibre link may have depending on the error rate caused by the wireless transport (influenced by the link quality) and the targeted raw error rate (i.e. before error detection). Typical target bit error rates are (remember: CTC error correction still is to be done, so the error rate on IP level will be significantly lower):

$$BER_{e2e} \in \left\lfloor 10^{-4}, 10^{-3}, 10^{-2}, 10^{-1} \right\rfloor \tag{10}$$

Therefore, we get:

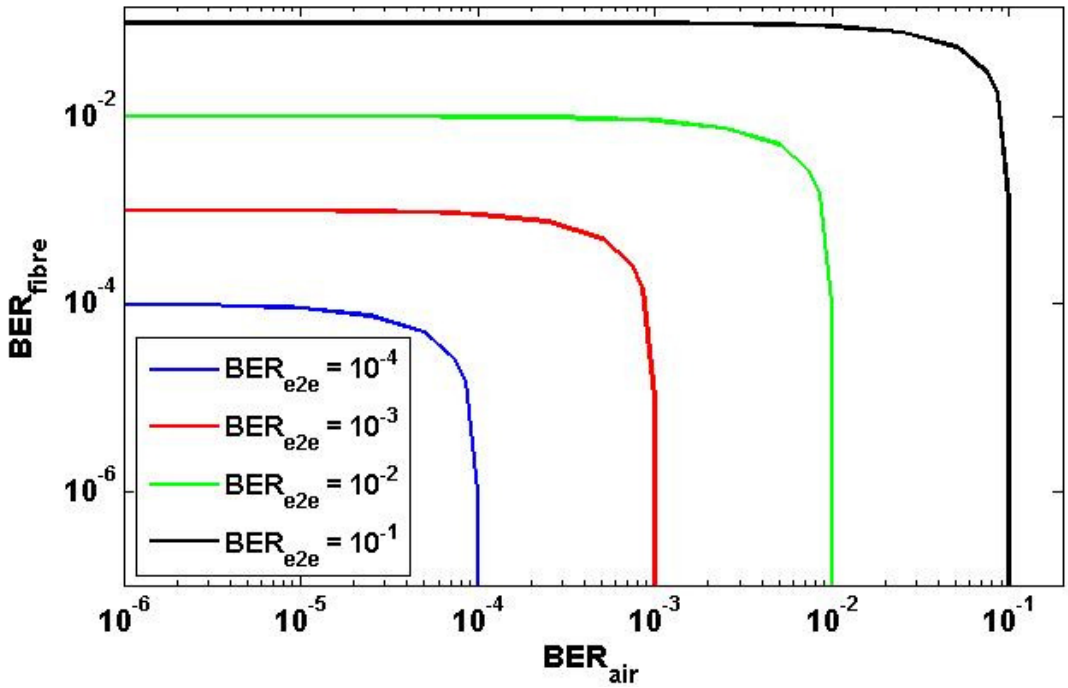

Figure 35: Acceptable BER_{fibre} depending on BER_{air} for various BER_{e2e}.

We can identify three ranges for BER_{air}:

$$\begin{aligned} &1.\ BER_{air} \le (1-\varepsilon) BER_{e2e} && \varepsilon \approx 0.9 \\ &2.\ (1-\varepsilon) BER_{e2e} \le BER_{air} \le BER_{e2e} \\ &3.\ BER_{e2e} \le BER_{air} \end{aligned} \tag{11}$$

1. BER_{air} significantly lower than BER_{e2e}
2. BER_{air} in the range of BER_{e2e}
3. BER_{air} higher than BER_{e2e}

The last case must not occur. If it does, the dimensioning of the wireless system is erroneous.

The first case assumes a conservatively dimensioned wireless system, relaxing the constraints for the fronthauling network. Here, the BER budget almost completely can be spent on the fibre link.

The second case assumes a throughput optimized wireless system. Here, the mapping between the modulation and coding scheme to the respective SINR range is rather aggressive. In this case the fronthauling link must be virtually error free.

In uplink the situation is completely different. Here a single bit transmitted via the PON does not carry a bit been transported via the air, but instead is part of a codeword reflecting a soft-bit amplitude. So, a bit error occurring on the PON does not directly translate into a bit error for the wireless transmission. Instead an amplitude error of the respective soft-bit is the consequence. Figure 36 shows the quantization characteristic and the codeword to amplitude mapping for N_{res}=4. The codeword alphabet consists of 2^{Nres} elements (here: 16, '0 0 0 0' up to '1 1 1 1'). A single bit error on the PON falsifies the respective codeword and thus the underlying amplitude.

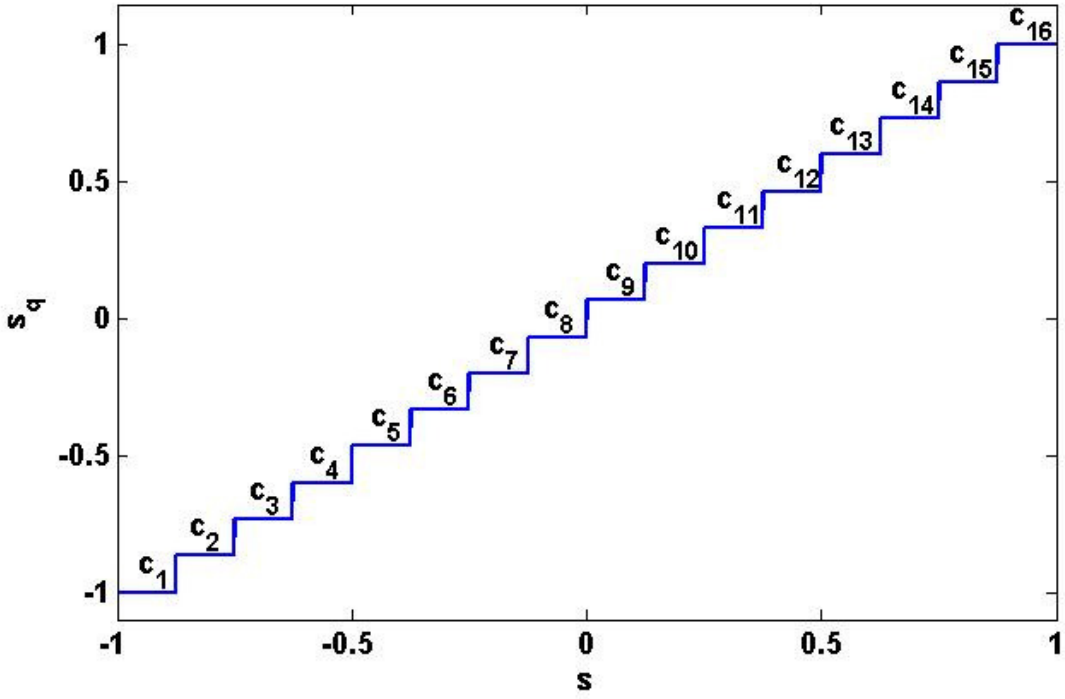

Figure 36: Quantization characteristic with codeword mapping (N_{res}=4).

We have performed link-level simulations to assess the quantitative impact of errors on the PON. The simulator performs the quantization and collects the respective codeword. Then, for each of the bits a dice has been tossed to determine, if it has been flipped or not according to a preset probability (the error probability on the PON). After this the codewords are substituted by the respective amplitude again (possibly leading to erroneous amplitudes). Then, wireless baseband processing continues. Outcome of the simulations are bit error rates characterising the quality of the wireless transport being affected by the amplitude errors due to the bit errors on the PON.

We have used three different codeword to amplitude mappings:

I. gray mapping: adjacent codewords differ only in a single bit
II. de2bi mapping: each codeword is the binary representation of the index of the codeword. The indices of the codewords are ascending with ascending amplitude (apparent in Figure 36).

III. inc-weight mapping: The lowest amplitude is mapped to the all-zeros codeword. The next higher amplitudes are mapped to the codewords with a single '1'. Then the codewords follow with two '1's until the highest amplitude gets the all-ones codeword.

For N_{res}=4 the used mappings are (mappings for further resolutions can be found within the appendix):

Table 11: Codeword space for N_{res}=4.

	gray	de2bi	inc-weight
c_1	0000	0000	0000
c_2	0001	0001	0001
c_3	0011	0010	0010
c_4	0010	0011	0100
c_5	0110	0100	1000
c_6	0111	0101	1001
c_7	0101	0110	1010
c_8	0100	0111	1100
c_9	1100	1000	0101
c_{10}	1101	1001	0011
c_{11}	1111	1010	0110
c_{12}	1110	1011	0111
c_{13}	1010	1100	1011
c_{14}	1011	1101	1101
c_{15}	1001	1110	1110
c_{16}	1000	1111	1111

The simulation framework is the same as already applied earlier (for assessing the impact of the quantization).

The resulting bit error rates depending on the signal-to-noise ratio at the antenna for various error rates on the PON applying the introduced mappings:

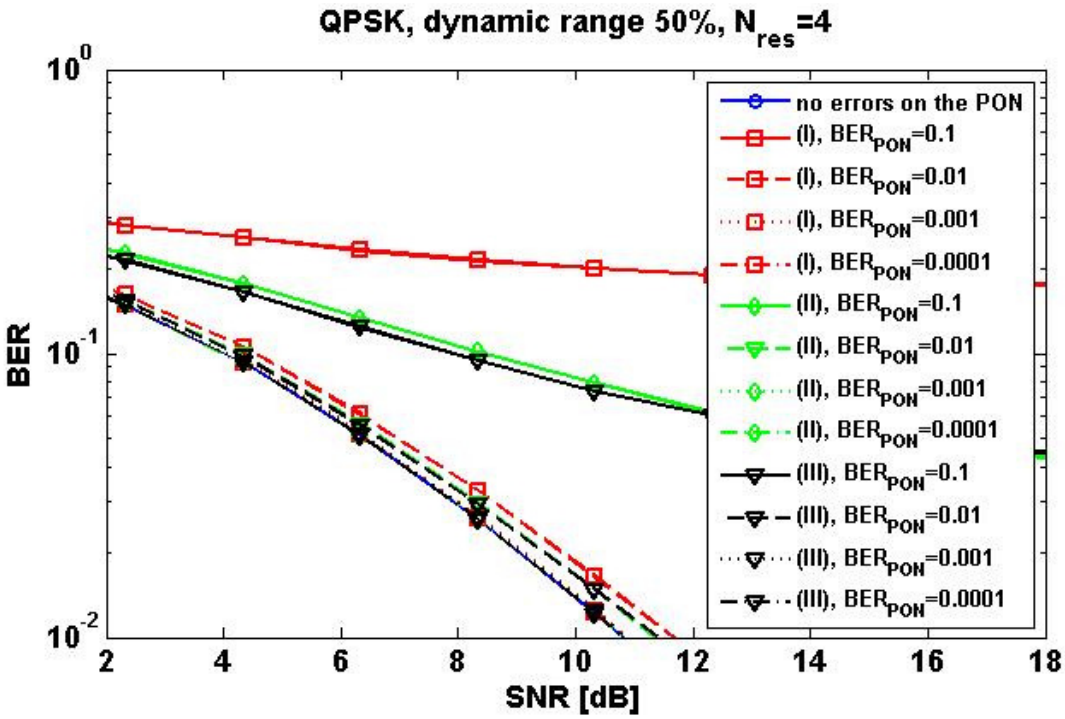

Figure 37: QPSK, N_{res}=4.

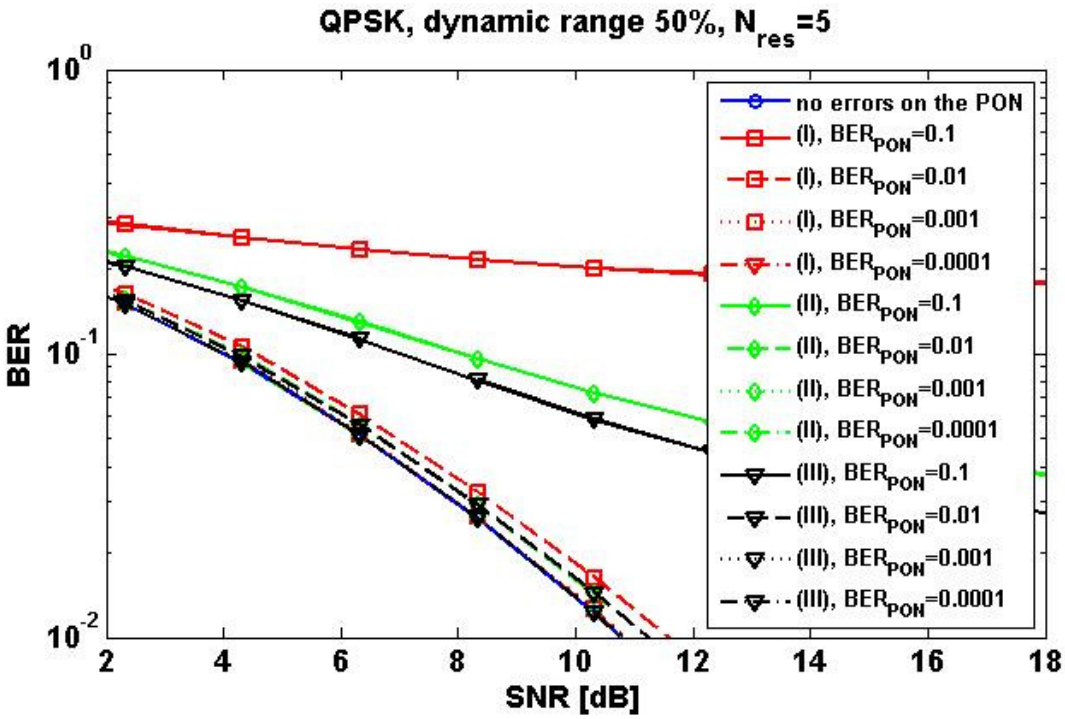

Figure 38: QPSK, N_{res}=5.

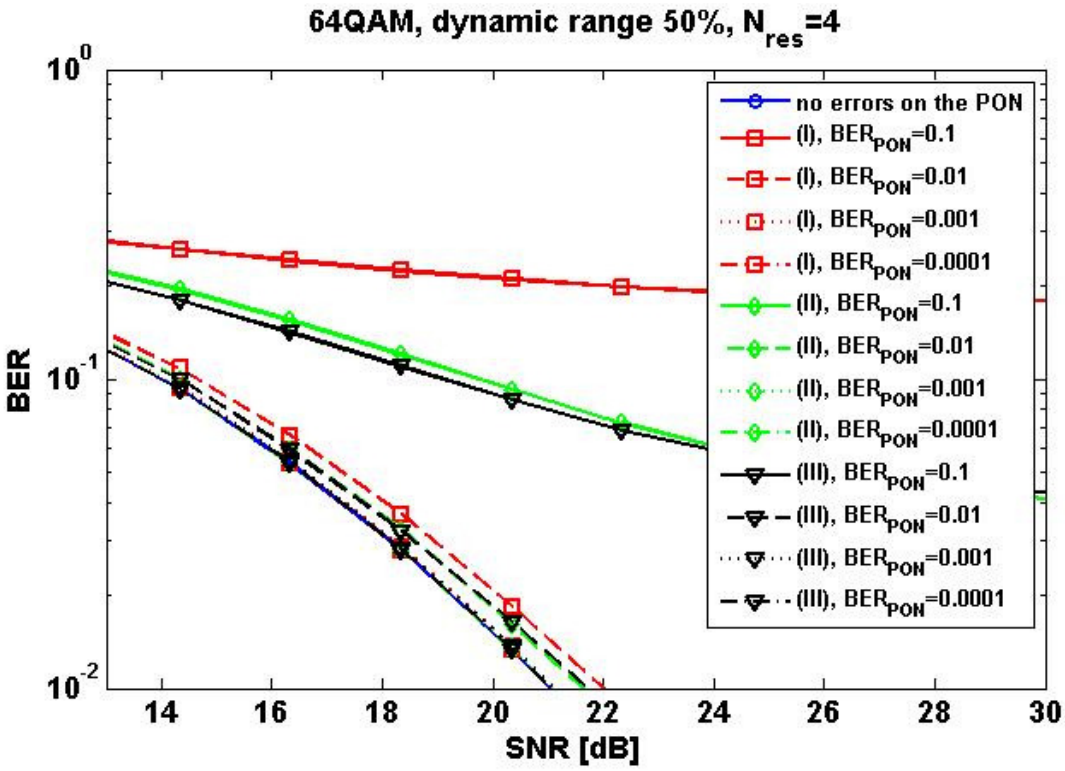

Figure 39: 64 QAM, Nres=4.

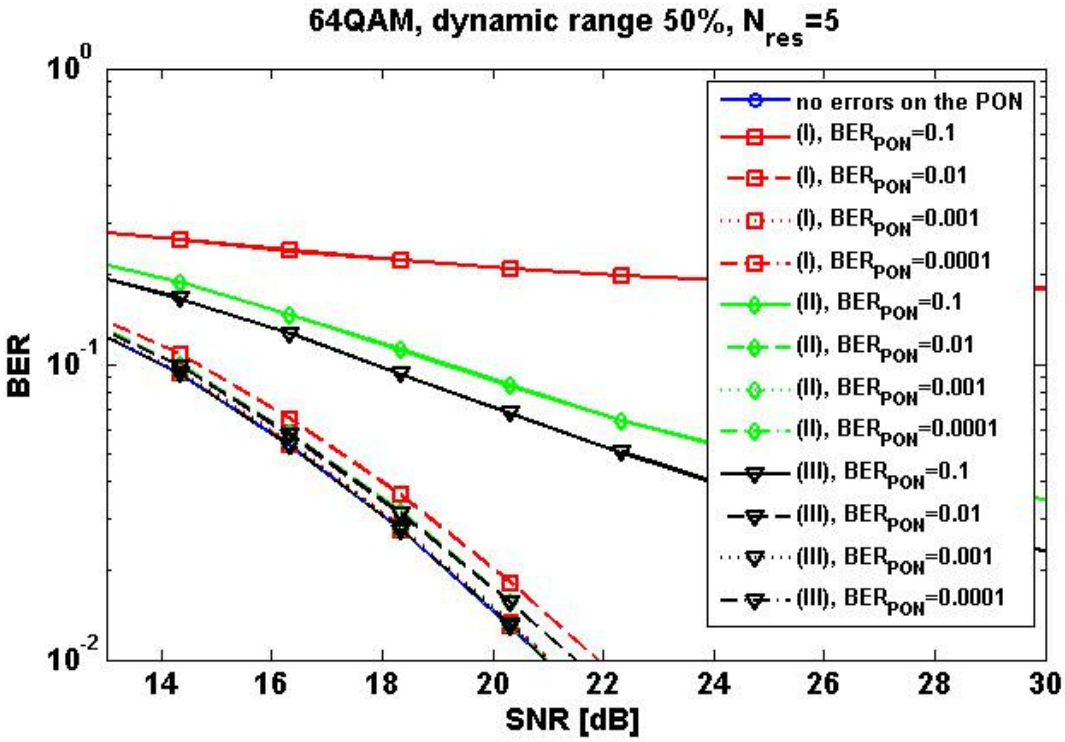

Figure 40: 64 QAM, Nres=5.

As expected bit errors on the PON are less devastating then in downlink. A bit error rate on the PON of 0.1% has almost no impact. With 1% a performance decrease (a SNR loss of around 1 dB) is observable. We have only a slight dependence on the chosen amplitude to codeword mapping with gray mapping being the worst.

Burst fronthauling:

With burst fronthauling we have to transport binary representations (codewords) of the actual symbols via the PON both in UL and in DL. We have used the same codeword spaces as already with soft-symbol fronthauling. The sensitivities to bit errors on the PON are as follows:

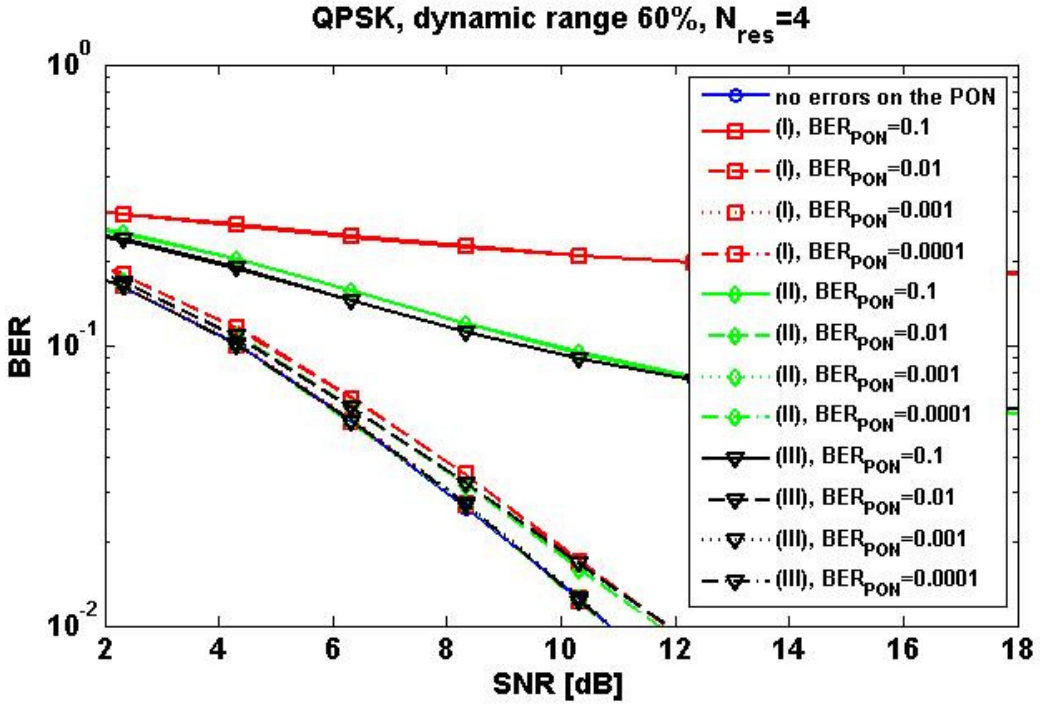

Figure 41: QPSK, N_{res}=4.

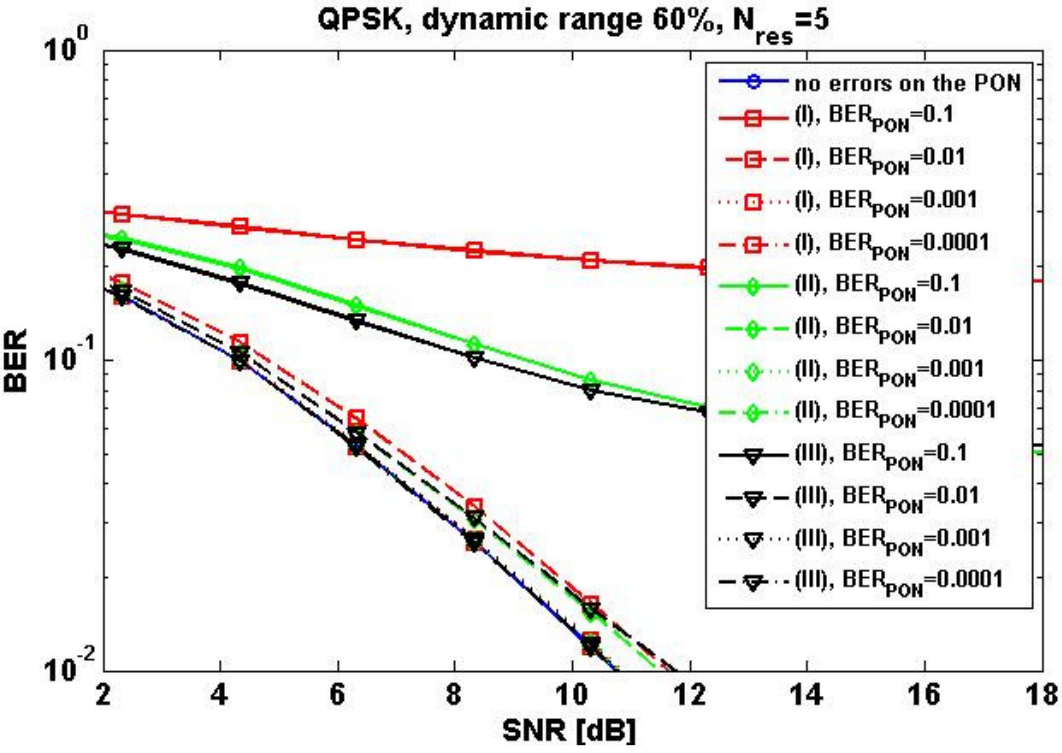

Figure 42: QPSK, N_{res}=5.

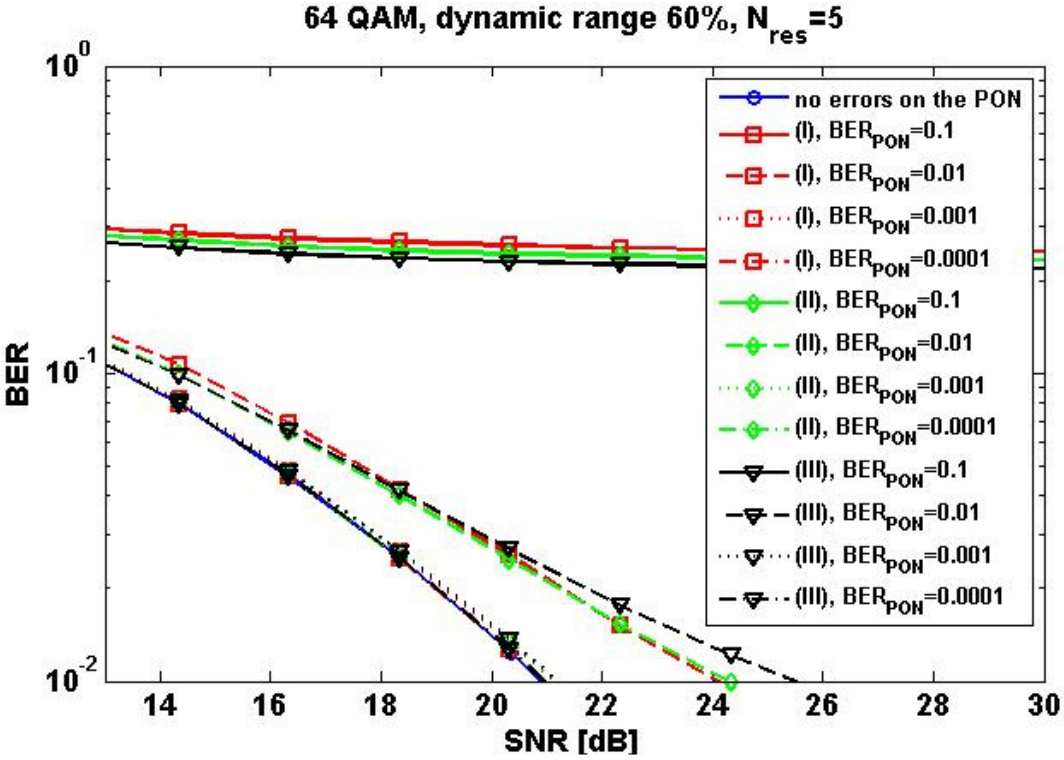

Figure 43: 64 QAM, N_{res}=5.

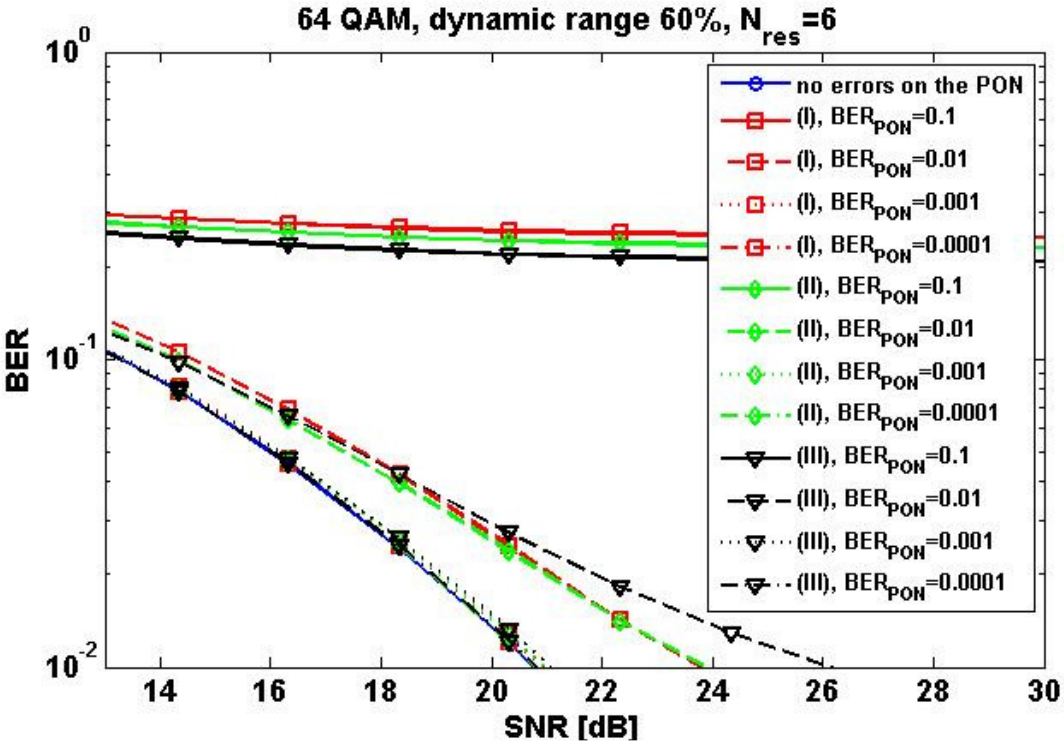

Figure 44: 64 QAM, N_{res}=6.

Again a bit error on the PON leads to an erroneous amplitude. As expected, sensitivity is similar to the former case. Once the error rate on the PON is below 0.1 % the impact to the wireless transport is negligible.

Frame fronthauling:

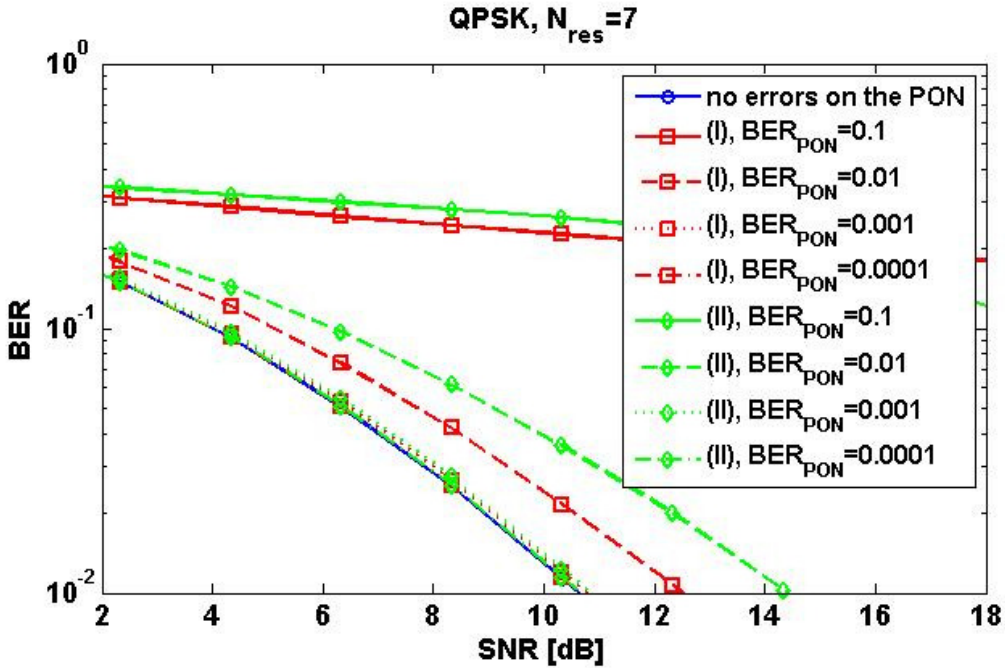

Figure 45: QPSK, N_{res}=7.

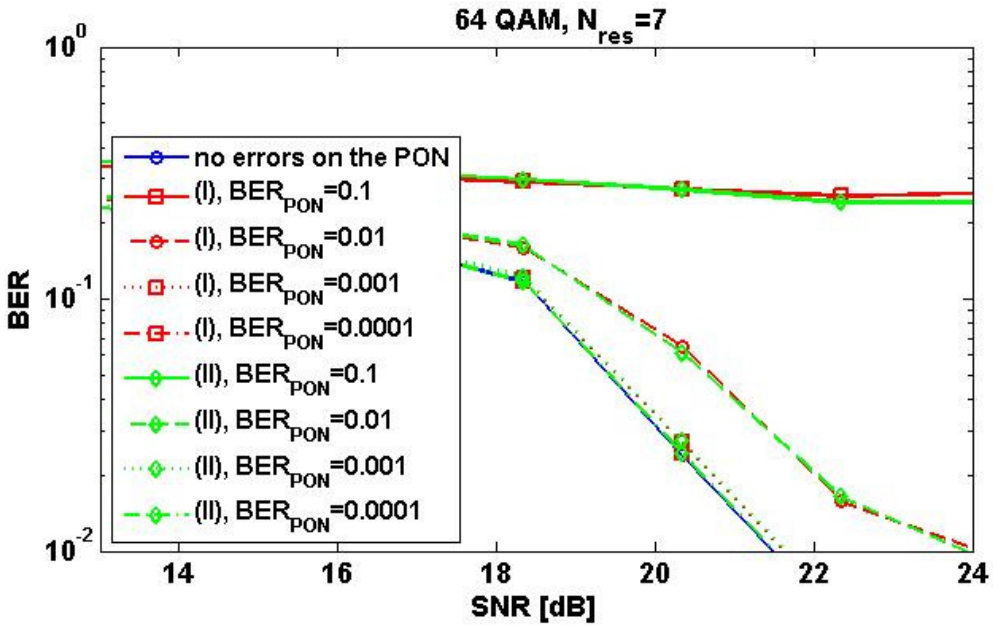

Figure 46: 64 QAM, N_{res}=7.

Once the constraints with respect to frame fronthauling delineated in the chapter covering the assessment of the required resolutions and dynamic ranges are met, the sensitivity to bit errors on the PON vanishes (with respect to the error rate on the air-link) again once the error rate on the PON is below 0.1 %.

CPRI fronthauling:

According to the CPRI standard [6] for CPRI fronthauling the error rate to be met is 10^{-12}. The performance evaluation of this option over the OFDMA PON via link level simulation is presented in D5.1 [5].

5.2. ANALOG FRONTHAULING

This section provides investigations for the analog fronthauling focusing on evaluation of the key performance figures of wireless signals transmitted over various lengths of PON. An outline of key advantages was initially presented for analog fronthauling.

Furthermore, detail description and up/down conversion techniques for RoF were described in D5.2 [2]. Due to its simplicity of implementation and low cost compared to other indentified options, the intensity modulation with direct detection (IM-DD) transmission technique is considered in these investigations.

One of the main focuses of this study is adjacent carrier leakage ratio (ACLR) figures obtained at remote radio heads (RRHs) since they can severely degrade performance over the wireless signals. These have not been extensively investigated in the literature for next generation wireless standards such as LTE and worldwide interoperability for microwave access (WiMAX). Although, ACLR plots have been scarcely drawn for point-to-point connections, they haven't been investigated for point-to-multipoint, various fibre distances and FDM transmission links targeted in ACCORDANCE.

To that extent, an experimental setup was devised in order to investigate the subcarrier spacing and ACLR with respect to different fibre distances. The general system architecture is given in Figure 47. The scenario is similar to ACCORDANCE setup with the exception of an optical amplifier at the first remote cabinet (named local exchange (LE)) and long feeder length. The investigations here include longer fibres in order to confirm RoF limitations for ACCORDANCE.

Evaluations are performed by means of optical single sideband (OSSB) modulation in the network downstream, to beat chromatic dispersion for longer standard single mode fibre (SSMF) reach, without using receiver pre-amplification, in order to reduce further deployment costs. In addition to ACLR, typical error vector magnitude (EVM) characteristics are also plotted.

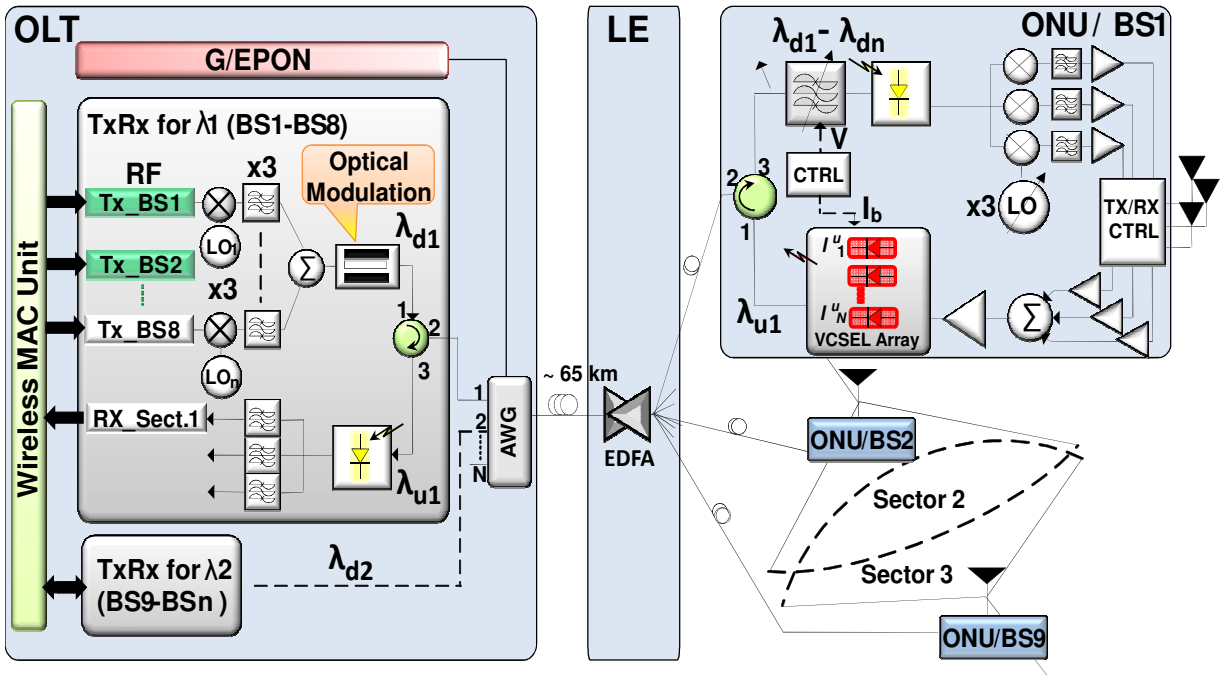

Figure 47: General description of the architecture for analog wireless fronthauling

For the topology, shown in Figure 47, the optical line terminal (OLT) is based at MCO. At the customer side, optical network unit/base stations (ONU/BSs), it means RRHs, are located at either the user premises or at remote antenna posts, providing connectivity to mobile terminals. Distinctively, the network utilizes a LE to connect the OLT through a single 65 km feeder fibre to multiple users. At the distribution side, the LE is used for broadcasting in DL or combining in UL signals to/from multiple network base stations via a passive splitter and link lengths spanning between 20km to 40km. In terms of new network deployment the LE can be simply placed at current OLT sides that would only perform amplification rather than the legacy OLT functionalities.

Another significant feature of this topology is the attainable scalability with respect to the number of supported BSs, through the application of extended wavelength band overlay, maintaining the splitter nature of existing G/EPON infrastructures. To comply with the standard, selected wireless channels generated in the network OLT/MCO are arranged in FDM windows and transmitted over individual wavelengths in the 1550-1600 nm range to selected ONU/BSs. Apart from different wavelengths transmitting different FDM windows, the proposed architecture also allows for a given FDM window to be propagated on multiple wavelengths. This relaxes significantly the bandwidth requirements of optical and electrical devices while enhancing the network scalability. The resulting reduction in the total FDM bandwidth provides for better optical modulation index (OMI) during modulation at the OLT and improved ACLR at remote antennas.

In practise the application of wavelength band overlay only requires an additional array waveguide grating (AWG) in the OLT and tuneable optical filters in individual ONU/BSs. Importantly the centralised AWG allows for multiple PONs to be serviced by a single OLT while maintaining the distribution network intact in support of smooth migration towards next generation PONs (NG-PONs). The final configuration will depend on the migration scenarios analysed in D2.4 [1].

Finally, to demonstrate colourless wireless-PONs upstream, long-wavelength vertical cavity surface emitting laser (VCSEL) arrays and tuneable optical band-pass filters (BPF) can be universally employed in the ONU/BSs. This results in simplification of network implementation and cost-reduction by excluding the use of wavelength-specific optical sources. The use of low-cost, VCSEL arrays upstream also demonstrates simple coupling optical terminations, not limited by the non-linear effects of the optical fibre. Although reflective semiconductor optical amplifiers (RSOAs) could be alternatively used, Rayleigh backscattering is known to degrade system performance. In the presence of VCSEL arrays, re-modulation of downstream carriers is not required for upstream transmission. Multi-wavelength propagation in upstream, with sufficient frequency spacing provided by the VCSEL, significantly reduces optical beat interference (OBI) at the PIN receiver in the OLT.

In this experiment the mobile WiMAX was used due to the availability of the hardware equipment. However, since another important aspect of analog fronthauling is that it is agnostic to any wireless signal formats it is expected that the outcome of investigations performed in this work for mobile WiMAX, could be also extended to LTE, particularly in downstream, since they are both based on OFDMA transmission technique.

To evaluate the transmission of mobile WiMAX channels over the long-reach PON links between the OLT and ONU/BS, received EVMs were experimentally investigated. EVMs give a measure of transmission quality by specifying the minimum acceptable value at each ONU/BS's antenna input. However, for radio transmission over highly nonlinear, power budget limited optical links, only EVM performance figures are not sufficient. As already mentioned before, ACLR measurements were also performed, in particular for the long reach

scenario, in order to establish the adjacent channel leakage power caused by the non-linearity of the optical link for various subcarrier spacing. The generation and specifications of the WiMAX signals as well as the experimental set-ups implemented for their transmission over short and long-reach ACCORDANCE PON is described below.

An Aeroflex PXI WiMAX Vector Signal Generator/Analyser unit was used in this experiment to generate and analyse the WiMAX channels. The specification for each generated WiMAX channel distinguishing between upstream and downstream transmission is given in Table 12.

For 1024 OFDMA subcarriers (corresponding to the FFT size), 10MHz bandwidth between the RF channels at the output of the Aeroflex VSG and 64-QAM modulation, the resulting aggregate data rate per sector for the downstream WiMAX link was 25.2 Mbps. In view of the 16-QAM modulation in the upstream, the corresponding figure was 18.9 Mbps. It is important to stress out at this point, these data rates were calculated in view of guard and pilot subcarriers which do not carry user data but rather used for synchronisation and estimation purposes. A worst case scenario, 25% cyclic prefix was also included. The downstream WiMAX channel transmitter relative constellation error (RCE) was -50 dB, a figure higher than the minimum required for 64-QAM modulation [7].

Finally, the time division duplex (TDD) mode of operation was adopted in the experiment with frame duration of 5ms.

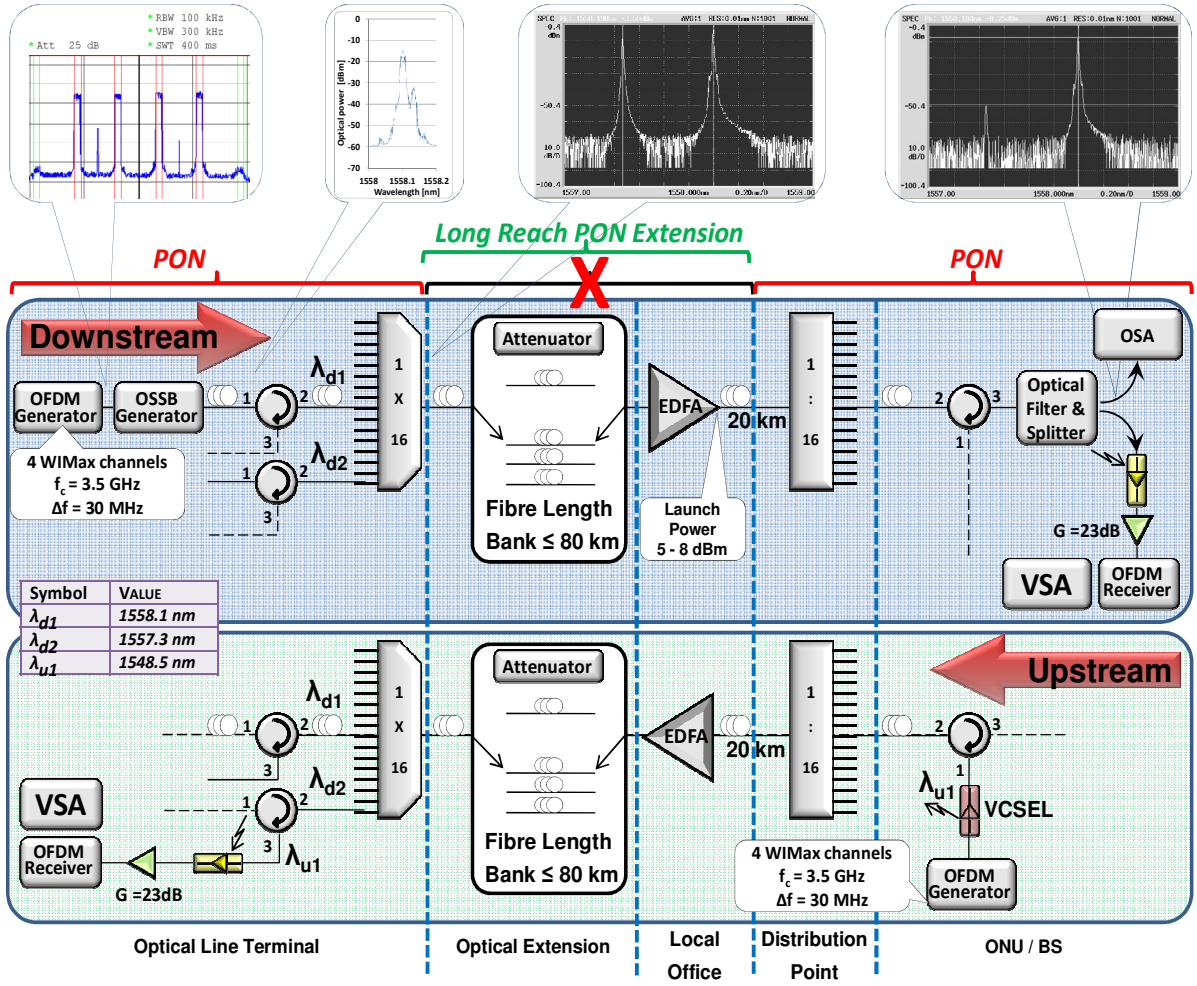

Figure 48: Experimental setup.

Table 12: WiMAX parameters.

Symbol	Downstream	Upstream
FFT size	1024	1024
Modulation	64-QAM	16-QAM
Coding	2/3	¾
Bandwidth	10MHz	10MHz
RCE	-50dB	-25.8dB
Data rate	25.2Mbps	18.9Mbps

5.2.1. MCO to RRH transmission

Figure 48 describes the experimental set-up. Four WiMAX channels, forming an FDM window, at the standard 3.5 GHz with 30 MHz subcarrier spacing were generated at the OLT. The number of generated WiMAX channels was limited by the capability of the Aeroflex device. Ideally the number of generated WiMAX channels should match the passive optical network split and as a result for a targeted 1:16 split to comply with current deployments of legacy PONs, a minimum of 16 channels should be generated (if power budget allows). This assumes that one or more ONU/BSs would require more than one WiMAX channels. The 30 MHz subcarrier spacing was chosen to match the Aeroflex receiver filter specifications.

To address individual ONU/BSs each WiMAX channel should be shifted in frequency from 3.5 GHz to any higher value that avoids adjacent channel interference. This was being achieved by using a predetermined local oscillator (LO) and BPFs in the OLT. In succession the WiMAX channels are combined and modulated onto an optical carrier. At the ONU/BS, a LO is required, operating at exactly the same frequency for a specific ONU/BS to downshift the appropriate WiMAX channels. Multiple BPFs are also needed to select each channel prior to transmission over the air.

The formed FDM signals in the OLT are then externally modulated using a Mach-Zehnder modulator (MZM) and a commercially available distributed feedback (DFB) laser source. Significantly, double sideband modulation of the subcarriers is used at this stage since the effect of fibre chromatic dispersion at 20km distances is expected to be insignificant. The MZM offers improved performance in terms of chirp compared to direct modulation but at higher cost. However, as it is typically shared by large number of users, cost is not a limiting factor.

The resulting signal was then transmitted on λ_{d1}=1558.1 nm, through a circulator and a 16x1 AWG to an ONU/BS, using various lengths of SSMF ranging from 23.2 km to 40.7 km. Having added the various optical component losses in the system's OLT, outlined in Table 13, 0.9 dBm optical power was launched into the fibre. An additional un-modulated wavelength at λ_{d2}=1557.3 nm was connected at one of the unused AWG inputs to investigate interference at ONU/BSs.

Continuing downstream an optical attenuator was used after the fibre to account for various splitter loses. At the ONU/BS, a readily available add/drop multiplexer (ADM) was utilised prior to PIN detection as a substitute for a commercial 50 GHz optical band pass filter. The ADM drop port, at the wavelength of 1558.1 nm, produced a signal to interference ratio of 42

dB. The resulting up-converted WiMAX signal was then down-shifted in frequency to get the original WiMAX channels and subsequently amplified by a 23 dB gain amplifier for performance evaluation measurements.

Table 13: Optical parameters.

Symbol	Loss (dB)
MZM	7.75
AWG	3.76
Circulator Pol. Control	0.9 0.45
Splitter (1 : 16)	13.5
Add/Drop filter	5

A single IEEE 802.16-2005, 3.5 GHz channel was generated in upstream to directly modulate a VCSEL at λ_{u1}=1548.5 nm. An 8.3 mA bias was used producing -0.94 dBm output power prior to being transmitted over the SSMF. Since the experimental investigations involve no signal transmission over a wireless channel, the upstream WiMAX transmitter relative constellation error (RCE) was set to -25.8 dB to conform to the figure expected to be received at the base station in a practical scenario. The resulting optical signal was then routed through the corresponding AWG output port to the destination receivers (Rx_Sect.X) in the OLT where individual EVMs are measured.

Performance evaluation:
The four frequency-shifted, 3.5 GHz, WiMAX channels, displayed as inset in Figure 48, at 10MHz bandwidth each, are transmitted downstream to address selected ONUs as described in the previous section. Each WiMAX channel displayed a 50 dB signal to noise ratio as specified by the Aeroflex PXI transmitter. Subsequently they were applied at the MZM RF input for optical modulation. In order to measure intermodulation distortion, and evaluate the associated degradation imposed on the received WiMAX channels at the ONU/BS receivers, the Aeroflex output power was varied between -2 dBm and +14 dBm.

The EVM characteristic of a selected WiMAX channel was measured at the remote antenna input of the corresponding ONU/BS as a function of the MZM RF drive power as shown in Figure 49 for varying fibre lengths and network splits to define the maximum reach and splitting ratio attainable with a fully passive infrastructure. The considered splits of 1:4, 1:8 and/or 1:16 are expected to be used between MCO and RRH as an intermediate node in order to reduce power budget limitations. The plots drawn in Figure 49 confirm in all cases that at low RF drive powers the signal is mainly distorted by noise. At high powers however, EVM increases due to the nonlinearities of the MZM.

To comply with the WiMAX downstream requirements for 64-QAM 2/3 [7], an EVM figure above -30 dB should be achieved at the bottom of the bathtub curve. This is achieved in the experimental setup for a 23.2 km fibre and 16 split with RF input power into the MZM ranging between +11dBm and +13 dBm and a moderate +1dBm optical power launched into the fibre. Suggested by the longer reach, reduced split responses in Figure 49, measuring 40.7 km and 8-split respectively, a justifiable increase in the fibre launch power would allow enhanced length-split ratios. This is expected to be achieved in a practical network by the optimisation of OLT network component losses. Comparable results were confirmed for all WiMAX channels.

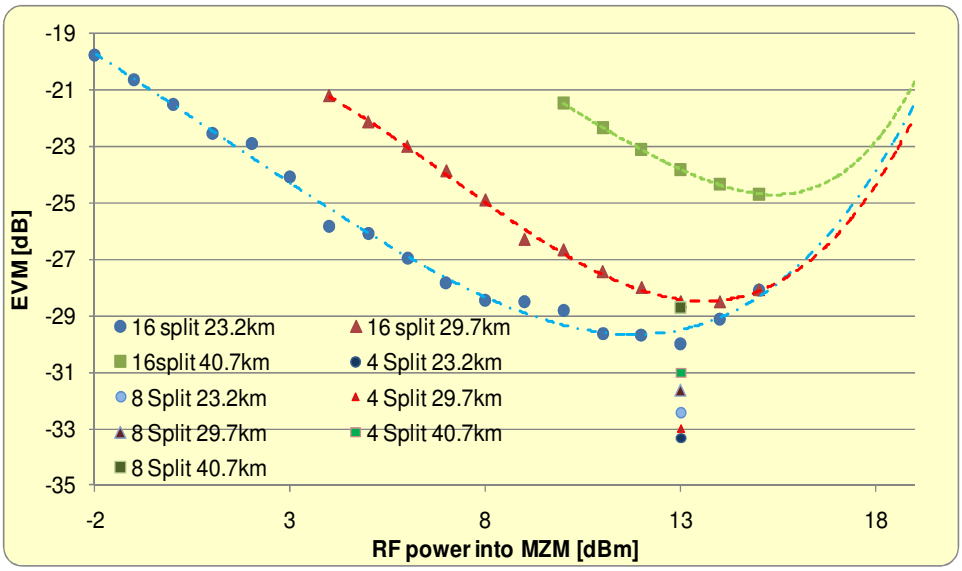

Figure 49: Obtained EVM for 3.5 GHz WiMAX channel at remote antenna downstream.

Similarly EVM measurements were performed at the OLT receiver in the upstream as shown in Figure 50, as a function of the VCSEL RF input power. This is purely investigated in order to establish the signal degradation between a base station and the OLT. To that extent, an EVM of -23 dB was recorded over 23.2 km of fibre with 16 split. The interaction of VCSEL laser chirp and fibre dispersion in analog optical modulation upstream had negligible effect on the received WiMAX channels in the OLT. Longer fibre lengths were not considered due to the VCSEL output power limitation (max 0dBm) however, higher output power VCSEL arrays [8] are expected to significantly reduce the EVM penalties.

Finally, the power of the received WiMAX signals at an ONU/BS was determined at approximately -30 dBm, within the range of input powers required for linear operation of the high power amplifier for transmission over the air. Also, the constellation diagrams obtained after phase and amplitude corrections at the remote antenna are displayed in Figure 51. The two outermost points represent the pilot tones used for estimation and synchronisation purposes.

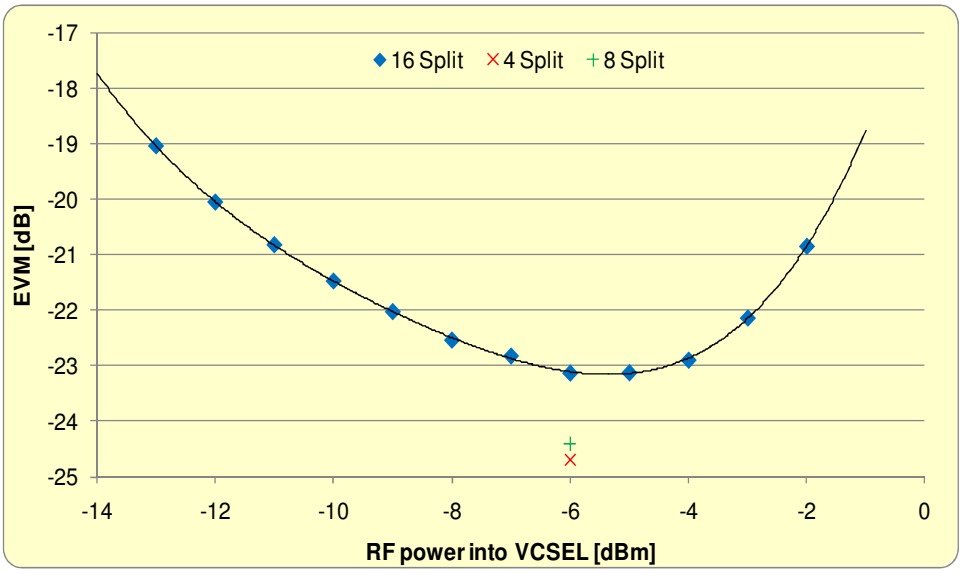

Figure 50: Obtained EVM at the WiMAX OLT receiver for 3.5 GHz channel upstream

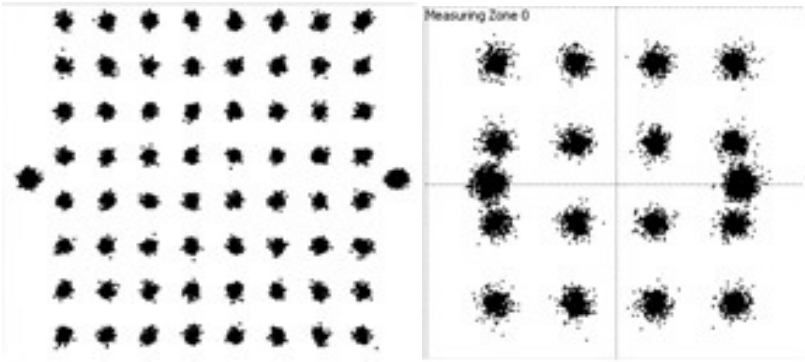

Figure 51: 64-QAM downstream (left) and 16-QAM upstream (right) modulation

5.2.2. Extended MCO to RRH transmission

Figure 48 also describes the experimental set-up expansion to accommodate long-reach networking. A variable-gain erbium doped fibre amplifier (EDFA) was used to compensate for the increased link losses, located in the LE where the feeder fibre terminates. The application of EDFA is widely acceptable for NG-PONs by operators and vendors for long reach scenarios. The EDFA utilised in the experiment has a noise figure of 6 dB and variable gain up to 28 dB.

Most significantly to be able to achieve long-reach spans, OSSB modulation is performed in downstream targeting the reduction of chromatic dispersion. Adding to the network's benefits OSSB signalling is generated using a dual arm MZM, significantly reducing the OLT implementation cost compared to alternative solutions based on optical band pass filters. WiMAX channels were fed to the MZM with a 90 degree phase shift between its two arms. The resulting spectrum is given as an inset in Figure 48. As it can be observed the upper sideband was selected for transmission over the fibre.

To complete downstream transmission, the output of the MZM is then fed to the optical circulator and an AWG as previously described. Power budget optimisation at varying feeder fibre spans was performed to estimate the maximum transmission distance as well as the optimum performance in terms of ACLR and EVM. The length of the distribution network from the LE to the ONU was kept fixed at 20km, complying with typical next generation access network targets for long-reach networks while the component losses measured in the previous section remained intact. The ONU/BS premises infrastructure also remained unchanged with the network upstream still utilising double sideband direct VCSEL modulation. Both the 40-80km feeder and 20km distribution fibres were of SSMF type, maintaining the nature of the network in the field to that of legacy PONs since the multi-wavelength overlay is provided over an already deployed passive splitter.

Performance evaluation:
The long reach network scenario performance extends to evaluating the effect of subcarrier spacing to sustain ACLRs. Only downstream measurements are required since for RoF designs it is imperative that the ACLR before transmission into the air conforms to regulatory requirements. In the upstream, since the received channels are terminated at the OLT, ACLR is not a critical issue.
ACLR depends on several factors including the length of the transmission link, the optical modulation index, the subcarrier spacing and number of subcarriers. The same four, frequency shifted WiMAX channels are similarly applied. The subcarrier spacing was varied between 10 MHz and 40 MHz (5 MHz increment), due to the specifications of the Aeroflex signal generator as shown in Figure 52.

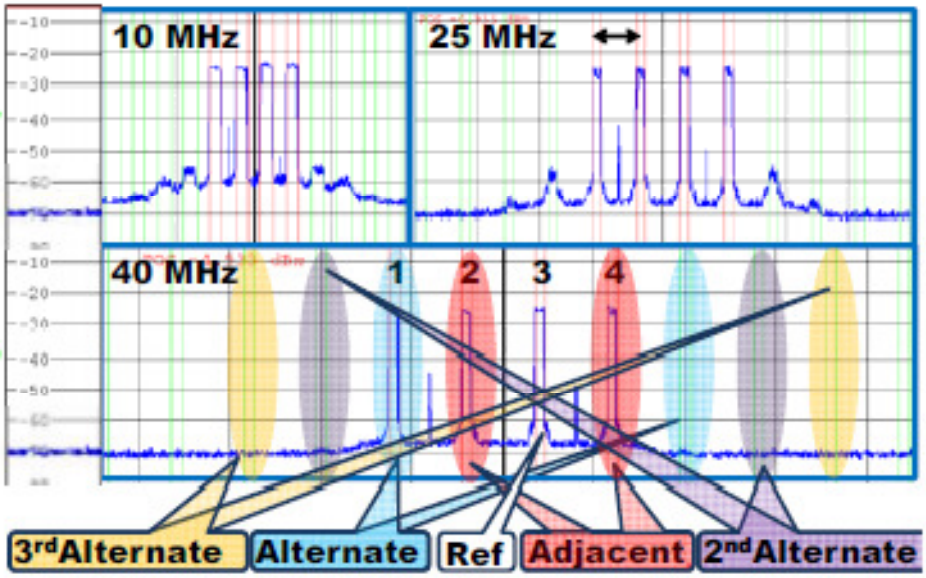

Figure 52: Subcarrier spacing for 10 MHz, 25 MHz & 40 MHz

A feeder fibre length of 65 km, sustained by an EDFA at the LE, was considered for these measurements. The distribution network of 20 km remains intact as previously described. The gain of the EDFA was varied to adjust the optical launch power from 5 dBm to 9 dBm into the distribution and feeder fibres to estimate the transmission performance. A plot of channel spacing versus measured ACLR with respect to the third WiMAX channel is plotted in Figure 53. The specific channel is selected since it represents the worst case scenario in terms of both adjacent and alternate channel interference. For mobile WiMAX applications the acceptable ACLR figure is usually specified by local regulators and for 10 MHz channel bandwidths, -35 dB for adjacent and -45 dB for alternate channels should be achieved [9]. Figure 53 confirms that for 40 MHz subcarrier spaced FDM windows both adjacent and alternate channels satisfy the specified requirements. At 20 MHz the ACLR condition for adjacent channels is also achieved although alternate channels fall above the threshold. This defines by no means a network limitation since 40 MHz subcarrier spacing for FDM applications still imposes a low bandwidth requirement on the PON infrastructure.

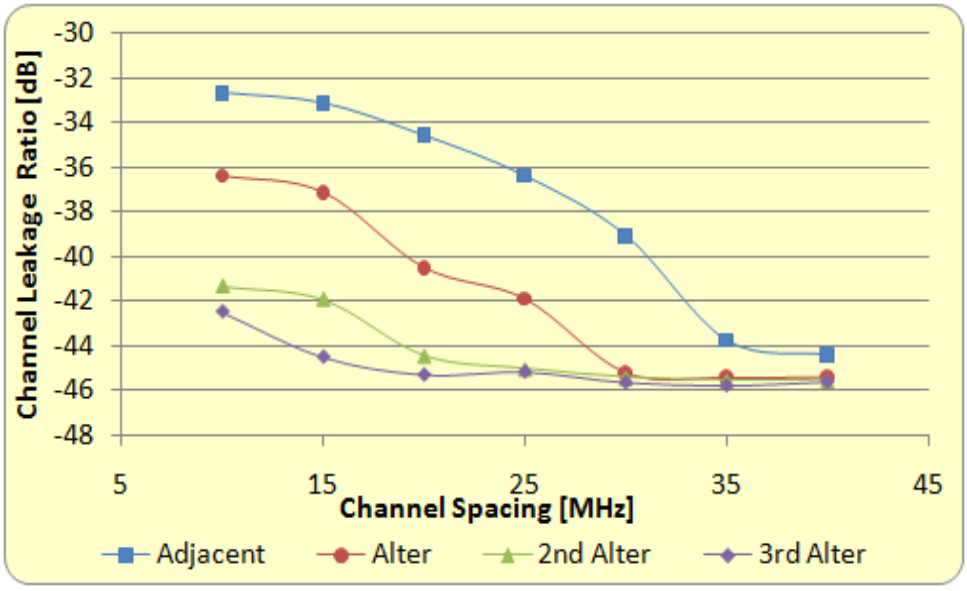

Figure 53: ACLR versus subcarrier spacing

In addition to the above, Figure 54 displays the obtained EVM at an antenna input with respect to MZM OMI and ACLR for 65 km feeder length and 40 MHz subcarrier spacing. The trace at the bottom of the bathtub curve confirms an EVM of -30 dB was obtained as specified in the standard [7].

Significantly, Figure 54 also demonstrates the specified OMI range meets the adjacent and alternate channels ACLR profile of -45 dB, declared in Figure 53 at 40 MHz subcarrier spacing.

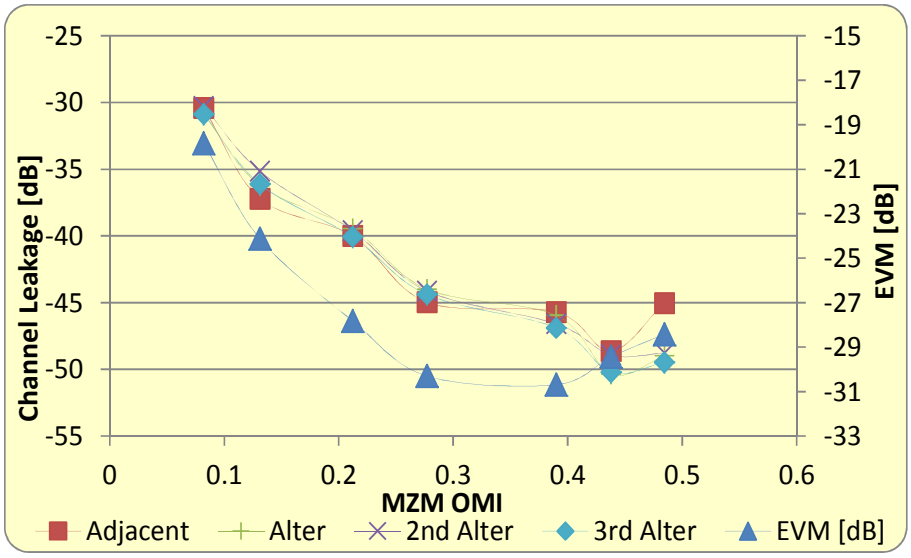

Figure 54: ACLR versus EVM

To define how much chromatic dispersion has affected EVM, experimental investigations were performed in both downstream and upstream. The obtained EVMs with and without the feeder were compared to establish the potential penalties imposed by the link. In the second scenario the corresponding attenuation that would have been acquired due to the transmission over the feeder fibre is still accounted for.

As demonstrated in Figure 55 the imposed degradation in downstream as a result of chromatic dispersion for various local office output powers is negligible. This characteristic is the property of the proposed OSSB scheme, compensating effectively the chromatic dispersion accumulated over the extended 65 km feeder reach. For an EVM of -30 dB the minimum required output power is +6.5 dBm. This has been achieved with an EDFA gain of 20 dB.

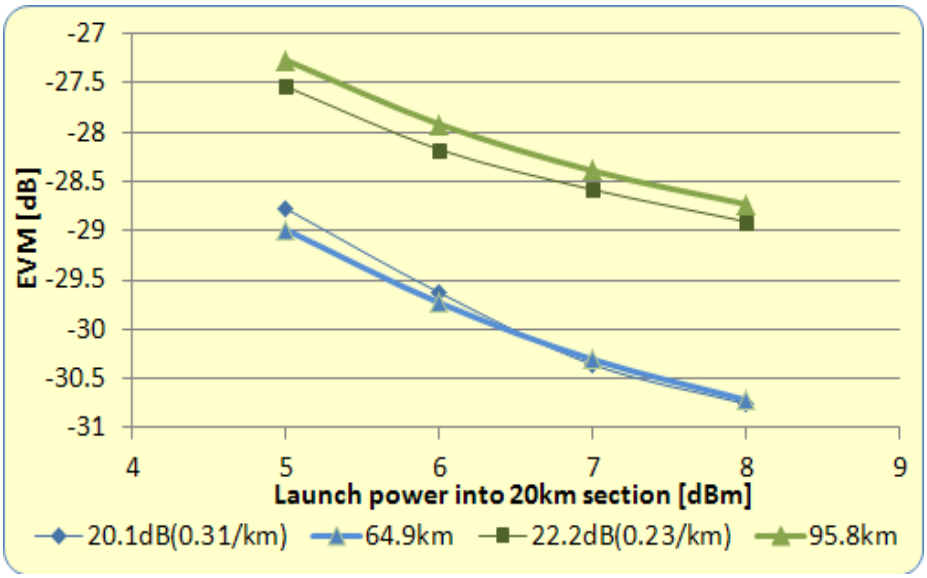

Figure 55: EVM with fibre and equivalent attenuation figures downstream

Similarly, an assessment of the fibre dispersion accumulation in measured EVMs at the OLT is plotted in Figure 56 for a range of middle office output powers. As expected, a power penalty of 1.8 dB is observed for the same transmission distance. This can be justified since upstream considers double sideband modulation of VCSELs. As a result this restricts feeder transmission to 45 km achieving a total 65 km upstream backhauling links, including the 20 km fibre. A straightforward approach achieving symmetrical links in downstream and upstream would be the application of OSSB also in upstream. This would only require an additional optical filter in the ONU/BS to select single sideband transmission.

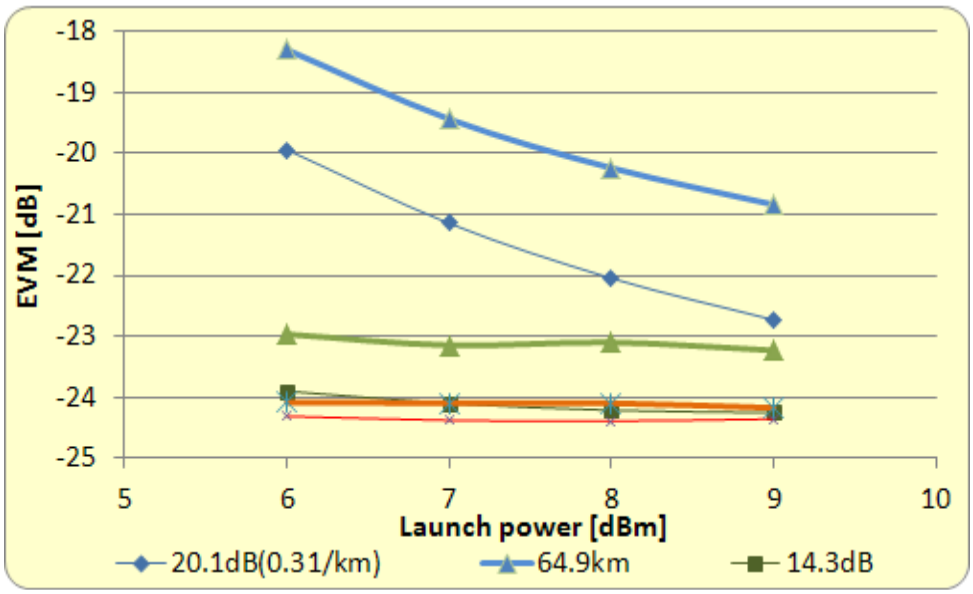

Figure 56: EVM with fibre and equivalent attenuation figures upstream

Finally, it can be conclude from the obtained results that although the targeted ACLR of -45 dB for 84.6 km downstream transmission was readily achieved, the total number of supportable RRHs is significantly reduced due to the limited power budget. If the requirement is to increase the split ratio the ACLR will notably degrade. In addition, such links would require optical amplifications (multi-channel EDFA preferably) as well as advance modulation formats to combat chromatic dispersion effects increasing the cost. Therefore, the RoF in ACCORDANCE should be only considered between MCO and RRH (as already described in section 3) due to shorter distances and lower split ratios.

Significantly, the results for both short and extended reach RoF links confirmed that low cost laser sources, such as VCSELs, can be used for upstream in RRHs. This could be especially advantageous since recent developments in VCSELs proved operation over long multiple wavelengths.

6. Inter-site communication

Two cell-edge types can be identified with the architecture discussed in ACCORDANCE:

1. both cells sharing the cell-edge are fed by the same main central office
2. both cells sharing the cell edge are fed by different main central offices

Naturally for both cases cell-edge performance ought to be good. In case one this is trivial, as here a single central office is in charge and thus the cells share the same global RLC/MAC unit. In case three this is different. We have three options to solve this issue:

- Implementation of a communication link between central offices feeding locally adjacent regions for the exchange of information.
- Implementation of a communication link between the sites.
- Sensible placement of such cell edges.

The first option is advised, but it is important to note that for most of the schemes making use of the global view (the ones relying on short term statistics, such as collaborative scheduling) this link introduces too much latency. This increased latency due to the transport between the central offices would devour all gains. Only schemes relying on long-term statistics like topology control might be feasible, as they do not suffer from the increased delay.

The second option again has certain flaws. Although those cells can interact this way, the central office still is not able to exploit the global view.

So, the third option might be the most simple and the most appropriate one. When assigning the cells to the central offices, the problematic cell-edges should be placed in rural, scarcely occupied regions. Here, the cells are not in full load most of the times and so a good cell-edge performance still can be guaranteed without the need of dedicated schemes.

7. Comparison of different options for optical/wireless access

Based on the outcomes of the above investigations, mainly in terms of interfacing and bandwidth requirements as well as link-level performance evaluation, the indentified integrated optical/wireless architectural options are compared in this section by outlining their key advantages and disadvantages.

Table 14: Comparison of different options.

Options		Advantages	Disadvantages
IP backhauling (a)		• Low bandwidth requirements on the PON • Load on the PON follows the load on the air link • Complete baseband and MAC/RLC processing performed at the site therefore latency requirements not an issue (HARQ anchored at the site) • Minimum interfacing with PON needed • Control planes of wireless and PON networks are independent (i.e. no special messages needed) • Transport via the optical OFDM possible • Digital transmission	• QoS radio/optical mapping required when transmission resources are shared • ONU and OLT should be aware of all eight LTE's standardized QCIs and corresponding DSCP values • Benefits (e.g. hardware sharing between sites) of the optical network not achieved due to the complete processing at the site • Highest equipment footprint at the site (compared to the other options) → highest cost and lowest acceptance from residents • Intense and cumbersome message exchange needed for inter-site cooperation schemes
Split eNB (b-e)	***Soft-bit (b)***	• Low bandwidth on the PON • Load on the PON follows the load on the air link • Transport via the optical OFDM possible • Hardware sharing at the MCO possible • No radio/optical mapping required • Digital transmission • Inter-site cooperation schemes applied more efficiently through MAC centralisation	• Still extensive (compared to CPRI fronthauling) baseband processing at the site (but reduced compared to IP backhauling) • HARQ anchored at the central point → feeder link eats away parts of the available latency budget
	Soft-symbol (c)	• Still comparatively low bandwidth requirement on the PON	• Still extensive (compared to CPRI fronthauling) baseband processing at the site (but

		• Load on the PON follows the load on the air link • Transport via the optical OFDM possible • Increased hardware sharing at the MCO possible • Digital transmission • No radio/optical mapping required • Inter-site cooperation schemes applied more efficiently through MAC centralisation	reduced compared to IP backhauling) • No binary processing steps (such as FEC for the optical transport) can be applied in downlink • The modulation grade cannot be adapted to the quality of the optical channel (therefore not preferred option) • HARQ anchored at the central point → feeder link eats away parts of the available latency budget
	Burst (d)	• Still comparatively (compared to CPRI fronthauling) low bandwidth requirement on the PON but higher than with soft-bit fronthauling • Load on the PON follows the load on the air link • Transport via the optical OFDM possible • Hardware sharing at the MCO possible (at the max, as all processing steps which are per user, are performed centrally) • Digital transmission • No radio/optical mapping required • Inter-site cooperation schemes applied more efficiently through MAC centralisation	• Still some baseband processing required at the site (compared to CPRI fronthauling), but less then soft-bit fronthauling • HARQ anchored at the central point → feeder link eats away parts of the available latency budget • Higher bandwidth requirement than soft-bit fronthauling
	Frame (e)	• Limited baseband processing at the site • Hardware sharing at the MCO possible (at the max, as all processing steps which are per user, are performed centrally) • Digital transmission • No radio/optical mapping required • Inter-site cooperation schemes applied more efficiently through MAC centralisation	• Relatively high bandwidth per site required • Load on the PON does not follow load on the air • HARQ anchored at the central point → feeder link eats away parts of the available latency budget

CPRI fronthauling	• Simple remote radio heads • Digital transmission • Hardware sharing between sites possible (at the max, as all processing steps which are per user, are performed centrally) • Supports all emerging wireless standards • No radio/optical mapping required • No communication link between wireless and optical MAC needed (i.e. minimum interfacing requirements with PON)	• High transmission bandwidth pipes needed on the PON • Load on the PON does not follow load on the air • Low BER requirements are to be met at remote antennas • Transport of CPRI traffic must be separated from wireline services • HARQ anchored at the central point → feeder link eats away parts of the available latency budget • No efficient transport of site control messages possible (e.g. for topology control)
RoF fronthauling	• Simple remote radio heads • Small transmission bandwidth pipes needed on the PON • Complete transparency to the optical MAC achieved • Hardware sharing between sites possible • No communication link between wireless and optical MAC needed due to transparency (i.e. minimum interfacing requirements with PON) • No radio/optical mapping required	• Susceptible to non-linearity of optical components • It might be limited to short fibre distances (depending on the number of BSs) • Shared budget (optical modulation index difficult to maintain) • Can not be transported with OFDMA spectrum. WDM/FDM transmission required • Multiple wavelengths required

8. xDSL over fibre transmission

In D5.2 “Requirements of wireless/wireline systems and their impact on the optical network” [2] was presented a study regarding how to transmit xDSL signals over fibre in analog mode without the need of a remote DSLAM and increasing the current coverage and capacity of xDSL access networks.

We proposed a distribution system for xDSL signals over fibre to provide xDSL services to final users up to 20 km from the central office with a maximum last drop based on copper between 200 and 300m. One of the advantages is that in the remote node located at the demarcation point there is only an electro-optical transceiver but not a small full featured DSLAM or mini-DSLAM.

The remote node is comprised of:

- A photodetector that receives the downstream optical signal and recovers the analog one.
- A frequency transceiver of the lower frequencies in addition to a FDM demultiplexer to split the downstream xDSL signals.
- A frequency transceiver of the upper frequencies in addition to a FDM multiplexer to group the upstream xDSL signals.
- A collection of solid state hybrids to split/combine the downstream/upstream signals to or from any copper pair.
- A laser and a modulator that converts and transmits the upstream analog signal up to the central office.

In this way, the downstream spectra are transmitted over a FDM multiplex over a wavelength while the upstream spectra are transmitted forming another FDM multiplex over a different wavelength.

In order to evaluate the performance of this kind of xDSL over fibre transmission, the analysis has been performed over the first alternative presented in D5.2 [2] and it is based on the power budget estimate. This first alternative considers a DSLAM in the CO collocated with a separated xDSL optical transceiver and an optical transmission using two different wavelengths.

The C/N degradation due to optical to electrical conversion is estimated to be 5 dB, and the optical loss of the WDM device (where the wavelengths that are carrying upstream and downstream signals are multiplexed together and with possible 3rd lambda that is dedicated to DTT signal) is assumed to be 1.5 dB. Also the assumption is that the optical power is related to the current for both laser diodes and photodiodes which leads to the doubling of the fibre attenuation. The attenuation of the fibre is assumed to be 0.4 dB per km including the losses at the splices. The attenuations considered are schematically shown in the figure below. The simulations were performed for the worst case where optical-electrical transceiver is assumed to be installed in additional rack to DSLAMs. Integration of the optical-electrical transceiver into the DSLAM line card could decrease 3 dB the performance losses.

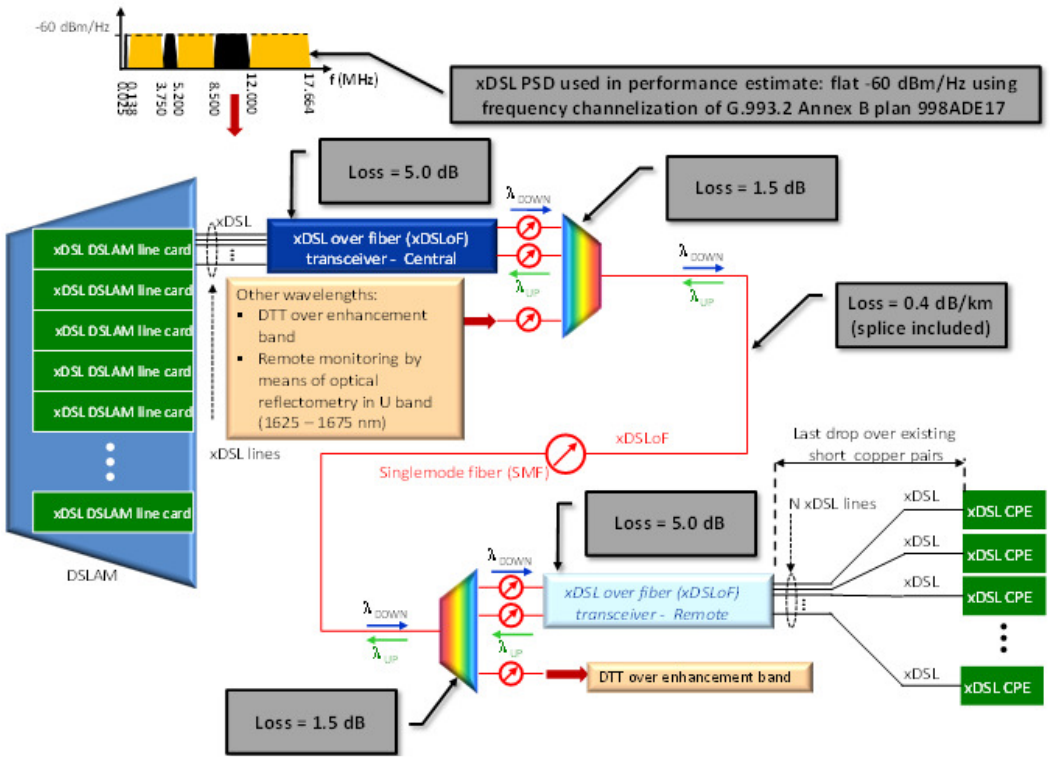

Figure 57: xDSLoF scenario with the assumed attenuation

Other considerations includes the VDSL2 signal according to the ITU-T G.993.2 Annex B, band plan 998AE17 with flat PSD of -60 dBm/Hz at U0 (0,025 MHz – 0,138 MHz) and D1 (0,138 MHz – 3,750 MHz) bands. The copper cables were modeled according to the ITU-T G 996.1 recommendation. Other parameters include, the background noise of -132 dBm/Hz, noise margin of 8 dBm, HAM band included, impulse noise protection (INP) set to 4 symbols and a maximum delay of 8 ms.

The following figure shows the achievable net data rates as a function of a distance from the distribution point for a 0.4 mm paper insulated copper cable used in a final drop. Different colors are for different lengths of the fibre (1 m, 5 km, 10 km, 15 km, 20 km, 25 km and 30 km). As can be noted, the net data rate decrease with the longer fibre but not as much as with the copper cable length.

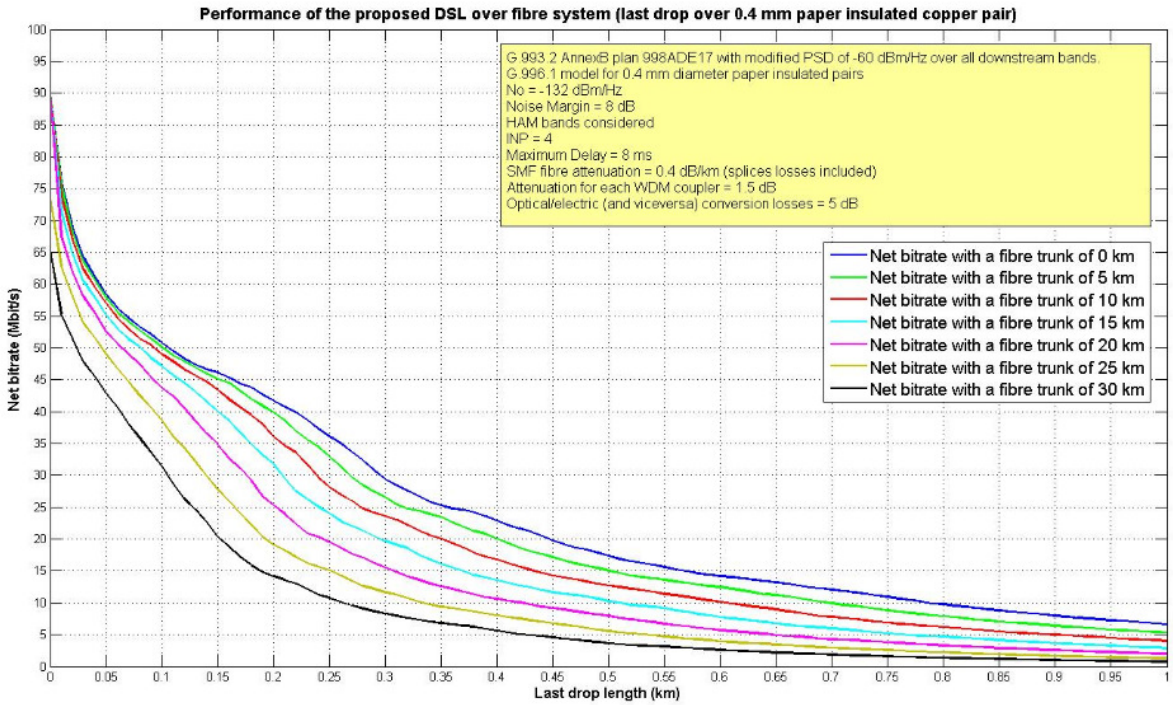

Figure 58: xDSLoF performance analysis for0.4 mm paper insulated copper cable

Next figure shows the achievable net data rates as a function of a distance from the distribution point for a 0.5 mm paper insulated copper cable used in a final drop. Different colors are for different lengths of the fibre (1 m, 5 km, 10 km, 15 km, 20 km, 25 km and 30 km). The same can be concluded as for the previous case with better results.

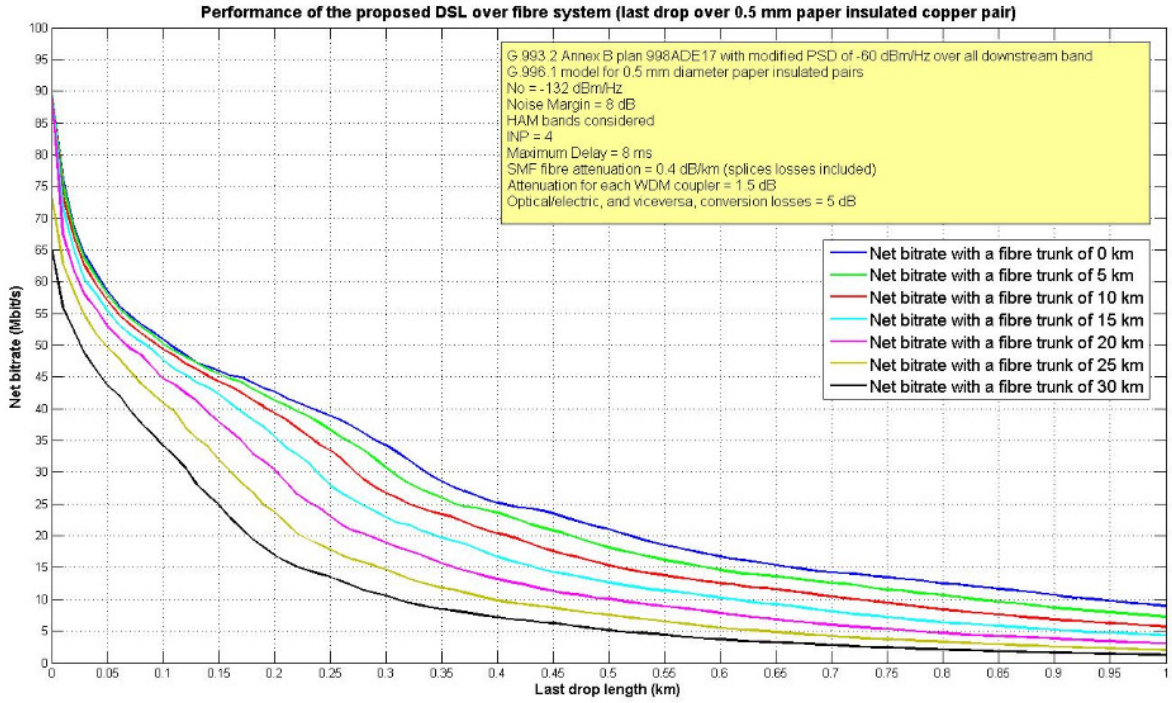

Figure 59: xDSLoF performance analysis for 0.5 mm paper insulated copper cable

The figure bellow shows the achievable net data rates as a function of a distance from the distribution point for a 0.4 mm with poly-ethylene insulation copper cable used in a final

drop. Different colors are for different lengths of the fibre (1 m, 5 km, 10 km, 15 km, 20 km, 25 km and 30 km). The same can be concluded as for the previous case.

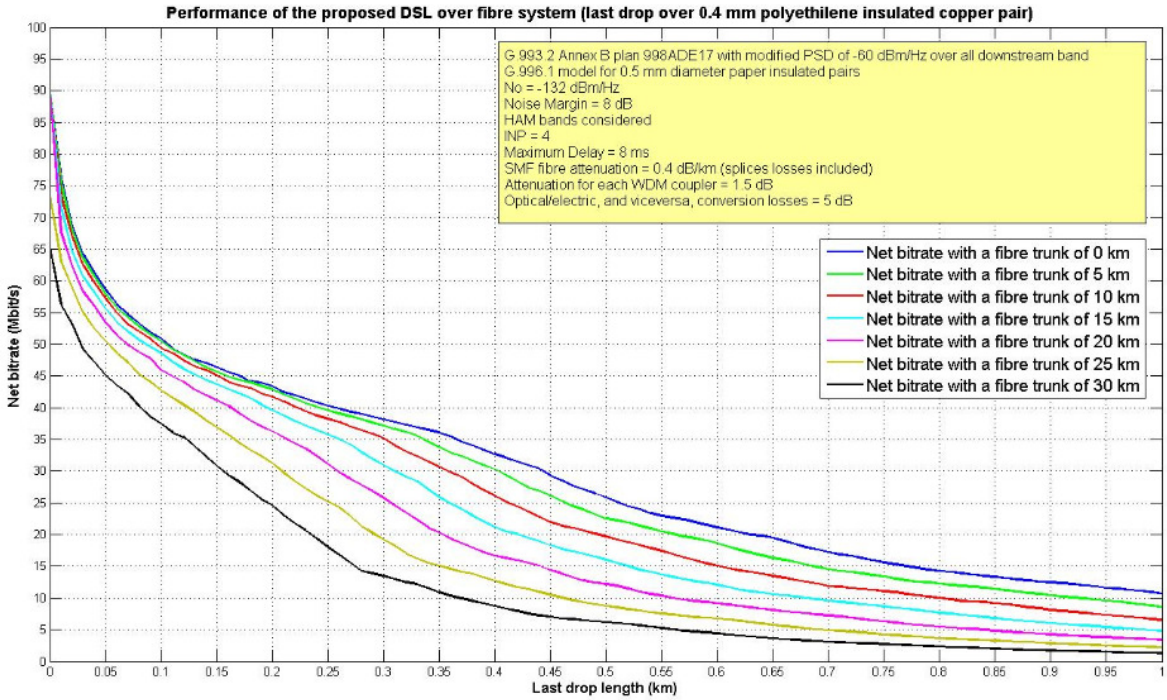

Figure 60: xDSLoF performance analysis for 0.4 mm poly-ethylene (PE) insulated copper cable

The last figure shows the achievable net data rates as a function of a distance from the distribution point for a 0.5 mm with poly-ethylene insulation copper cable used in a final drop. Different colors are for different lengths of the fibre (1 m, 5 km, 10 km, 15 km, 20 km, 25 km and 30 km). The same can be concluded as for the previous case.

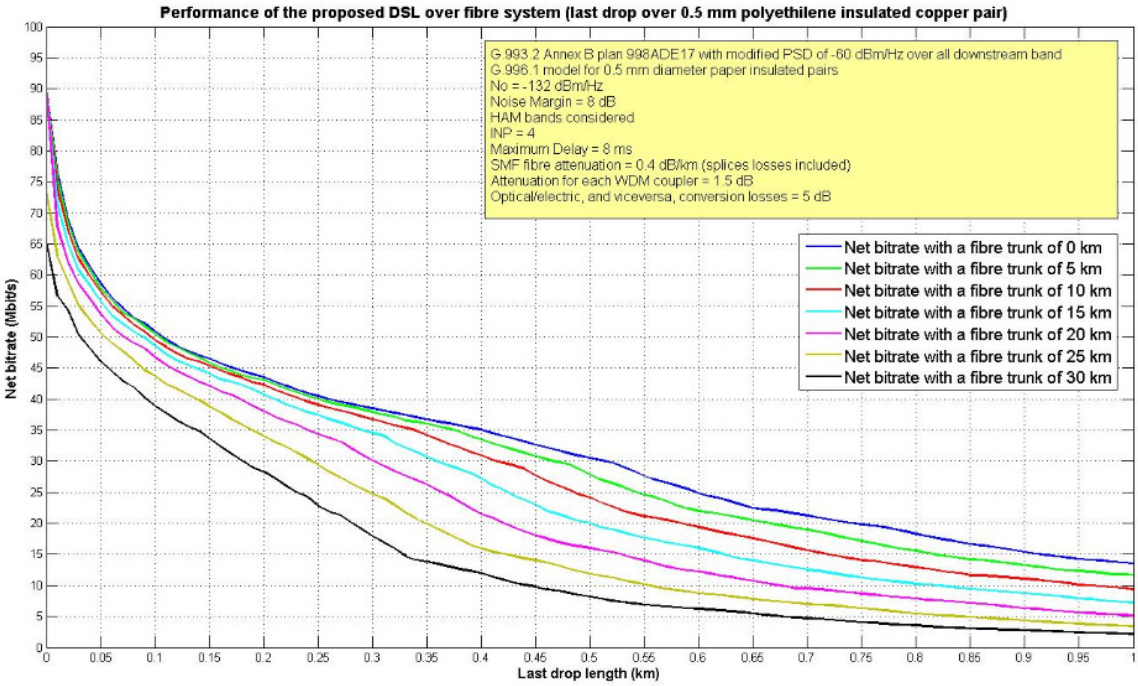

Figure 61: xDSLoF performance analysis for 0.5 mm poly-ethylene (PE) insulated copper cable

The following table summarizes the performance of the xDSL over fibre scenario evaluated as the copper cable distance from the distribution point able to deliver 10 Mbps, 20 Mbps, 30 Mbps, 40 Mbps and 50 Mbps net data rates to the end users. These data rates are obtained with the 20 km long fibre and with the hypothesis mentioned at the beginning of this section. As can be noted, the 20 Mbps service can be easily delivered to the users that are 20 km plus the drop cooper end of around 300 m from the head end (central office).

Table 15: Distances from the fibre endpoint (SMF 20 km length)

Copper pair drop type: diameter and isolation	Achievable Net Data Rate				
	10 Mbps	20 Mbps	30 Mbps	40 Mbps	50 Mbps
	Distance from the fibre endpoint				
0.4 mm paper	425 m	250 m	175 m	125 m	60 m
0.5 mm paper	490 m	280 m	200 m	140 m	70 m
0.4 mm PE	570 m	350 m	260 m	160 m	70 m
0.5 mm PE	680 m	420 m	300 m	175 m	70 m

Figures shown in the above table have been obtained considering only one copper pair per connected home. So, bonding has not been considered but it could be used to achieve a higher capacity.

As a result, as shown in the next image, the whole area of Madrid can be covered with only one head end (central office and MDF). The correction factor of 0.707 is used to take into account the deviation of the fibre from the direct path. Therefore, the length of 14 km corresponds to 20 km fibre length, 10.5 km corresponds to the 15 km of the fibre, 7 km corresponds to 10 km of fibre and 3.5 km corresponds to 5 km fibre.

Figure 62: Coverage analysis of xDSL over fibre solution over Madrid area

Taking as an example the Sao Paulo area, four head ends would be sufficient to cover the whole area, as demonstrated in the figure bellow.

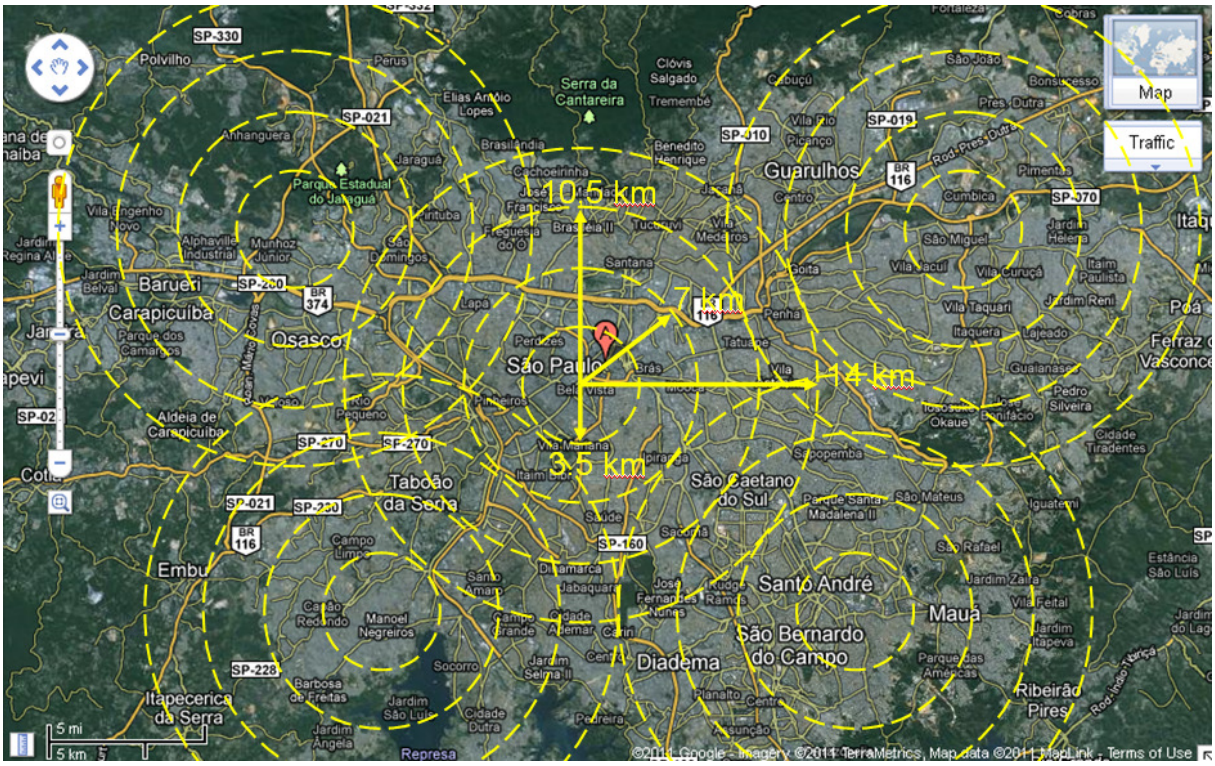

Figure 63: Coverage analysis of xDSL over fibre solution over Sao Paolo area

Typically a broadband service of 30 Mbps based on copper access can be delivered only to a limited number of users that are around 300 m from the Central Office. A lower capacity of 6 Mbps can be typically offered for users that are 2 km from the Central Office and a maximum capacity of 4 Mbps can be offered to higher distances. xDSL over fibre can provide a broadband connection of 20 - 30 Mbps to the users that are around 300 m from the remote distribution point. The figure below clarifies graphically this concept and shows how it can help to CO consolidation reducing the number of the operator's building.

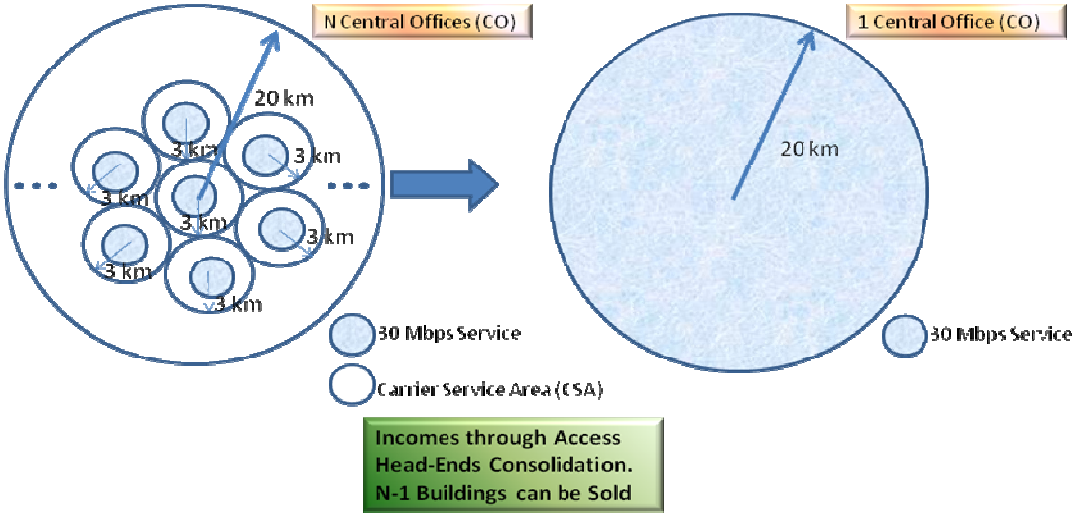

Figure 64: Coverage comparison for the 30 Mbit/s service between FTTEx and xDSLoF solutions

8.1. xDSL OVER FIBRE DEPLOYMENT

In xDSL, the longer the loop, the lower the access bit rate that can be provided. xDSL over fibre solves this problem by means of the usage of fibre in the loop, using copper only in the last drop.

The main drawbacks that appear are:

- How to house the xDSL over fibre Transceiver – Remote in the building proximity.
- How to feed the xDSL over fibre Transceiver - Remote.

There are two options:

- The first one consists of take advantage of current regulation referred to the deployment of common telecommunications infrastructures in buildings (e.g. Spanish ICT regulation, [10]).
- The second option consists of leverage xDSL over fibre deployment on 3G/HSPA/LTE macro and micro cellular deployment facilities (i.e. sites and active equipments remote feeding). Coverage extension needed to face Mobile Broadband increase requires much more cellular radio access sites (i.e. base stations, Nodes B and eNodes B) that has to be connected through fixed ultra-high broadband connections. xDSL over fibre can provide the backhaul for this cellular radio access deployment, and simultaneously, the xDSL over fibre transceiver – Remote can be fed the feeding equipment used to fed radio access sites equipments.

In the next section, both options are analyzed.

8.1.1. Deployment based on building's common telecommunications infrastructures

New buildings provide telecommunications infrastructure facilities that must be shared between all the telecommunication operators whose customers are in those buildings. These facilities, hereinafter Telecommunications Common Infrastructures, can be used by a telecommunications operator to make easier the deployment of both FTTB and xDSL over fibre access solutions.

In this point the Spanish Telecommunications Common Infrastructures, called ICT[1] (*Infraestructuras Comunes de Telecomunicaciones*) is analyzed, trying to find the ways it can be used to make easier the deployment of the *xDSL over Fibre – Remote* in the building, and the way it can reuse the building's internal copper drops.

In Spain there are approximately 24.647 Million homes (2009). The new ICT regulation came into effect in 1998 and was updated in 2003. The following table shows the figures of new homes build since 2002 a year where 1998 ICT regulation was fully operative, and it also includes the total homes which include ICT facilities.

[1] ICT: *Infraestructuras Comunes de Telecomunicaciones*.

Table 16: Building's telecommunication internal ducts (Spanish ICT regulation)

Homes up to 2001	20.946.554			
Homes built from 2002 to 2009	**New**	**Restored**	**Demolished**	**Total**
	3,725,808	138,032	162,824	3,701,016
Total (may 2009)	24,647,570			
Homes with ICT facilities	5,132,274 (20.82%)			
Homes without ICT facilities	19,515,296 (79.18%)			

In accordance to above figures, in Spain more than 20% of the homes (5.132 Million), and by extension, buildings, include telecommunications housing and wiring facilities. And the 60% of this figure, 3.1 Million are primary residences. It is a significant percentage which can be addressed by xDSL over fibre solutions. Which are facilities offered by Spanish ICT regulation? These facilities are summarized in the following tables.

Spanish ICT requires that each building has a telecommunication cabinet to house all requires elements to provide telecommunications services (POTS, ISDN, terrestrial, cable and satellite TV, etc). The size of this cabinet depends on the number of homes in the building. This cabinet can be used to deploy the xDSL over fibre transceiver – Remote. The next table shows the size of this cabinet.

Table 17: Building's telecommunication cabinets size (Spanish ICT regulation)

Building's internal cabinets size, one in the floor (RITI[2]) and a second one in the roof (RITS[3])			
Number of homes per building (PAUs[4])	**Width (m)**	**Height (m)**	**Depth (m)**
Up to 20	1.00	2.00	0.50
From 21 to 30	1.50	2.00	0.50
From 31 to 45	2.00	2.00	0.50
More than 45	2.00	2.30	0.50

The number of copper pairs in a building will be a 40% higher than the estimated demand, according to the number of houses, offices and business in that building. These pairs will have to be distributed into standard 25, 50, 75 or 100 pair's cables, which will be hung in the building's internal duct for POTS and ISDN services. These pairs will be poly-ethylene insulated and the minimum diameter will be 0.5 mm.
In order to make possible that each operator can access to any building pair, there will be two types of MDFs in the building cabinet:

- A group of input MDFs where pairs from operators are connected. There will be an input MDF per operator, so two input MDFs in the building cabinet (RITI and RITS).
- And an output MDF where building pairs are connected.

[2] RITI: *Recinto Interior de Telecomunicaciones Interior*. Building's internal telecommunications cabinet located in the building's floor.
[3] RITS: *Recinto Interior de Telecomunicaciones Superior*. Building's internal telecommunications cabinet located in the building's roof.
[4] PAU: *Punto de Acceso al Usuario*. The connection point between building's common telecommunications infrastructure and the home connectivity infrastructure.

If N is the total number of pairs in the cables inside building's duct for POTS and ISDN service, the number of positions of input and output MDF will fulfill the following expressions:

$$1.5 \times N_{OUT-MDF} = N_{IN-MDF-A} + N_{IN-MDF-B}$$

Where:

- NOUT-MDF: is the number of positions of building's cabinet output MDF.
- NIN-MDF-A: is the number of positions of building's cabinet input MDF for operator A.
- NIN-MDF-B: is the number of positions of building's cabinet input MDF for operator B.

Finally, depending on the number of required copper pairs, one or more cables containing up to 100 pairs must be used, providing an additional number of spare pairs.

Table 18: Building's POTS and ISDN internal cables (Spanish ICT regulation)

Number of pairs	Number of cables	Type of cable
25 < N ≤ 50	1	50 pairs (1 (50 p.))
50 < N ≤ 75	1	75 pairs (1 (75 p.))
75 < N ≤ 100	1	100 pairs (1 (100 p.))
100 < N ≤ 125	2	1 (100 p.) + 1 (25 p.) or 1 (75 p.) + 1 (50 p.)
125 < N ≤ 150	2	1 (100 p.) + 1 (50 p.) or 2 (75 p.)
150 < N ≤ 175	2	1 (100 p.) + 1 (75 p.)
175 < N ≤ 200	2	2 (100 p.)
200 < N ≤ 225	3	2 (100 p.) + 1 (25 p.) or 3 (75 p.)
225 < N ≤ 250	3	2 (100 p.) + 1 (50 p.) or 1 (100 p.) + 2 (75 p.)
250 < N ≤ 275	3	2 (100 p) + 1 (75 p.)
275 < N ≤ 300	3	3 (100 p.)

So deploying the xDSL over fibre transceiver – Remote into the building's communications cabinet, it will be possible to reuse copper pairs available that provide POTS and ISDN and additional cables from building's multi-pair cables. So, leveraging xDSL over fibre transceiver –Remote on building's telecommunications Common Infrastructures, xDSL over fibre deployment becomes simpler and cheaper and it can be used simultaneously with copper pair bonding solutions.

There is another point that must be solved related to remote feeding. There are two options in the case the xDSL over fibre transceiver – Remote is housed in one of the building's telecommunications cabinet:

- Remote powering from the Central Office. Spare loops can be used for feeding. There are available systems from main vendors, like Alcatel-Lucent or Ericsson which can be used for this purpose. Depending on pair gauge and the number of available pairs, the remote feeding solution can extend beyond 10 km. This option requires other copper Central Offices for remote powering issues.
- Local powering using in-building power supply sources. It is a possibility which is considered in the Spanish ICT regulation that allows housing two Telco's power metering devices.

8.1.2. Deployment from radio cellular access sites

An integrated operator can take advantage from its cellular radio access deployment for the xDSL over fibre deployment. It can leverage a possible xDSL over fibre deployment on its 3G/HSPA/LTE macro and micro cellular deployment facilities (i.e. sites and active equipments remote feeding).

The coverage and access bit rate increase needed to face Mobile Broadband traffic increase requires a much more cellular radio access sites (i.e. base stations, *Nodes B* and *eNodes B*) that has to be connected through fixed ultra-high broadband connections. xDSL over fibre can provide the backhaul for this cellular radio access deployment, and simultaneously, xDSL over fibre transceivers – Remote can be fed by feeding facilities used to fed cellular radio access sites equipments.

In this scenario, last copper drops will start at cellular radio access sites, where remote feeding facilities (batteries, remote feeding solutions from operator's CO over existing copper pairs or AC power supply) are located. The next figure describes this deployment option. This deployment strategy requires the usage of xDSL pair bonding (ITU-T G.998.2) at the xDSL over fibre transceiver – Remote in order to be able to provide the required downstream and upstream aggregated access bit rates for HSPA or LTE.

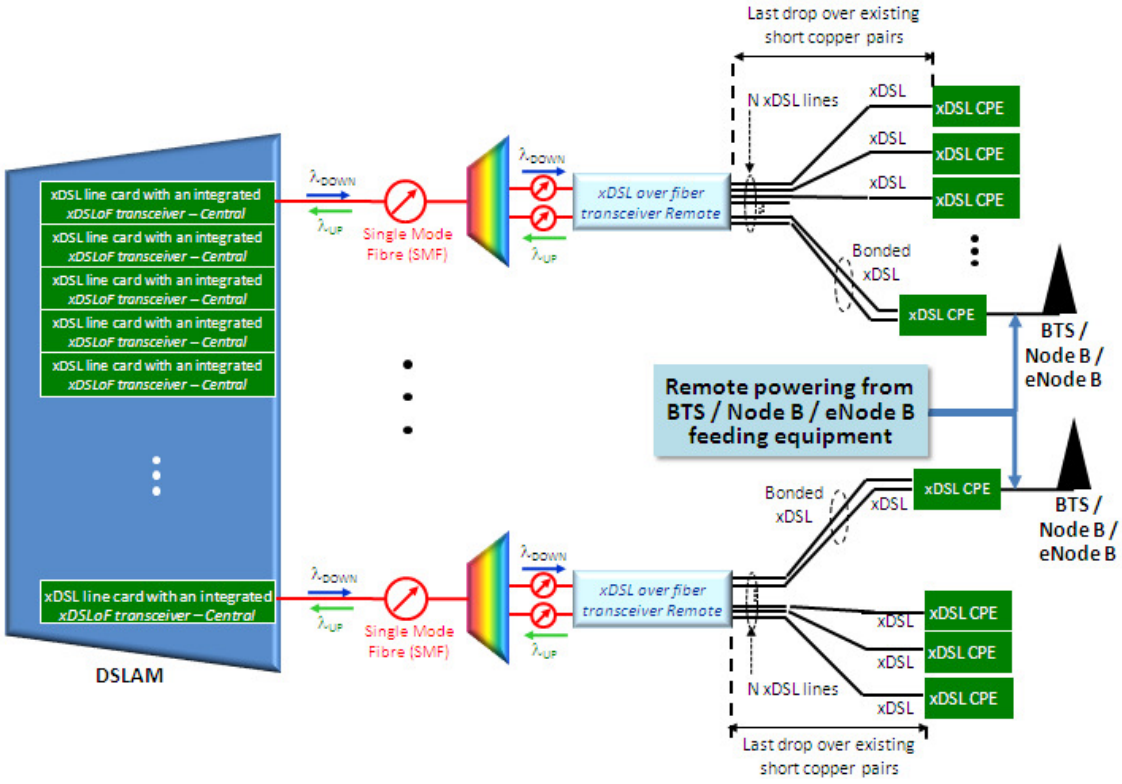

Figure 65: xDSL over fibre deployment strategy leveraged on cellular radio access sites

8.1.3. xDSL over fibre implementation in Accordance

There are two main scenarios in which the proposed solution of xDSL over fibre can be implemented in an ACCORDANCE type access network. Both of them are based on the potential ACCORDANCE solutions for DSL signals; see D2.1 ACCORDANCE report, chapter 6.2 "Options for carrying DSL signals over ACCORDANCE" [11].

- The first scenario is based on Ethernet connectivity in the CO, using only xDSL in the access segment. In this alternative, all DSLAM are located in the CO and are connected to the metro network using the ACCORDANCE network. This way the high capacity and long reach of the ACCORDANCE network can be use to perform the xDSL backhaul of a huge area.

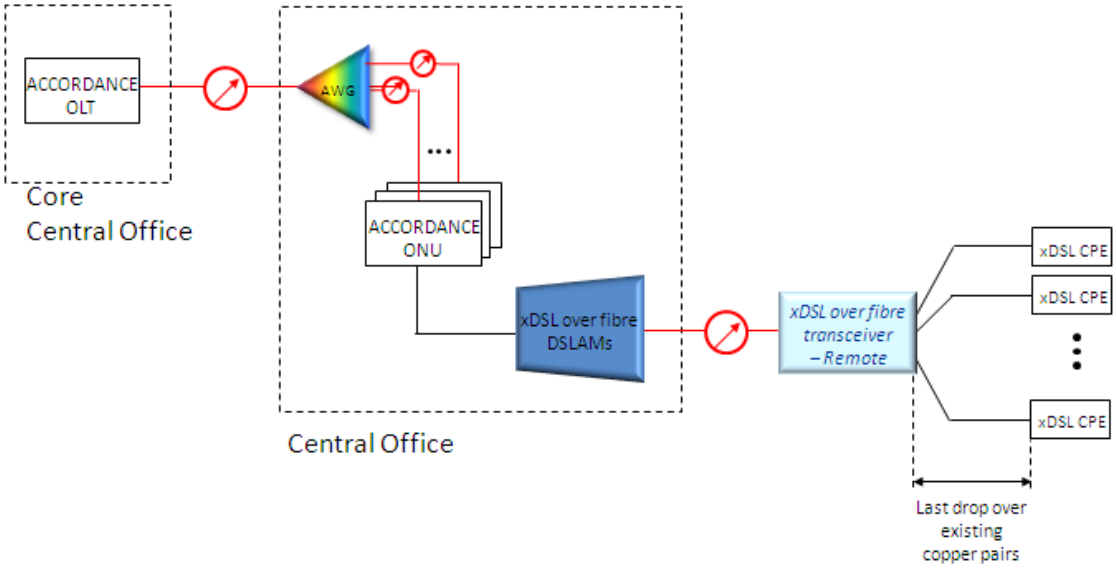

Figure 66: Ethernet connectivity using ACCORDANCE network

- The second scenario is based on a centralized DSLAM with analogue transport of the xDSL signals and sharing the ODN with other ACCORDANCE signals. This scenario is oriented to provide more capacity to final users and can be used as a candidate scenario in a future migration of xDSL users. In this case, the metro connectivity can be provided by the ACCORDANCE network or other kind of connectivity. The xDSL over fibre downlink signal is multiplexed using a WDM device with the ACCORDANCE wavelengths in the CO. The ODN can consist of one or several splitting levels for all ACCORDANCE and xDSL users, and the insertion loss that splitters add can be reduced using a by-pass solution of the xDSL over fibre signal, as can be seen in the following figure.

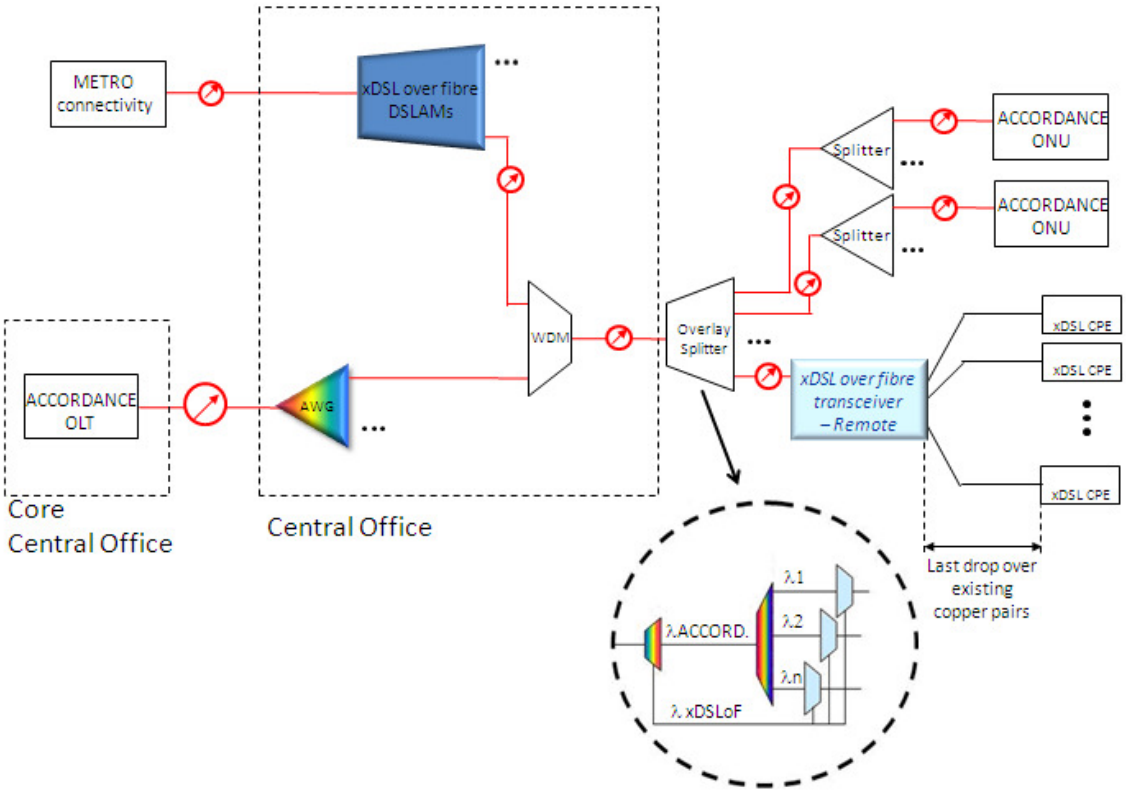

Figure 67: Centralized DSLAM with analogue transport using ACCORDANCE network

9. Conclusions

The purpose of this chapter is to summarise the concepts presented in this deliverable for combined optical and wireless/wireline access over ACCORDANCE for efficient back- and fronthauling. The fronthauling was referred to in the deliverable in a scenario where parts of the wireless baseband processing are performed at the central office.

In that direction, the document started by providing a detail analysis of interfacing requirements for the various interfacing points in the wireless chain. Description of the layer-1 and layer-2 components was presented. With IP backhauling baseband and MAC processing is performed at the base station. However, MAC centralisation was still possible leading to intolerable latencies. In contrast, split-eNB variants, namely soft-bit, soft-symbol, burst and frame fronthauling, perform certain degree of baseband centralisation and complete MAC processing at the CO. With the application of CPRI and RoF on the other hand, full baseband and MAC centralisation is achieved.

The bandwidth requirements on the PON of all the above options vary significantly and it is important factor to consider. For instance, with some system level simulations it was determined that the peak data rate for soft-bit fronthauling under 100 % network load is in the range of 200 Mbps while for the CPRI it is 2.5 Gbps. Therefore, as the interface point is shifted to the right (i.e. more baseband processing steps are performed centrally) the bandwidth requirement increases.

None of the given options can be treated as the best. Each option has advantages and disadvantages (as described in Section 7) compared to the alternatives. Instead, the boundary conditions of the setting determine which of the advantages/disadvantages are dominating and thus which of the fronthauling/backhauling options is to be favoured. A key point of this deliverable is the provision of reasonable implementation guidelines depending on the setting (urban/rural).

To that extent, performance evaluation of digital and analog fronthauling options was presented via link-level simulations. For the IP backhauling the QoS mapping will be analysed in the future deliverables of this work package.

Finally, this deliverable presented wireless/wireline, in the view of xDSL transmission, convergence options. The corresponding deployment scenarios were also discussed showing the feasibility of transmitting xDSL signals over fibre and how it could be implemented with the ACCORDANCE network.

10. Appendix

Table 19: Codeword space for N_{res}=5.

	gray	de2bi	inc-weight		gray	de2bi	inc-weight
c_1	00000	00000	00000	c_{17}	11000	10000	11100
c_2	00001	00001	00001	c_{18}	11001	10001	11010
c_3	00011	00010	00010	c_{19}	11011	10010	10110
c_4	00010	00011	00100	c_{20}	11010	10011	01110
c_5	00110	00100	01000	c_{21}	11110	10100	00111
c_6	00111	00101	10000	c_{22}	11111	10101	01011
c_7	00101	00110	10001	c_{23}	11101	10110	10011
c_8	00100	00111	01001	c_{24}	11100	10111	10101
c_9	01100	01000	00101	c_{25}	10100	11000	01101
c_{10}	01101	01001	00011	c_{26}	10101	11001	11001
c_{11}	01111	01010	00110	c_{27}	10111	11010	11101
c_{12}	01110	01011	01010	c_{28}	10110	11011	11110
c_{13}	01010	01100	10010	c_{29}	10010	11100	11011
c_{14}	01011	01101	10100	c_{30}	10011	11101	10111
c_{15}	01001	01110	01100	c_{31}	10001	11110	01111
c_{16}	01000	01111	11000	c_{32}	10000	11111	11111

Table 20: Codeword space for N_{res}=6.

	gray	de2bi	inc-weight		gray	de2bi	inc-weight
c_1	000000	000000	000000	c_{33}	110000	100000	110100
c_2	000001	000001	000001	c_{34}	110001	100001	111000
c_3	000011	000010	000010	c_{35}	110011	100010	110010
c_4	000010	000011	000100	c_{36}	110010	100011	110001
c_5	000110	000100	001000	c_{37}	110110	100100	101001
c_6	000111	000101	010000	c_{38}	110111	100101	100101
c_7	000101	000110	100000	c_{39}	110101	100110	100110
c_8	000100	000111	110000	c_{40}	110100	100111	100011
c_9	001100	001000	101000	c_{41}	111100	101000	101010
c_{10}	001101	001001	100100	c_{42}	111101	101001	101100
c_{11}	001111	001010	100010	c_{43}	111111	101010	111100
c_{12}	001110	001011	100001	c_{44}	111110	101011	111010
c_{13}	001010	001100	010001	c_{45}	111010	101100	111001
c_{14}	001011	001101	010010	c_{46}	111011	101101	110011
c_{15}	001001	001110	010100	c_{47}	111001	101110	110101
c_{16}	001000	001111	011000	c_{48}	111000	101111	110110
c_{17}	011000	010000	001100	c_{49}	101000	110000	101110
c_{18}	011001	010001	001010	c_{50}	101001	110001	101101
c_{19}	011011	010010	001001	c_{51}	101011	110010	101011
c_{20}	011010	010011	000101	c_{52}	101010	110011	100111
c_{21}	011110	010100	000110	c_{53}	101110	110100	001111

c_{22}	011111	010101	000011	c_{54}	101111	110101	010111
c_{23}	011101	010110	000111	c_{55}	101101	110110	011011
c_{24}	011100	010111	001011	c_{56}	101100	110111	011101
c_{25}	010100	011000	001101	c_{57}	100100	111000	011110
c_{26}	010101	011001	001110	c_{58}	100101	111001	011111
c_{27}	010111	011010	010110	c_{59}	100111	111010	101111
c_{28}	010110	011011	010101	c_{60}	100110	111011	110111
c_{29}	010010	011100	010011	c_{61}	100010	111100	111011
c_{30}	010011	011101	011001	c_{62}	100011	111101	111101
c_{31}	010001	011110	011010	c_{63}	100001	111110	111110
c_{32}	010000	011111	011100	c_{64}	100000	111111	111111

Table 21: Codeword space for N_{res}=7.

	gray	de2bi		gray	de2bi
c_1	0000000	0000000	c_{65}	1100000	1000000
c_2	0000001	0000001	c_{66}	1100001	1000001
c_3	0000011	0000010	c_{67}	1100011	1000010
c_4	0000010	0000011	c_{68}	1100010	1000011
c_5	0000110	0000100	c_{69}	1100110	1000100
c_6	0000111	0000101	c_{70}	1100111	1000101
c_7	0000101	0000110	c_{71}	1100101	1000110
c_8	0000100	0000111	c_{72}	1100100	1000111
c_9	0001100	0001000	c_{73}	1101100	1001000
c_{10}	0001101	0001001	c_{74}	1101101	1001001
c_{11}	0001111	0001010	c_{75}	1101111	1001010
c_{12}	0001110	0001011	c_{76}	1101110	1001011
c_{13}	0001010	0001100	c_{77}	1101010	1001100
c_{14}	0001011	0001101	c_{78}	1101011	1001101
c_{15}	0001001	0001110	c_{79}	1101001	1001110
c_{16}	0001000	0001111	c_{80}	1101000	1001111
c_{17}	0011000	0010000	c_{81}	1111000	1010000
c_{18}	0011001	0010001	c_{82}	1111001	1010001
c_{19}	0011011	0010010	c_{83}	1111011	1010010
c_{20}	0011010	0010011	c_{84}	1111010	1010011
c_{21}	0011110	0010100	c_{85}	1111110	1010100
c_{22}	0011111	0010101	c_{86}	1111111	1010101
c_{23}	0011101	0010110	c_{87}	1111101	1010110
c_{24}	0011100	0010111	c_{88}	1111100	1010111
c_{25}	0010100	0011000	c_{89}	1110100	1011000
c_{26}	0010101	0011001	c_{90}	1110101	1011001
c_{27}	0010111	0011010	c_{91}	1110111	1011010
c_{28}	0010110	0011011	c_{92}	1110110	1011011
c_{29}	0010010	0011100	c_{93}	1110010	1011100
c_{30}	0010011	0011101	c_{94}	1110011	1011101
c_{31}	0010001	0011110	c_{95}	1110001	1011110

c_{32}	0010000	0011111	c_{96}	1110000	1011111
c_{33}	0110000	0100000	c_{97}	1010000	1100000
c_{34}	0110001	0100001	c_{98}	1010001	1100001
c_{35}	0110011	0100010	c_{99}	1010011	1100010
c_{36}	0110010	0100011	c_{100}	1010010	1100011
c_{37}	0110110	0100100	c_{101}	1010110	1100100
c_{38}	0110111	0100101	c_{102}	1010111	1100101
c_{39}	0110101	0100110	c_{103}	1010101	1100110
c_{40}	0110100	0100111	c_{104}	1010100	1100111
c_{41}	0111100	0101000	c_{105}	1011100	1101000
c_{42}	0111101	0101001	c_{106}	1011101	1101001
c_{43}	0111111	0101010	c_{107}	1011111	1101010
c_{44}	0111110	0101011	c_{108}	1011110	1101011
c_{45}	0111010	0101100	c_{109}	1011010	1101100
c_{46}	0111011	0101101	c_{110}	1011011	1101101
c_{47}	0111001	0101110	c_{111}	1011001	1101110
c_{48}	0111000	0101111	c_{112}	1011000	1101111
c_{49}	0101000	0110000	c_{113}	1001000	1110000
c_{50}	0101001	0110001	c_{114}	1001001	1110001
c_{51}	0101011	0110010	c_{115}	1001011	1110010
c_{52}	0101010	0110011	c_{116}	1001010	1110011
c_{53}	0101110	0110100	c_{117}	1001110	1110100
c_{54}	0101111	0110101	c_{118}	1001111	1110101
c_{55}	0101101	0110110	c_{119}	1001101	1110110
c_{56}	0101100	0110111	c_{120}	1001100	1110111
c_{57}	0100100	0111000	c_{121}	1000100	1111000
c_{58}	0100101	0111001	c_{122}	1000101	1111001
c_{59}	0100111	0111010	c_{123}	1000111	1111010
c_{60}	0100110	0111011	c_{124}	1000110	1111011
c_{61}	0100010	0111100	c_{125}	1000010	1111100
c_{62}	0100011	0111101	c_{126}	1000011	1111101
c_{63}	0100001	0111110	c_{127}	1000001	1111110
c_{64}	0100000	0111111	c_{128}	1000000	1111111

11. Abbreviations

ACCORDANCE	A Converged Copper-Optical-Radio OFDMA-based Access Network with high Capacity and flexibility
A/D	Analog to Digital
ACLR	Adjacent Channel Leakage Ratio
ADM	Add/Drop Multiplexer
AWG	Array Waveguide Grating
BB	Baseband
BER	Bit Error Rate
BLER	Block Error Rate
BPF	Band Pass Filter
BS	Base Station
CO	Central Office
CPRI	Common Public Radio Interface
D/A	Digital to Analog
DFB	Distributed Feedback
DL	Downlink
DBA	Dynamic Bandwidth Allocation
DoF	Digital-over-Fibre
DSCP	Diffserv Code Point
DSL	Digital Subscriber Line
DSLAM	Digital Subscriber Line Access Multiplexer
eNB	E-UTRAN NodeB
EDFA	Erbium Doped Fibre Amplifier
EPON	Ethernet Passive Optical Network
E-UTRAN	Evolved Universal Terrestrial Radio Access Network
EVM	Error Vector Magnitude
FDM	Frequency Division Multiplexing
FEC	Forward Error Correction
FFT	Fast Fourier Transform
FTTB	Fibre to the Building
FTTH	Fibre to the Home
GPON	Gigabit PON
HARQ	Hybrid Automatic Repeat Request
IF	Intermediate Frequency
IFFT	Inverse Fourier Transform
IM-DD	Intensity Modulation – Direct Detection
INP	Impulse Noise Protection
IP	Internet Protocol
LE	Local Exchange
LO	Local Oscllator
LTE	Long Term Evolution
MAC	Medium Access Control
MCS	Modulation and Coding Scheme
MDF	Main Distribution Frame
MCO	Metro Central Office
MZM	Mach Zehnder Modulator

OBI	Optical Beat Interference
ODN	Optical Distribution Network
ODSB	Optical Double Sideband Modulation
OFDM	Orthogonal Frequency Division Multiplexing
OFDMA	Orthogonal Frequency Division Multiple Access
OLT	Optical Line Termination
OMI	Optical Modulation Index
ONU	Optical Network Unit
OSSB	Optical Single Sideband
PCFICH	Physical Control Format Indicator Channel
PDCCH	Physical Downlink Control Channel
PHICH	Physical Hybrid ARQ Indicator Channel
PHY	Physical layer
PON	Passive Optical Network
PRACH	Physical Random Access Channel
PSD	Power Spectral Density
PUCCH	Physical Uplink Control Channel
QAM	Quadrature Amplitude Modulation
QCI	QoS Class Identifier
QoS	Quality of Service
QPSK	Quadrature Phase Shift Keying
RCE	Relative Constellation Error
RF	Radio Frequency
RLC	Radio Link Control
RoF	Radio-over-Fibre
RSOA	Reflective Semiconductor Amplifier
RRH	Remote Radio Head
SDH	Synchronous Digital Hierarchy
SSMF	Standard Single-mode Fibre
SINR	Signal to Interference Ration
SNR	Signal To Noise Ratio
TDD	Time Division Duplex
TTI	Transmission Time Interval
UE	User equipment
UL	Uplink
VCSEL	Vertical Cavity Surface Emitting Laser
VDSL2	Very high-speed Digital Subscriber Line2
VSG	Vector Signal Generator
WDM	Wavelength Division Multiplexing
WiMAX	Worldwide Interoperability for Microwave Access
WLAN	Wireless Local Area Network
xDSL	x-type Digital subscriber line

--- End of Document ---